



**UNIVERSIDADE DE BRASÍLIA**  
**INSTITUTO DE CIÊNCIAS BIOLÓGICAS**  
**DEPARTAMENTO DE FITOPATOLOGIA**  
**PROGRAMA DE PÓS-GRADUAÇÃO EM FITOPATOLOGIA**

***Xanthomonas phaseoli* pv. *manihotis*: avaliação de genótipos de  
mandioca quanto à resistência e desenvolvimento de novos  
métodos de detecção**

**Ian Carlos Bispo de Carvalho**

**Tese de Doutorado**

**Brasília - DF**

**2025**

**IAN CARLOS BISPO DE CARVALHO**

***Xanthomonas phaseoli* pv. *manihotis*: avaliação de genótipos de mandioca quanto  
à resistência e desenvolvimento de novos métodos de detecção**

Tese apresentado à Universidade de  
Brasília como requisito parcial para  
obtenção do título de Doutor em  
Fitopatologia pelo Programa de Pós-  
Graduação em Fitopatologia

**Orientador**

Dr. Maurício Rossato

**Brasília – DF**

**2025**

**FICHA CATALOGRÁFICA**

## **Dedicatória**

*Dedico esse trabalho à minha esposa Alice Maria e à minha filha Luísa Maria,  
vocês foram o farol que iluminaram a minha jornada até aqui.*

*“Honra e glória a Deus para todo o sempre! Ele é o Rei eterno, invisível e imortal; Ele é o único Deus. Amém.”*

1Timóteo 1:17 (NVT)

## **Agradecimentos**

A Deus, fonte e autor de todas as coisas, pela infinita bondade manifestada em cada momento da minha vida. *Soli Deo Gloria.*

À minha querida esposa, Alice Carvalho, minha companheira de vida e de pesquisa, pelo amor, pela cumplicidade, pelo cuidado e pelo apoio indispensável, que tornaram possível o sucesso desta jornada.

À minha filha, Luísa Carvalho, meu pequeno raio de sol, por iluminar meus dias.

Aos meus pais, Edimilson Carvalho e Isadôra Carvalho, por todo amor, carinho e apoio que me deram em todos os momentos. Vocês me ajudaram a enxergar que todos os sonhos são possíveis.

Aos meus irmãos, Isa, Ianne e Carlos Eduardo, pelo apoio, amor e confiança depositados em mim.

Ao casal que me acolheu com tanto amor e carinho durante meu doutorado em Brasília: meus tios Edilson Moura e Ednara Moura.

Ao meu orientador, Maurício Rossato, pela dedicação, confiança e pelos valiosos conselhos que contribuíram de forma especial para o meu crescimento e amadurecimento ao longo desta jornada. Obrigado por ser um exemplo de profissional e ser humano.

Aos amigos e colegas do programa de Pós-graduação em Fitopatologia da UnB, em especial à equipe de pesquisa do Laboratório de Bacteriologia Vegetal: Luciellen, Angelica, Henrique e Julieth, pela parceria, auxílio, troca de experiências e convívio enriquecedor.

Aos meus amigos, Erivaldo e Izaías, pela amizade, apoio e companheirismo indispensáveis ao longo de toda essa trajetória. Vocês tornaram essa jornada mais leve e agradável.

A todos os professores do Programa de Fitopatologia da Universidade de Brasília, pela contribuição valiosa à minha formação.

À Coordenação de Aperfeiçoamento de Pessoal de Nível Superior (CAPES), pelo apoio financeiro por meio da bolsa de doutorado.

À Fundação de Apoio à Pesquisa do Distrito Federal (FAP-DF), por financiar o presente projeto de pesquisa.

Ao Programa de Pós-Graduação em Fitopatologia da Universidade de Brasília (PPG-FIT), pelo suporte acadêmico e pela oportunidade de desenvolvimento científico.

Trabalho realizado junto ao Departamento de Fitopatologia do Instituto de Ciências Biológicas da Universidade de Brasília, sob orientação do Dr. Prof. Maurício Rossato. Apoio Coordenação de Aperfeiçoamento de Pessoal de Nível Superior (CAPES) e da Fundação de Apoio à Pesquisa do Distrito Federal (FAPDF).

***Xanthomonas phaseoli* pv. *manihotis*: avaliação de genótipos de mandioca quanto à resistência e desenvolvimento de novos métodos de detecção**

**Ian Carlos Bispo de Carvalho**

TESE APROVADA em 27 /01/2024 por:

---

Dr. Jayme Garcia Arnal Barbedo – Embrapa Agricultura Digital  
Examinador

---

Profº. Dr. Everaldo Antônio Lopes - Universidade Federal de Viçosa - UFV  
Examinador

---

Prof.<sup>a</sup> Dra. Marisa Alvares da Silva Velloso Ferreira – Universidade de Brasília - UnB  
Examinadora

---

Prof<sup>a</sup>. Dra. Thaís Ribeiro Santiago – Universidade de Brasília - UnB  
Examinadora

---

Profº. Dr. Maurício Rossato  
Orientador (Presidente)

BRASÍLIA – DF

2025

## SUMÁRIO

<b>LISTA DE FIGURAS .....</b>	<b>X</b>
<b>LISTA DE TABELAS.....</b>	<b>XIII</b>
<b>RESUMO GERAL .....</b>	<b>XIV</b>
<b>GENERAL ABSTRACT .....</b>	<b>XVI</b>
<b>INTRODUÇÃO GERAL.....</b>	<b>18</b>
Objetivos .....	20
Objetivo geral .....	20
Objetivos específicos.....	20
<b>CAPÍTULO 1.....</b>	<b>21</b>
<b>REVISÃO DE LITERATURA.....</b>	<b>21</b>
1. Origem, taxonomia e importância da cultura da mandioca.....	22
2. A bacteriose da mandioca .....	24
2.1. Etiologia.....	24
2.2. Ecologia do patógeno e ciclo da doença.....	26
2.3. Sintomatologia .....	28
2.4. Distribuição geográfica e diversidade genética do patógeno .....	29
3. Manejo da doença e resistência genética .....	31
4. Métodos moleculares para detecção da bactéria .....	33
4.1. Loop-mediated isothermal amplification - LAMP .....	34
4.2. Análises dos produtos do LAMP .....	35
5. Emprego de sensores na detecção de alterações fisiológicas em plantas infectadas por fitopatógenos .....	38
6. Aplicação de aprendizado de máquina no processamento de dados hiperespectrais .....	39
<b>REFERÊNCIAS .....</b>	<b>41</b>
<b>CAPÍTULO 2.....</b>	<b>53</b>
<b>Colorimetric lamp assay for detection of <i>Xanthomonas phaseoli</i> pv. <i>manihotis</i> in cassava through genomics: a new approach to an old problem.....</b>	<b>53</b>
Introduction .....	56
Material and Methods.....	57
Genomic region selection and LAMP primer design .....	57
Bacterial isolates, culture conditions, and DNA extraction .....	59
LAMP assay .....	62
Specificity and sensitivity tests .....	62
Detection in cassava leaves with Xpm by LAMP assay and sample preheating.....	63
Results .....	64
Genomic region selection and LAMP primer design .....	64
LAMP assay optimization.....	64

Sensitivity and specificity of LAMP assay.....	65
Detection in cassava leaves infected with Xpm by LAMP assay .....	69
Discussion.....	72
References .....	74
Supplementary material .....	79
CAPÍTULO 3.....	84
Resistance classification to bacterial blight ( <i>Xanthomonas phaseoli</i> pv. <i>manihotis</i> ) in cultivars, clones and accessions of Brazilian cassava ( <i>Manihot esculenta</i> ) based on a new qualitative ordinal scale .....	84
Introduction .....	87
Material and methods .....	88
Results .....	91
Discussion.....	96
References .....	99
Supplementary material .....	104
CAPÍTULO 4.....	105
Hyperspectral imaging and machine learning for detecting physiological changes in cassava caused by <i>Xanthomonas phaseoli</i> pv. <i>manihotis</i> .....	105
Introduction .....	108
Material and methods .....	109
Xpm inoculation on cassava plants.....	109
Image capture .....	110
Hyperspectral image processing .....	111
Discriminant Spectral Parameters.....	112
Data analysis .....	112
Classification Methods .....	113
Hyperparameter optimization.....	115
Model validation.....	115
Results .....	116
Model performance .....	116
Spectral reflectance characterization .....	119
Discussion.....	120
References .....	124
CONCLUSÕES GERAIS .....	130

## LISTA DE FIGURAS

### CAPÍTULO 1- REVISÃO DE LITERATURA

<b>Figura 1.</b> Maiores produtores de mandioca fresca do mundo (FAOSTAT 2024).....	22
<b>Figura 2.</b> Principais estados produtores de mandioca do Brasil (IBGE 2024).....	23
<b>Figura 3.</b> Representação esquemática do ciclo da doença causada por <i>Xanthomonas phaseoli</i> pv. <i>manihotis</i> , ilustrando as etapas de infecção, colonização, disseminação e sobrevivência do fitopatógeno (Adaptado de Zárate-Chaves et al., 2021).....	27
<b>Figura 4.</b> Sintomatologia da doença causada por <i>Xanthomonas phaseoli</i> pv. <i>manihotis</i> , ilustrando os principais sintomas visíveis em folhas, hastes e outras partes da planta. A imagem destaca manifestações típicas da doença, incluindo lesões, murcha e necrose. (A) lesões foliares do tipo anasarca; (B) necrose em folhas; (C) necrose no caule; (D) exsudação gomosa no caule; (E) murcha das folhas; e (F) murcha do caule.....	28
<b>Figura 5.</b> Representação da distribuição mundial de <i>Xanthomonas phaseoli</i> pv. <i>manihotis</i> , destacando as áreas de ocorrência registradas (Adaptado de Zárate-Chaves et al., 2021).....	31

### CAPÍTULO 2 - COLORIMETRIC LAMP ASSAY FOR DETECTION OF *Xanthomonas phaseoli* pv. *manihotis* IN CASSAVA THROUGH GENOMICS: A NEW APPROACH TO AN OLD PROBLEM

<b>Figure 1.</b> Schematic representation of the position and sequence of the designed LAMP primer set Xpm_Lp1 within the nucleotide sequence.....	59
<b>Figure 2.</b> LAMP assay using different primer proportions (4:1 / 8:1) of primer set Xpm_Lp1 at different time intervals with the DNA of the type strain of <i>Xanthomonas phaseoli</i> pv. <i>manihotis</i> , IBSBF 278. The DNA amplification product was visualized by color change of the pH indicator dye (left) and by agarose gel electrophoresis (right). M: DNA Ladder 1 kb Plus (Invitrogen), NC: Negative control.....	65
<b>Figure 3.</b> Sensitivity of the LAMP primer set Xpm_Lp1 using different dilutions of the genomic DNA of the type strain of <i>Xanthomonas phaseoli</i> pv. <i>manihotis</i> , IBSBF 278, ranging from 10 ng ( $10^7$ fg) to 1 fg. The DNA amplification product was visualized by color change of the pH indicator dye (top) and by agarose gel electrophoresis (bottom). M: DNA Ladder 1 kb Plus (Invitrogen), NC: Negative control.....	67
<b>Figure 4.</b> Evaluation of the LAMP assays specificity with the primer set Xpm_Lp1. A) LAMP assays are able to detect Xpm isolates from the plant bacteriology collection at UnB. B) LAMP assays do not detect other pathovars or species. Xcm: <i>Xanthomonas citri</i> pv. <i>malvacearum</i> , Xc:	

*Xanthomonas citri*, Xea: *Xanthomonas euvesicatoria* pv. *allii*, Xep: *Xanthomonas euvesicatoria* pv. *perforans*, Xhg: *Xanthomonas hortorum* pv. *gardneri*, Rsol: *Ralstonia solanacearum*, Cff: *Curtobacterium flaccumfaciens* pv. *flaccumfaciens*, Pto: *Pseudomonas syringae* pv. *tomato*. Type strain (IBSBF 278) was used as a positive control. The DNA amplification product was visualized by observing the change in color of the pH indicator dye (top) and by agarose gel electrophoresis (bottom). M: DNA Ladder 1 kb Plus (Invitrogen), NC: Negative control.....68

**Figure 5.** Effect of pre-heating treatment for LAMP assay with primers Xpm\_Lp1 for detection of *Xanthomonas phaseoli* pv. *manihotis* (Xpm) in inoculated with strain UnB 17 and non-inoculated cassava leaves. The DNA amplification product was visualized by observing the change in color of the pH indicator dye. Xpm type strain (IBSBF\_278) was used as positive control. NC: Negative control.....70

**Figure 6.** LAMP assay with primer set Xpm\_Lp1 for detection of *Xanthomonas phaseoli* pv. *manihotis* (Xpm) in naturally infected cassava leaves collected from four cassava production fields. DNA from Xpm type strain (IBSBF 278) was used as positive control. The DNA amplification product was visualized by observing the change in color of the pH indicator dye (top) and by agarose gel electrophoresis (bottom). M: DNA Ladder 1 kb Plus (Invitrogen), NC: Negative control.....71

**Figure S1.** Multiplex nested-PCR with primers by Bernal-Galeano et al. (2018) to assess the concentration limit of detection using a genomic DNA dilution of *Xanthomonas phaseoli* pv. *manihotis* type strain IBSBF 278 ranging from 10 ng ( $10^7$  fg) to 1 fg. M: DNA Ladder 1 kb Plus (Invitrogen), NC: Negative control.....83

### **CAPÍTULO 3 - RESISTANCE CLASSIFICATION TO BACTERIAL BLIGHT (*Xanthomonas phaseoli* pv. *manihotis*) IN CULTIVARS, CLONES AND ACCESSIONS OF BRAZILIAN CASSAVA (*Manihot esculenta*) BASED ON A NEW QUALITATIVE ORDINAL SCALE**

**Figure 1.** Clustering of cassava genotypes assessed for resistance to CBB in the first (A) and second (B) trials using the area under the disease progress curve .....92

**Figure 2.** Response of different cassava genotypes to CBB in the first (A) and second (B) trials, assessed using three parameters: final score, disease index (%), and AUDPC (Area Under the Disease Progress Curve).....93

**Figure 3.** Disease progress curve of CBB in the first (A) and second (B) trials. MR, moderately resistant; MS, moderately susceptible; S, susceptible .....96

**CAPÍTULO 4 - HYPERSPECTRAL IMAGING AND MACHINE LEARNING FOR  
DETECTING PHYSIOLOGICAL CHANGES IN CASSAVA CAUSED BY  
*Xanthomonas phaseoli* pv. *manihotis***

<b>Figure 1.</b> Schematic representation and setup of a benchtop hyperspectral imaging system for cassava leaf analysis. (A) Diagram of the hyperspectral imaging system components, including the FX10e camera, halogen lamps for illumination, and a motorized translation stage for sample movement. (B) Practical setup capturing cassava leaf samples under halogen lamp illumination.....	111
<b>Figure 2.</b> Workflow of the image classification process, including data collection, processing, hyperparameter optimization, training, testing, and performance evaluation.....	113
<b>Figure 3.</b> Balanced accuracy results of classification methods differentiating healthy cassava leaves from those infected with <i>Xpm</i> . K-Nearest Neighbors (KNN); Decision Tree (DT); Random Forest (RF); Extreme Gradient Boosting (XGBoost); Multi-Layer Perceptron (MLP); Support Vector Machine (SVM).....	118
<b>Figure 4.</b> Cassava leaves spectral reflectance characterization: normalized spectral reflectance curves (a); normalized sensitivity value (b); normalized spectral difference (c).....	120

## LISTA DE TABELAS

### **CAPÍTULO 2 - COLORIMETRIC LAMP ASSAY FOR DETECTION OF *Xanthomonas phaseoli* pv. *manihotis* IN CASSAVA THROUGH GENOMICS: A NEW APPROACH TO AN OLD PROBLEM**

<b>Table 1.</b> Set of Xpm_Lp1 LAMP primers designed for <i>Xanthomonas phaseoli</i> pv. <i>manihotis</i> and their sequences.....	58
<b>Table 2.</b> Bacterial isolates used to validate the specificity and sensitivity of the LAMP assay for detection of <i>Xanthomonas phaseoli</i> pv. <i>manihotis</i> .....	61
<b>Table S1.</b> List of bacterial species, pathovars and isolate names used on the comparative genomics for the selection of regions for LAMP primer design.....	79

### **CAPÍTULO 3 - RESISTANCE CLASSIFICATION TO BACTERIAL BLIGHT (*Xanthomonas phaseoli* pv. *manihotis*) IN CULTIVARS, CLONES AND ACCESSIONS OF BRAZILIAN CASSAVA (*Manihot esculenta*) BASED ON A NEW QUALITATIVE ORDINAL SCALE**

<b>Table 1.</b> Cassava genotypes evaluated for resistance to <i>Xanthomonas phaseoli</i> pv. <i>manihotis</i> .....	89
<b>Table 2.</b> Classification of resistance levels of cassava genotypes in the first and second trials.....	94

### **CAPÍTULO 4 - HYPERSPECTRAL IMAGING AND MACHINE LEARNING FOR DETECTING PHYSIOLOGICAL CHANGES IN CASSAVA CAUSED BY *Xanthomonas phaseoli* pv. *manihotis***

<b>Table 1.</b> Result of the performance evaluation metrics of the models on the test set.....	118
-------------------------------------------------------------------------------------------------	-----

## RESUMO GERAL

CARVALHO, Ian Carlos Bispo. *Xanthomonas phaseoli* pv. *manihotis*: avaliação de genótipos de mandioca quanto à resistência e desenvolvimento de novos métodos de detecção. Universidade de Brasília, Brasília, DF, Brasil. 2025. 131p. Doutorado em Fitopatologia\*

A cultura da mandioca desempenha papel de grande relevância econômica e social, sendo amplamente cultivada devido à robustez e à capacidade da planta de tolerar estresses hídricos. No entanto, a produção está sujeita a adversidades que podem comprometer seu potencial produtivo, destacando-se a bacteriose da mandioca, causada por *Xanthomonas phaseoli* pv. *manihotis* (Xpm). Essa doença é uma séria ameaça à produção nacional de mandioca, sendo uma das mais importantes da cultura e figurando entre as dez principais bacterioses globais em termos científicos e econômicos. Diante desse cenário, o presente estudo tem como objetivo aprofundar o conhecimento sobre a bacteriose da mandioca por meio do desenvolvimento de métodos sensíveis de detecção baseados na amplificação isotérmica mediada por loop (*Loop-Mediated Isothermal Amplification – LAMP*) e em imagens hiperpectrais (*Hyperspectral Imaging - HSI*) combinadas com aprendizado de máquina, além de avaliar a resistência de genótipos de mandioca à bacteriose. Os genótipos avaliados pertencem ao banco de germoplasma da UnB e da EMBRAPA Cerrados. Para os testes, foram utilizados isolados da coleção do Laboratório de Bacteriologia Vegetal e novos isolados foram obtidos em áreas produtoras de mandioca em diferentes regiões do país. Os DNAs de todos os isolados foram extraídos e quantificados. A partir da análise comparativa dos genomas de Xpm e outras espécies do gênero *Xanthomonas*, foram desenhados primers específicos para detecção por LAMP. Além disso, imagens hiperpectrais de folhas sadias e infectadas foram utilizadas para o treinamento e teste de seis modelos de aprendizado de máquina: Decision Tree (DT), Random

---

\* Orientador: Prof. Dr. Maurício Rossato, Universidade de Brasília - UnB

Forest (RF), Support Vector Machine (SVM), K-Nearest Neighbors (KNN), Extreme Gradient Boosting (XGBoost) e Multi-Layer Perceptron (MLP). Para a avaliação da resistência de 11 genótipos de mandioca, as plantas foram cultivadas em casa de vegetação e inoculadas com o isolado de Xpm UnB 17 e submetidas a avaliações periódicas da severidade e do índice da doença. O teste LAMP desenvolvido neste estudo demonstrou alta sensibilidade, detectando até 100 fg de DNA do isolado tipo (IBSBF 278), e alta especificidade, sem reações cruzadas com outras espécies bacterianas ou patovares, amplificando apenas isolados de Xpm. O método foi eficiente para detectar Xpm em folhas de mandioca infectadas e maceradas, sem necessidade de tratamento adicional das amostras, sendo adequado para monitoramento da doença em laboratório e campo. A avaliação da resistência de genótipos de mandioca revelou três grupos: moderadamente resistentes, moderadamente suscetíveis e suscetíveis, com base na escala de severidade e na Área Abaixo da Curva de Progresso da Doença (AUDPC). Nenhum genótipo foi classificado como resistente, destacando a importância de múltiplos ensaios sob diferentes condições ambientais para compreender melhor o comportamento dos genótipos. Na análise por imagens hiperespectrais, o SVM obteve o melhor desempenho, com 91,41% de acurácia e AUC-ROC de 0,9684, seguido por MLP (87,5%), RF (76,56%) e XGBoost (80,08%). KNN e DT tiveram os piores resultados, com acurárias de 70,31% e 71,88%, respectivamente. Esses resultados indicam que o HSI combinado com SVM é um método rápido e preciso para diagnosticar a bacteriose da mandioca, com potencial para aplicações em larga escala. Pesquisas futuras podem melhorar o desempenho dos modelos e explorar alternativas mais econômicas.

**Palavras chaves:** *Manihot esculenta*, LAMP, imagens hiperespectrais, aprendizado de máquina

## GENERAL ABSTRACT

CARVALHO, Ian Carlos Bispo. *Xanthomonas phaseoli* pv. *manihotis*: Evaluation of Cassava Genotypes for Resistance and Development of New Detection Methods.

Universidade de Brasília, Brasília, DF, Brasil. 2025. 131p. Doctorate in Plant Pathology\*

The cassava crop plays a significant economic and social role, being widely cultivated due to its robustness and ability to tolerate water stress. However, production is subject to adversities that can compromise its productive potential, with cassava bacterial blight (CBB), caused by *Xanthomonas phaseoli* pv. *manihotis* (Xpm), being a major concern. This disease poses a serious threat to cassava production in Brazil, ranking among the most important diseases of the crop and one of the top ten bacterial plant diseases globally in scientific and economic terms. In this context, the present study aims to deepen the understanding of cassava bacterial blight through the development of sensitive detection methods based on Loop-Mediated Isothermal Amplification (LAMP) and Hyperspectral Imaging (HSI) combined with machine learning, as well as evaluating the resistance of cassava genotypes to the disease. The evaluated genotypes belong to the germplasm bank of the University of Brasília (UnB) and EMBRAPA Cerrados. For testing, bacterial isolates from the Plant Bacteriology Laboratory's collection were used, and new isolates were obtained from cassava-producing regions across different areas of the country. The DNA of all isolates was extracted and quantified. Through comparative genome analysis of Xpm and other species of the *Xanthomonas* genus, specific primers were designed for LAMP detection. Additionally, hyperspectral images of healthy and infected leaves were used to train and test six machine learning models: Decision Tree (DT), Random Forest (RF), Support Vector Machine (SVM), K-Nearest Neighbors (KNN), Extreme Gradient Boosting (XGBoost), and Multi-Layer Perceptron (MLP). To evaluate the resistance of 11 cassava genotypes, plants were grown in a greenhouse, inoculated with the Xpm isolate UnB 17, and

---

\* Advisor: Prof. Dr. Maurício Rossato, Universidade de Brasília - UnB

subjected to periodic assessments of disease severity and index. The LAMP test developed in this study demonstrated high sensitivity, detecting as little as 100 fg of DNA from the reference isolate (IBSBF 278), and high specificity, with no cross-reactions with other bacterial species or pathovars, amplifying only Xpm isolates. The method effectively detected Xpm in infected and macerated cassava leaves without requiring additional sample processing, making it suitable for disease monitoring in both laboratory and field conditions. The evaluation of cassava genotype resistance revealed three groups: moderately resistant, moderately susceptible, and susceptible, based on severity scales and the Area Under the Disease Progress Curve (AUDPC). No genotype was classified as resistant, highlighting the importance of multiple trials under different environmental conditions to better understand genotype behavior. In hyperspectral image analysis, the SVM model achieved the best performance, with 91.41% accuracy and an AUC-ROC of 0.9684, followed by MLP (87.5%), RF (76.56%), and XGBoost (80.08%). KNN and DT had the lowest results, with accuracies of 70.31% and 71.88%, respectively. These findings indicate that HSI combined with SVM is a fast and accurate method for diagnosing cassava bacterial blight, with potential for large-scale applications. Future research can improve model performance and explore more cost-effective alternatives.

**Keywords:** *Manihot esculenta*, LAMP, hyperspectral Imaging, machine learning

## INTRODUÇÃO GERAL

A mandiocultura é uma atividade de grande valor econômico e social, predominantemente desenvolvida por pequenos agricultores, contribuindo para a redução do êxodo rural e a fixação da população no campo. Isso se deve à sua robustez, menor demanda por insumos em comparação com culturas como soja e milho e maior tolerância à escassez hídrica (Parmar et al. 2017; Olarinde et al. 2020; Santos et al. 2020). Apesar de sua relevância, a cultura da mandioca pode ser suscetível a fatores que podem comprometer sua produtividade e rentabilidade, a exemplo de doenças.

Entre os patógenos que afetam a mandioca, destaca-se a *Xanthomonas phaseoli* pv. *manihotis*, agente causal da bacteriose da mandioca. Essa bactéria possui ampla distribuição geográfica, estando presente em 50 países (CABI 2023; Taylor et al. 2017; Zárate-Chaves et al. 2024). As plantas infectadas apresentam manchas translúcidas e encharcadas nas folhas, que evoluem para manchas necróticas, podendo levar à murcha foliar em infecções sistêmicas. A disseminação da bactéria a longas distâncias ocorre principalmente por material propagativo infectado (Elango e Lozano 1980; Verdier et al. 2012), além de sua capacidade de sobrevivência em plantas daninhas (Elango e Lozano 1981; Fanou et al. 2017).

Para um manejo eficiente, métodos moleculares de detecção são cruciais. Protocolos baseados em PCR (*Polymerase Chain Reaction*) foram desenvolvidos com sucesso (Verdier et al. 1998; Ojeda e Verdier 2000; Bernal-Galeano 2018; Flores et al. 2019; Cerqueira-Melo et al. 2019), embora sejam considerados mais caros e trabalhosos do que métodos como a amplificação isotérmica mediada por loop (LAMP) (Panno et al. 2020). Além disso, estratégias baseadas em resistência genética também são fundamentais, mas genótipos resistentes à bacteriose da mandioca ainda são escassos (Teixeira et al. 2021; Aquiles et al. 2021). Essa limitação é atribuída à diversidade genética do patógeno e sua rápida adaptação local (Oliveira et al. 2023).

O sucesso de uma lavoura depende da antecipação e mitigação de estresse biótico como doenças de plantas, tornando essencial o desenvolvimento de tecnologias rápidas e precisas, como o sensoriamento remoto (Ang e Lew 2022). Os sensores ópticos capturam variações espectrais de 350 a 2500 nm causadas por estressores abióticos e bióticos, permitindo diagnósticos mais eficientes (Oerke 2020; Yang 2010; Zhang et al. 2019).

Algoritmos de aprendizado de máquina têm revolucionado a análise de dados espectrais, permitindo reconhecer e classificar doenças com rapidez e precisão. Estudos mostram aplicações bem-sucedidas para identificar doenças bacterianas como a mancha bacteriana do tomateiro (Abdulridha et al. 2020), a murcha bacteriana do amendoim (Chen et al. 2020), e o fogo bacteriano da macieira (Skoneczny et al. 2020) e doenças fúngicas como a pinta-preta da batata (Van De Vijver et al. 2020). A combinação de imagens hiperespectrais e aprendizado de máquina pode alcançar valores em torno de 90% de acurácia em diagnósticos complexos (Li et al. 2012; Nagasubramanian et al. 2019).

Neste contexto, este estudo busca ampliar a compreensão do patossistema Xpm-mandioca, focando no desenvolvimento de métodos práticos de detecção do patógeno, aplicação de dados hiperespectrais e aprendizado de máquina para diagnosticar alterações fisiológicas e avaliação da resistência em genótipos de mandioca. Os resultados poderão auxiliar produtores na prevenção do plantio de material infectado e na celeridade da tomada de decisões de controle.

## **Objetivos**

### **Objetivo geral**

Desenvolver métodos rápidos e eficazes para a detecção do patógeno e das alterações fisiológicas causadas por *Xanthomonas phaseoli* pv. *manihotis* em plantas de mandioca, além de avaliar a resistência de diferentes genótipos de mandioca do banco de germoplasma da Embrapa Cerrados.

### **Objetivos específicos**

- Desenvolver um método molecular baseado na amplificação isotérmica LAMP, utilizando *primers* específicos para a detecção de *Xanthomonas phaseoli* pv. *manihotis* em material vegetal;
- Identificar genótipos de mandioca com potencial para programas de melhoramento genético, focando na resistência à bacteriose da mandioca;
- Avaliar o uso de imagens hiperespectrais associadas ao aprendizado de máquina para a detecção de alterações fisiológicas causadas por *Xanthomonas phaseoli* pv. *manihotis* em plantas de mandioca.

# **CAPÍTULO 1**

---

---

## **REVISÃO DE LITERATURA**

## REVISÃO DE LITERATURA

### 1. Origem, taxonomia e importância da cultura da mandioca

A mandioca (*Manihot esculenta* Crantz), juntamente com o milho, cana-de-açúcar e arroz constitui-se como a mais importante fonte de carboidratos nas regiões tropicais, sendo considerado um alimento básico para mais de 800 milhões de pessoas em todo o mundo (Burns et al., 2010; Nassar et al., 2012). Em termos botânicos, a mandioca faz parte da família Euphorbiaceae e tem seu centro de origem na América do Sul, nas planícies tropicais ao longo da fronteira sul bacia amazônica (Olsen e Schaal 1999; Wang et al. 2014).

O Brasil é o quinto maior produtor de mandioca do mundo com uma produção de 18.514.317 toneladas, atrás apenas da Nigéria, República Democrática do Congo, Tailândia e Gana (Figura 1) (FAO, 2023). No Brasil, os principais estados produtores de mandioca são Pará, Paraná, São Paulo, Mato Grosso do Sul, Amazonas, Bahia e Ceará (Figura 2) (IBGE, 2023).

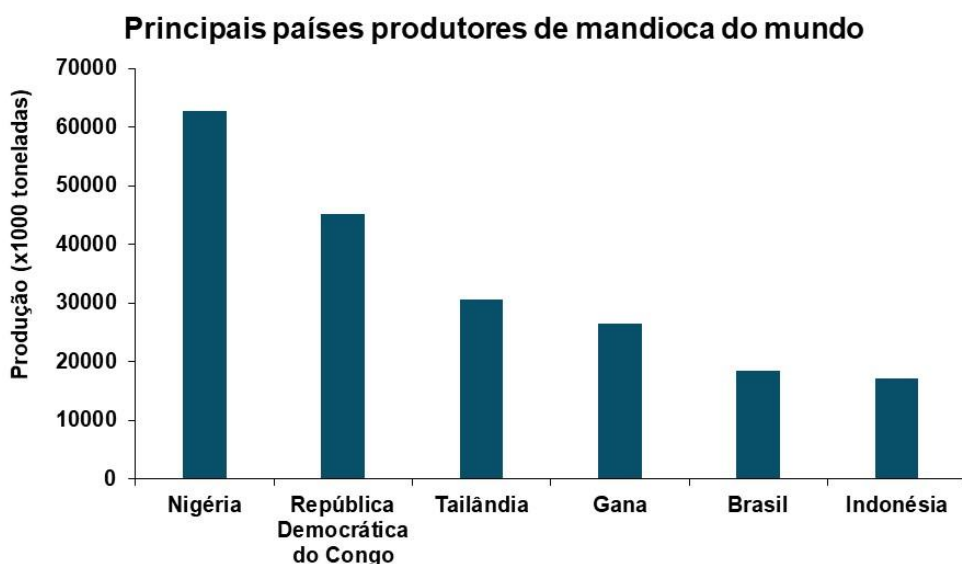


**Figura 1.** Maiores produtores de mandioca do mundo (FAOSTAT 2023).

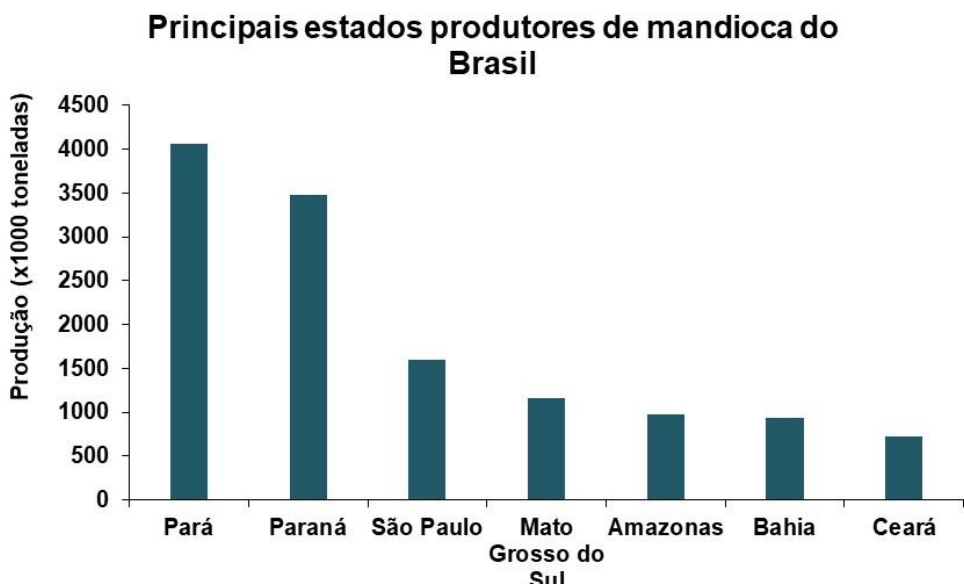


**Figura 2.** Principais estados produtores de mandioca do Brasil (IBGE 2023).

A mandiocultura é considerada uma atividade de grande valor econômico e social, pois em sua maioria é desenvolvida por pequenos agricultores, além de apresentar grande robustez, maior tolerância à seca e menor necessidade de insumos quando comparada com outras espécies cultivadas (Parmar et al. 2017; Olarinde et al. 2020; Santos et al. 2020). Apesar do grande potencial da cultura, como qualquer planta de interesse agronômico, a presença de doenças pode limitar o seu cultivo quando não manejadas adequadamente.

Em uma perspectiva histórica, o cultivo e uso da mandioca para consumo humano no Brasil está associado à cultura indígena do país e remonta o período da colonização portuguesa (Silva et al., 2016). Outrora considerada o “alimento dos pobres”, a mandioca tem emergido como uma cultura polivalente para o século 21, que responde às prioridades dos países em desenvolvimento, às tendências da economia global e aos desafios das mudanças climáticas (FAO, 2018). Nas regiões Norte e Nordeste do país, a tuberosa é amplamente utilizada para a alimentação, sendo consumida in natura, mas também há forte predomínio da indústria, principalmente a de farinha (Felipe et al., 2010).

Apesar de sua relevância nos aspectos econômicos e social, a cultura da mandioca pode ser suscetível a fatores que podem comprometer sua produtividade e rentabilidade, com destaque para as doenças.

## 2. A bacteriose da mandioca

### 2.1. Etiologia

A bacteriose da mandioca causada pela bactéria *Xanthomonas phaseoli* pv. *manihotis* (Xpm) foi registrada pela primeira vez no Brasil em 1912 pelo pesquisador Gregório Bondar, sendo relatada posteriormente em outras partes do mundo (Manicom et al. 1981; Wonni et al. 2015; Kante et al. 2020). À época, a bactéria recebeu a denominação de *Bacillus manihotus* (Bondar, 1912), sendo em seguida renomeada como *Bacillus manihotis* (Berthet e Bondar, 1915). Desde o seu primeiro relato, a nomenclatura e a taxonomia do agente etiológico da bacteriose da mandioca sofreram uma série de alterações no decorrer dos anos (Lozano e Booth 1974; Maraite e Meyer 1975; Vauterin et al. 1995).

Em períodos mais recentes, com o avanço das técnicas moleculares, houve alterações na classificação taxonômica do agente causal da bacteriose da cultura da mandioca. A primeira delas foi realizada com base em testes de hibridização DNA-DNA e atividade metabólica envolvendo substratos de carbono, a bactéria foi classificada anteriormente como *Xanthomonas axonopodis* pv. *manihotis* (Vauterin et al. 1995). A segunda, e atual, foi um estudo de comparação entre sequencias de sete genes *housekeeping* (*atpD*, *dnaK*, *efp*, *glnA*, *gyrB*, *lrp*, *rpoD*), hibridização DNA-DNA e identidade média de nucleotídeos (*Average Nucleotide Identity* - ANI) utilizando o genoma completo de diferentes isolados permitiram reclassificá-la como *Xanthomonas phaseoli* pv. *manihotis* (Constantin et al. 2016).

De acordo com o List of Prokaryotic names with Standing in Nomenclature (LPSN), a *Xanthomonas phaseoli* pv. *manihotis* é classificada taxonomicamente da seguinte forma: domínio bactéria; filo *Pseudomonadota*; classe *Gammaproteobacteria*; ordem *Lysobacteriales*;

família *Lysobacteraceae*; gênero *Xanthomonas*; espécie *Xanthomonas phaseoli* pv. *manihotis*. Essa nova classificação contempla as mudanças na ordem e família da Xpm, que anteriormente era *Xanthomonadales* e *Xanthomonadaceae*, respectivamente. Essa alteração se deu em função de um estudo baseado em sequências 16 S rRNA e análise filogenômica envolvendo genomas de 92 isolados tipos de diversas espécies de bactérias, que demonstrou que o gênero *Xanthomonas* estava inserido na ordem *Lysobacterales* e na família *Lysobacteraceae* (Kumar et al. 2019).

Devido à sua importância científica e econômica, esse patógeno foi considerado uma das principais bactérias fitopatogênicas (Mansfield et al. 2012). O impacto da doença em termos de produção pode variar a depender das condições ambientais, com variações entre 30% e 90%, com pico de incidência entre 60% e 70%. Além disso, considera-se que as perdas podem chegar até 100% em dois ou três ciclos da cultura, caso medidas de manejo adequadas não sejam adotadas (Mansfield et al. 2012; Zárate-Chaves et al. 2021).

A *Xpm* é uma bactéria gram-negativa, aeróbica obrigatória, em formato de bastonete, móvel e com flagelos polares, apresentando colônias convexas e mucilaginosas, lisas e brilhantes (Ogunjobi et al., 2008). Diferentemente de outras bactérias do gênero *Xanthomonas*, a *Xpm* não sintetiza a xantomonadina, que é o pigmento que confere às colônias a coloração amarela típica. Deste modo, as colônias de Xpm possuem uma coloração esbranquiçada (Van Den Mooter et al. 1987; Chege et al. 2017).

Um exame do cluster de xantomonadina no genoma do isolado CIO151 de Xpm revelou que os genes de biossíntese de xantomonadina eram funcionais, mas apenas um gene que codifica a proteína transportadora acil desidratase havia sido interrompido. De acordo com os autores, isso se deve a um *frameshift* na posição 110, o que resultou em uma proteína de 50 aminoácidos em vez dos 95 aminoácidos previstos (Arrieta-Ortiz et al. 2013). Existem relatos de que esta proteína possui uma função crucial na coloração amarelada típica das colônias em *Xanthomonas oryzae* pv. *oryzae* (Goel et al. 2002; He et al. 2020).

## **2.2. Ecologia do patógeno e ciclo da doença**

A Xpm pode apresentar duas fases distintas no campo: epifítica e parasitária (Figura 3).

Na fase epifítica, as células bacterianas crescem na superfície foliar das plantas de mandioca, em um estágio pré-infecção. Essa etapa é crucial para a manutenção do inóculo no ambiente durante a estação de cultivo e para a sua sobrevivência entre estações de cultivo (Elango e Lozano 1981; Daniel et al. 1985; Fanou et al. 2017). Na fase parasitária, a bactéria penetra no tecido foliar através de aberturas naturais, como estômatos, ou por ferimentos. Uma vez nos espaços intercelulares do mesófilo, a bactéria se multiplica e inicia o processo de colonização dos tecidos da planta (Verdier et al. 1994). As condições ambientais são extremamente fundamentais para o crescimento da população bacteriana, de modo que durante o período vegetativo da mandioca, médias de temperaturas entre 25 e 29°C e umidade relativa entre 59 e 85% favorecem a rápida multiplicação da bactéria (Fanou et al. 2018).

A sobrevivência da Xpm em campo já foi relatada em plantas daninhas próximas ou dentro das áreas de cultivo (Elango e Lozano 1981). Inicialmente, acreditava-se que a sobrevivência da bactéria em plantas daninhas não grande importância (Daniel et al. 1985). Contudo, Fanou et al. (2017) demonstraram que, em condições de campo, a Xpm sobreviveu por até 30 dias, em concentrações moderadas, na superfície de *Brachiaria deflexa* (Poaceae), *Mariscus alternifolius* (Cyperaceae), *Pupalia lappacea* (Amaranthaceae) e *Solanum nigrum* (Solanaceae). Em outro experimento do mesmo estudo, realizado em casa de vegetação, as células bacterianas sobreviveram por até 60 dias em *Vernonia cinerea* (Asteraceae), *Dactyloctenium aegyptium* e *Brachiaria deflexa* infiltradas com Xpm. Já Yameogo et al. (2023) não detectaram a presença da Xpm na superfície foliar das diferentes espécies de plantas daninhas coletadas em cultivos de mandioca. No entanto, quando inocularam 21 espécies de plantas daninhas em condições controladas, os autores conseguiram isolar novamente a bactéria do tecido previamente infectado após duas semanas.

A principal forma de disseminação do patógeno a longas distâncias se dá através do plantio de material propagativo infectado. Adicionalmente, o intercâmbio de sementes infectadas, frequentemente usadas em programas de melhoramento, embora não sejam usadas necessariamente em cultivos convencionais, permite a transferência do patógeno entre países e continentes (Elango e Lozano 1980; Verdier et al. 2012). A ocorrência de populações viáveis e patogênicas da bactéria no interior de sementes já foi relatada (Daniel et al. 1985). Somado a isso, células bacterianas foram detectadas em sementes de mandioca armazenadas sob condições controladas, temperatura de 5°C e umidade relativa de 60%, por até 18 meses (Persley 1979). Ademais, a *Xpm* também é capaz de sobreviver em restos vegetais na superfície do solo por mais de 150 dias, o que depende das condições ambientais, especialmente de umidade presente nos resíduos (Fanou et al. 2017).

A princípio, especulava-se a possibilidade da ação de insetos na sobrevivência da *Xpm* (Daniel et al. 1985). Mas somente com os trabalhos desenvolvidos por Zandjanakou-Tachin et al. (2007) foi comprovada a capacidade da *Xpm* de sobreviver no trato digestivo da espécie de inseto *Zonocerus variegatus* por pelo menos 1 semana e pelo menos 5 semanas nas fezes desse inseto mantidas sob condições controladas.

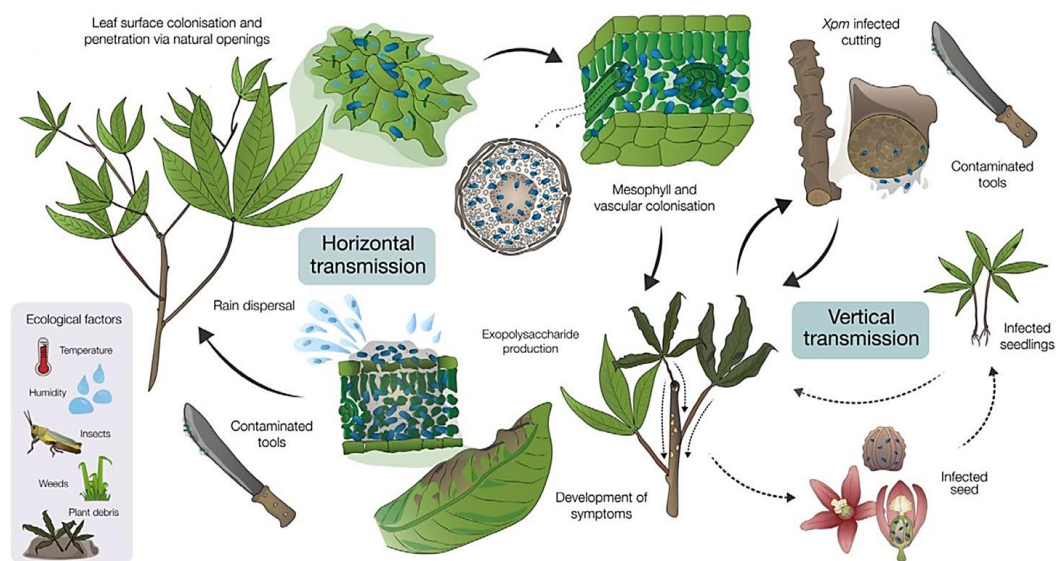


**Figura 3.** Representação esquemática do ciclo da doença causada por *Xanthomonas phaseoli* pv. *manihotis*, ilustrando as etapas de infecção, colonização, disseminação e sobrevivência do fitopatógeno (Adaptado de Zárate-Chaves et al. 2021).

### 2.3. Sintomatologia

O patógeno penetra os tecidos das folhas através de ferimentos na epiderme e/ou de aberturas naturais. Após alguns dias, surgem manchas translúcidas e encharcadas nas folhas, que aumentam e se coalescem, formando grandes manchas marrons (Figura 4). As bactérias se movem e se multiplicam por toda a planta, bloqueando o movimento da água e nutrientes no sistema vascular, o que induz a murchezza das folhas (Sandino et al. 2015; Rubio et al. 2017; Kante et al. 2020).

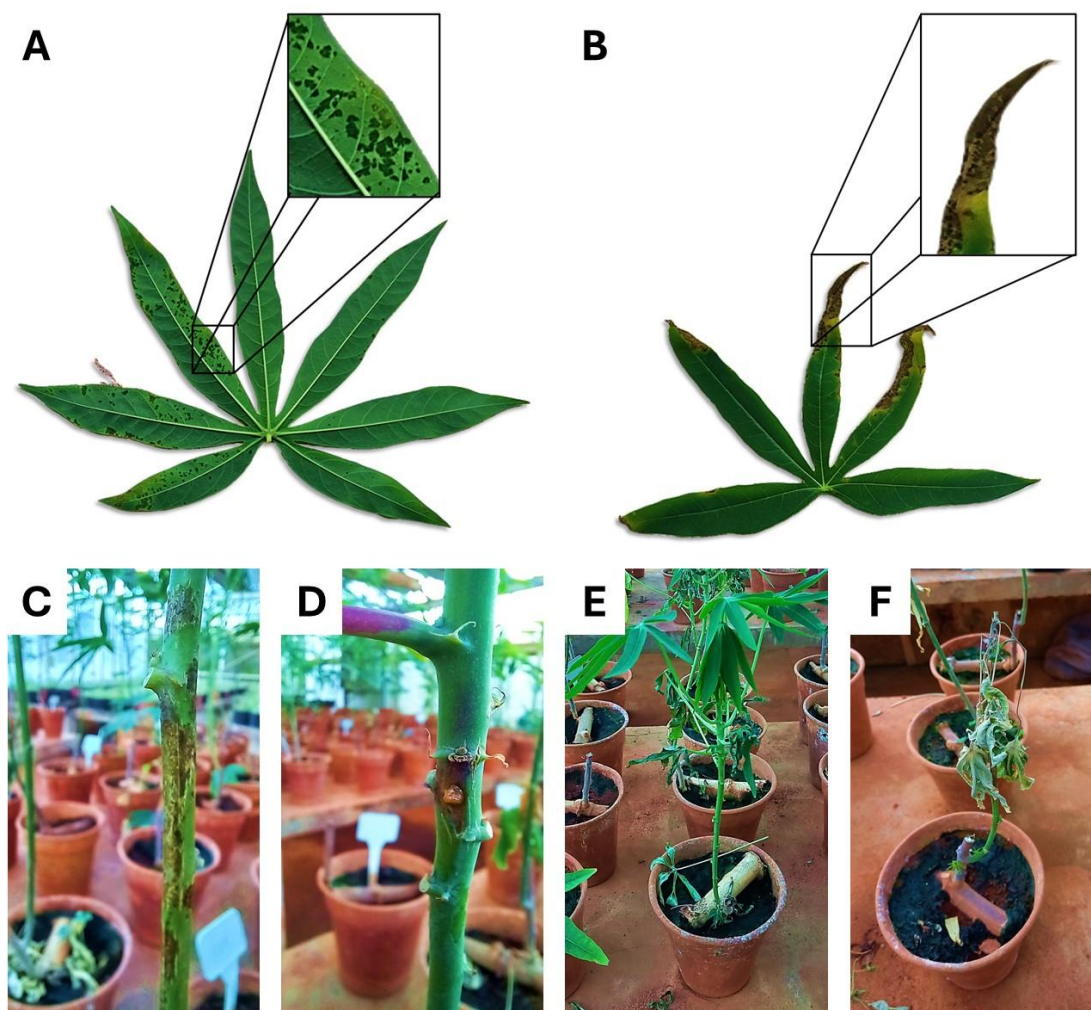


**Figura 4.** Sintomatologia da doença causada por *Xanthomonas phaseoli* pv. *manihotis*, ilustrando os principais sintomas visíveis em folhas, hastes e outras partes da planta. A imagem destaca manifestações típicas da doença, incluindo lesões, murcha e necrose em plantas inoculadas. (A) lesões foliares do tipo anasarca; (B) necrose em folhas; (C) necrose no caule; (D) exsudação gomosa no caule; (E) murcha das folhas; e (F) murcha da planta.

#### **2.4. Distribuição geográfica e diversidade genética do patógeno**

A Xpm apresenta uma ampla distribuição ao redor do mundo, estando presente nas Américas, Ásia, África e na Oceania (Figura 5). Até o momento, a Xpm foi relatada em 50 países (CABI 2023; Taylor et al. 2017; Zárate-Chaves et al. 2024).

O estudo da diversidade genética de fitopatógenos é indispensável para a compreensão da estrutura de populações de microrganismos (Rache et al., 2019). Além disso, esse conhecimento permite obter uma visão mais ampla de como os efeitos do manejo das culturas em cada agroecossistema pode influenciar as variações genéticas das espécies de bactérias fitopatogênicas (Chege et al. 2017).

Nesta perspectiva, a utilização de marcadores moleculares têm sido uma estratégia frequentemente utilizada para a caracterização genética e o estudo de populações de *Xpm* (Chege et al. 2017; Ogunjobi et al. 2006, 2007, 2010; Restrepo et al. 2000; Restrepo et al. 1999, 2004; Restrepo e Verdier, 1997; Trujillo et al. 2014; Verdier et al. 1993; Bart et al. 2012; Zárate-Chaves et al. 2021).

A utilização do *restriction fragment length polymorphism* (RFLP) no início dos anos de 1990 em 326 isolados de diferentes partes do mundo permitiu observar que os isolados obtidos da América do Sul eram heterogêneos, ao passo que os isolados da África não possuíam qualquer tipo de polimorfismo. O alto nível de diversidade observado nos isolados da América do Sul pode ser consequência da diversidade de genótipos do hospedeiro (Verdier et al. 1993).

Esses resultados foram corroborados com pesquisas subsequentes na Colômbia, uma vez que foi observada elevada diversidade genética em função da ampla gama de condições na qual a cultura da mandioca era cultivada, bem como da variedade de genótipos de mandioca utilizados (Restrepo et al. 2000; Restrepo et al. 1999; Restrepo e Verdier 1997). Em uma perspectiva temporal, constatou-se que existe a tendência de redução da diversidade genética no decorrer do tempo dentro de um mesmo campo de cultivo. Além disso, a migração do patógeno em material propagativo contaminado atua moldando a estrutura populacional da Xpm (Silvia Restrepo et al., 2004).

Na Nigéria, foi observada a existência de uma elevada diversidade genética entre os isolados de Xpm analisados, demonstrando que não existe uma homogeneidade genética (Ogunjobi et al. 2006, 2007, 2010), ao passo que no Quênia foi constatada uma baixa variabilidade genética entre os isolados, o que fornece indícios de que as populações de Xpm tenham evoluído a partir de um ponto de origem comum (Chege et al. 2017).

Recentemente, foi desenvolvido um sistema de marcadores microssatélites para essa espécie (Rache et al. 2019), que obteve maior acurácia, apresentando-se com uma abordagem capaz de fornecer informações úteis para a escolha de isolados a serem usados em *screenings* para resistência, além de fornecer dados da distribuição da diversidade do patógeno no país.

No Brasil, um levantamento utilizando os marcadores rep-PCR (BOX-PCR e ERIC-PCR) e *variable number of tandem repeats* (VNTRs) com o objetivo de avaliar a diversidade genética de oito populações de Xpm de cinco estados produtores foi realizado. Neste estudo, verificou-se que a diversidade genética poderia estar associada a alterações genéticas rápidas e à adaptação local do patógeno (Oliveira et al. 2023). Além disso, os autores destacaram que a introdução de variedades resistentes em cada região deve levar em consideração o grau de diversidade genética, a estrutura populacional e a agressividade do patógeno.

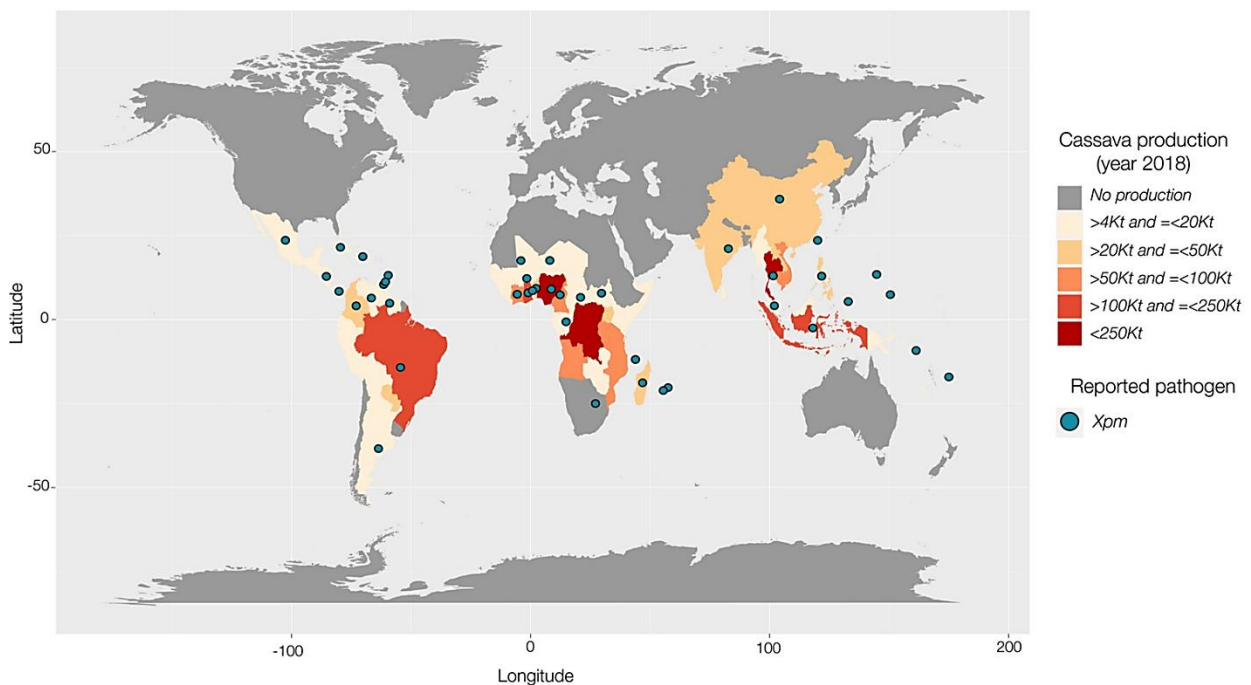


**Figura 5.** Representação da distribuição mundial de *Xanthomonas phaseoli* pv. *manihotis*, destacando as áreas de ocorrência registradas (Adaptado de Zárate-Chaves et al. 2021).

### 3. Manejo da doença e resistência genética

O manejo eficaz de doenças bacterianas em plantas requer um conhecimento aprofundado do patossistema. Isso permite identificar os períodos mais adequados para controlar as populações da bactéria fitopatogênica e determinar as fases em que os tecidos do hospedeiro apresentam maior suscetibilidade ao processo infeccioso (Sundin et al. 2016). Partindo desse princípio, a utilização conjunta de estratégias de manejo baseadas em práticas culturais, medidas sanitárias e resistência genética podem reduzir consideravelmente as perdas causadas pela doença a nível de campo (Lozano 1986; Zárate-Chaves et al. 2021).

O manejo cultural abrange práticas como a rotação de culturas, a eliminação de restos vegetais, o pousio e a eliminação de plantas daninhas. Essas técnicas desempenham um papel crucial na redução das fontes de inóculo para os cultivos subsequentes (Lozano 1986; Zárate-Chaves et al. 2021). Nesse sentido, a eliminação adequada dos restos vegetais e o manejo de plantas daninhas são essenciais para minimizar a presença de inóculo e prevenir infecções nos

cultivos futuros (Fanou et al. 2017). Em se tratando de medidas sanitárias, o uso de material propagativo sadio é essencial para evitar a introdução de inóculos de doenças em campos de cultivo de mandioca. Essa estratégia, fundamentada no princípio de controle conhecido como exclusão, tem como objetivo impedir a entrada da bactéria em áreas livres do patógeno.

Entre todas as estratégias de manejo, a resistência genética é considerada a mais eficaz, pois plantas resistentes possuem mecanismos capazes de inibir ou retardar o desenvolvimento do patógeno nos tecidos vegetais (Jones e Dangl 2006; Andersen et al. 2018). Essa abordagem é, portanto, fundamental no conjunto de estratégias de manejo dessa bacteriose. De maneira geral, a resistência genética pode ser quantitativa ou qualitativa, dependendo do tipo de interação entre a planta e o patógeno (Jorge e Verdier 2002; Mora et al. 2019; Díaz-Tatis et al. 2022). A resistência quantitativa geralmente confere à planta um nível parcial de resistência à doença. Ela não impede o processo infeccioso, mas apenas reduz a multiplicação do patógeno, a colonização da planta e/ou a gravidade dos sintomas (Pilet-Nayel et al. 2017). Por outro lado, na resistência qualitativa, a resposta da planta é uma resistência completa, que envolve uma resposta de hipersensibilidade ou morte celular programada (Kushalappa et al. 2016).

Dois estudos independentes para a identificação de genótipos com potencial para resistência genética à bacteriose da mandioca foram conduzidos no Brasil. No primeiro estudo, realizado em condições de campo, nenhum dos genótipos testados apresentou resistência completa à doença (Teixeira et al. 2021). No segundo estudo, conduzido em uma estufa, apenas um dos 12 acessos testados foi classificado como resistente, com base na reação média de três isolados diferentes de *Xpm* (Aquiles et al. 2021). Esses resultados revelam uma dificuldade significativa em encontrar genótipos resistentes a essa doença no Brasil (Teixeira et al. 2021; Aquiles et al. 2021).

#### **4. Métodos moleculares para detecção da bactéria**

A detecção e identificação de bactérias fitopatogênicas são essenciais para o desenvolvimento de estratégias de manejo adequadas a cada patossistema. Nesse contexto, diversas pesquisas utilizando técnicas moleculares para a detecção de Xpm foram desenvolvidas ao longo dos anos. Verdier et al. (1998) propuseram o primeiro protocolo de PCR, no qual o par de primers XV-XK amplificava uma sequência-alvo de 898 pb localizada no plasmídeo p44, que contém genes relacionados à patogenicidade da Xpm em plantas de mandioca.

Em seguida, Ojeda e Verdier (2000) desenvolveram um ensaio de nested-PCR para detecção de Xpm em sementes infectadas. Nesse estudo, os autores projetaram primers específicos para a segunda rodada de PCR, com o objetivo de aumentar a sensibilidade na amplificação de uma região específica do produto gerado na primeira rodada, que utilizou os *primers* previamente desenvolvidos por Verdier et al. (1998). Anos mais tarde outro nested-PCR multiplex, desta vez usando as regiões *Cterm* e *rpoB* foi apresentado por Bernal-Galeano et al. (2018).

Cerqueira-Melo et al. (2019) desenvolveram e aprimoraram um método de PCR utilizando um conjunto de primers redesenhados a partir dos previamente publicados por Verdier et al. (1998). O novo conjunto, denominado XV/XK\_MOD, foi criado devido à incapacidade dos primers originais de amplificar fragmentos de determinados isolados de Xpm, provavelmente em decorrência de polimorfismos nas duas primeiras bases do primer XK. Além desses métodos, Flores et al. (2019) desenvolveram um ensaio duplex-PCR para a detecção simultânea de Xpm e *Xanthomonas cassavae*, permitindo a identificação separada de ambas as bactérias.

Essa capacidade de diferenciação na detecção entre *X. cassavae* e *Xpm* é especialmente importante, pois a primeira é uma praga quarentenária ausente no Brasil (MAPA 2017). Ademais, essa bactéria teve sua presença confirmada apenas no continente africano até o

momento. E, embora a *X. cassavae* possa causar manchas encharcadas e necróticas nas folhas de mandioca, ela não é sistêmica como a Xpm (Zárate-Chaves et al. 2024).

#### **4.1. Loop-mediated isothermal amplification - LAMP**

A técnica de Amplificação Isotermal Mediada por Loop (*Loop-mediated isothermal amplification* - LAMP), foi desenvolvida por Notomi et al. (2000) para detecção do *Hepatite B virus* (HBV), sendo considerada uma técnica de amplificação de DNA com alta especificidade, eficiência e rapidez em condição de temperatura constante.

Inicialmente, essa técnica consistia na utilização de dois conjuntos de *primers*, um conjunto de *primers* externo (F3 e B3) e um conjunto interno (FIP e BIP). Posteriormente, foram adicionados os *primers* do loop (FL e BL) à técnica de LAMP, totalizando três conjuntos de *primers*. Estes *primers* permitiram uma otimização do processo de amplificação, de modo a aumentar a velocidade e reduzir o tempo necessário para a realização da análise (Nagamine et al. 2002).

De maneira geral, o processo de amplificação ocorre a uma temperatura constante, graças à *Bst* polimerase, oriunda da bactéria *Geobacillus stearothermophilus* (sinonímia: *Bacillus stearothermophilus*), que é utilizada no processo de amplificação, e que apresenta uma alta capacidade de deslocamento das fitas de DNA, de modo que não há a necessidade dos ciclos de variação de temperatura, como ocorre na reação em cadeia da polimerase (PCR) (Notomi et al. 2000).

O LAMP possui três fases fundamentais no processo de amplificação: não cíclica, cíclica e de elongação. Inicialmente, após a abertura da dupla fita de DNA, os *primers* F2 e F3 se ligam à sequência complementar na extremidade 3' da fita molde para sintetizar uma nova fita, F2c e F3c, respectivamente. Durante o processo de polimerização da fita de DNA iniciado a partir do *primer* F3, a *Bst* polimerase realiza o deslocamento, síntese e separação da fita filha gerada a partir do *primer* F2. Posteriormente, os *primers* B3 e F3 se ligam na extremidade da

fita formada, dando início ao processo de síntese de mais uma fita semelhantemente ao processo anterior. Depois disso, é possível perceber a formação de estruturas de loops nas extremidades da fita sintetizada, finalizando a etapa não cíclica (Notomi et al. 2000).

Em seguida, ocorre a fase cíclica de amplificação do DNA. Para tanto, os *primers* FIP e BIP hibridizam nas regiões complementares presentes nos loops, permitindo a síntese de novas fitas de DNA e promovendo o deslocamento das fitas à medida que são formados sucessivos loops nas sequências geradas. Esse processo se repete ciclicamente inúmeras vezes. Desse modo, em LAMP, a sequência alvo é amplificada 3 vezes a cada ciclo (Notomi et al. 2000; Nagamine et al. 2002).

Frequentemente, após a fase cíclica, é possível observar a formação de cadeias longas de DNA ligadas por loops, de modo a produzir fragmentos de tamanhos variados, conhecida como fase de elongação. Neste momento, é possível verificar a formação de algumas estruturas intermediárias que retornam para a fase cíclica da reação (Notomi et al. 2000; Nagamine et al. 2002).

Em termos comparativos, existe um número variado de trabalhos que revelam que a técnica LAMP possui uma elevada sensibilidade e especificidade, podendo ser comparado com a PCR. Ademais, estima-se que uma reação LAMP custe em torno de US\$ 3, o que torna esse teste barato, quando comparado com uma reação de PCR convencional, que exige um custo de pelo menos US\$ 12, uma vez que demanda a extração do ácido nucleico, ensaio de PCR e eletroforese (Panno et al. 2020).

#### **4.2. Análises dos produtos do LAMP**

Uma das vantagens na utilização do LAMP é a variedade de métodos para analisar o produto da amplificação. Um dos métodos clássicos é, indubitavelmente, a eletroforese em gel de agarose, haja vista o fato de que após a reação são formados fragmentos de diferentes tamanhos, apresentando um padrão de cascata ou escada e que são visualizados em luz

ultravioleta com corantes intercalantes como brometo de etídeo, gel red ou SYBR green I. Contudo, nos casos em que se pretende utilizar o LAMP em campo, torna-se necessário lançar mão de outras estratégias mais simples para a visualização do resultado.

É possível observar a olho nu a turbidez da reação presente no tubo, graças à formação de um precipitado de pirofosfato de magnésio oriundo da amplificação do DNA alvo (Fukuta et al. 2003). Ademais, são utilizados equipamentos para leitura óptica das amostras, como espectrofotômetro, o que auxilia na interpretação dos resultados e diminui possíveis erros de observação (Nie 2005; Kubota et al. 2008).

Existe uma diversidade de corantes na literatura que são usados na técnica LAMP, tais como corantes fluorescentes, indicadores de íons e indicadores de pH. Os corantes fluorescentes geralmente se ligam às novas cópias de DNA sintetizados gerando fluorescência, e quanto maior a quantidade de *amplicons* criados, maior a fluorescência observada. Esses corantes frequentemente são adicionados na mistura de reação LAMP, uma vez que não inibem o processo de amplificação, e os resultados podem ser visualizados a olho nu ou em luz ultravioleta, sem a necessidade da abertura dos tubos de reação. Dentre os corantes encontrados na literatura, pode-se citar: brometo de etídeo (Zoheir and Allam 2010), SYBR green I (Parida et al. 2005), iodeto de propídio (Hill et al. 2008), e GelRed (Woźniakowski et al. 2012)

A compreensão do funcionamento da reação LAMP permitiu o desenvolvimento da visualização do resultado pela adição de corantes indicadores de metal e de pH. Os corantes indicadores de metal, tais como calceína e azul de hidroxinaftol (HNB), se ligam a diferentes cátions como cálcio e magnésio, e à medida que ocorrem alterações na concentração desses íons na reação, ocorre, por consequência, mudança na coloração da solução.

Em se tratando do HNB, a reação LAMP produz uma grande quantidade de íon pirofosfato, que se ligam aos íons  $Mg^{2+}$  para formar o produto insolúvel pirofosfato de magnésio. O aumento na concentração desse íon durante o processo de amplificação de DNA

acarreta uma diminuição na disponibilidade do cátion  $Mg^{2+}$ , resultando na mudança de cor da solução de violeta para azul claro (Goto et al. 2009).

No caso da calceína, primeiramente, o íon manganês encontra-se ligado à calceína, e à medida que a reação ocorre, o pirofosfato gerado por LAMP tem uma maior preferência por se ligar a esse íon, removendo-o da calceína. Em seguida, o magnésio disponível na solução passa a ocupar o sítio que antes continha o manganês, resultando na formação do complexo calceína-magnésio, o que gera uma fluorescência verde (Tomita et al. 2008).

Os indicadores de pH, por outro lado, mudam de cor como resultado da liberação do próton  $H^+$  na reação em função da incorporação de desoxinucleotídeos trifosfato (dNTPs) na fita de DNA formada. Essa acidificação do meio durante o processo de amplificação torna-se perceptível pela ação de corantes indicadores de pH, a exemplo do vermelho de fenol (Tanner et al. 2015). Apesar do potencial de uso desses corantes, é imprescindível salientar que reações LAMP fortemente tamponadas podem sofrer resistência às variações de pH, tornando-se, consequentemente, incapazes de serem avaliadas por essa abordagem. Partindo desse princípio, torna-se necessária a utilização de soluções fracamente tamponadas nas reações LAMP (Tanner et al. 2015).

A técnica LAMP tem sido aplicada com sucesso na detecção de diferentes bactérias fitopatogênicas do gênero *Xanthomonas*, como *Xanthomonas euvesicatoria* em tomate (Larrea-Sarmiento et al. 2018), *Xanthomonas fragariae* em morango (Gétaz et al. 2017) e *Xanthomonas citri* pv. *fusca*s e *Xanthomonas phaseoli* pv. *phaseoli* em feijão (Paiva et al. 2019). No entanto, nenhuma técnica LAMP havia sido desenvolvida para detectar Xpm em mandioca, evidenciando a necessidade do desenvolvimento dessa metodologia.

## **5. Emprego de sensores na detecção de alterações fisiológicas em plantas infectadas por fitopatógenos**

O sucesso de uma lavoura está ligado à capacidade do produtor de entender as alterações que ocorrem no campo, de maneira que seja possível antever e mitigar os efeitos deletérios causados por agentes estressores, especialmente as doenças de plantas. Deste modo, o desenvolvimento de estratégias para detecção e identificação de fitopatógenos pode ser crucial para o monitoramento da sua distribuição na área, bem como para a adoção de medidas de controle de forma sustentável e economicamente viável.

Tendo em vista esses fatores, o uso de tecnologias que permitam a coleta de dados de maneira rápida, precisa e de forma não destrutiva torna-se importante no contexto do manejo de doenças de plantas (Ang e Lew 2022). Partindo desse princípio, o sensoriamento remoto de doenças de plantas apresenta-se como uma alternativa promissora e com amplo potencial de uso.

Dentre as abordagens de sensoriamento para o estudo de doenças de plantas, pode-se citar: imagens térmicas, de fluorescência e espectrais. Os sistemas de imagens térmicas estendem nossa visão, permitindo observar mudanças fisiológicas no objeto pela variação de temperatura. Nesta perspectiva, com o uso de câmera térmica tem sido possível registrar a o progresso de diferentes doenças causadas por fitopatógenos em plantas hospedeiras, tais como a mancha bacteriana em plantas de arroz infectadas com *Xanthomonas oryzae* pv. *oryzae* (Bhakta et al. 2018) e *Oidium neolyccopersici* em tomateiro (Raza et al. 2015).

O método de fluorescência de clorofila permite mensurar mudanças no metabolismo fotossintético em plantas submetidas a estresses bióticos de maneira não invasiva e não destrutiva, e é considerada acessível devido aos preços relativamente baixos de fluorômetros comerciais (Rolfe and Scholes 2010; Pérez-Bueno et al. 2019). A aplicação dessa tecnologia para detecção de alterações fisiológicas no patossistema tomate-*Xanthomonas gardneri*, permitiu verificar uma redução significativa da atividade fotossintética, bem como da

concentração das clorofilas a e b e carotenoides em tomateiros em decorrência do desenvolvimento da doença (Silveira et al. 2015). O uso de imagem de fluorescência induzida por laser para monitorar a doença *huanglongbing* em plantas de citros inoculadas com *Candidatus Liberibacter asiaticus* possibilitou a detecção do patógeno em estágios iniciais da doença, ainda no primeiro mês (Pereira et al. 2011).

A utilização de informações espectrais é possível graças ao uso de sistemas detectores sensíveis à radiação, sendo capazes de dividi-la em seus componentes espectrais, que variam de 350 a 2500 nm (Oerke 2020). Esses sensores são capazes de detectar variações espectrais causadas por diferentes agentes estressores abióticos e bióticos que venham afetar a fisiologia da planta, como é o caso das infecções por fitopatógenos e o ataque de pragas. Essas alterações podem ocorrer tanto na intensidade de reflectância, quanto na assinatura espectral (Yang 2010; Zhang et al. 2019).

A aplicação de imagem hiperespectral na diagnose de doenças não se limita apenas aos laboratórios, mas se estende para o campo. Isto se deve ao uso de veículos aéreos não tripulados (VANTs) equipados com câmera hiperespectral permitindo obter informações suficientes para identificar plantas doentes, além de diferenciar mais de um tipo de doença. Em plantas de tomate já é possível diagnosticar e diferenciar a nível de campo infecções causadas por *Xanthomonas perforans* e *Corynespora cassiicola*, os quais causam mancha foliar (Abdulridha et al. 2020), obtendo-se resultados superiores ao da análise visual feita por seres humanos, o qual são especialistas, em plantas de tomate infectadas com *Xanthomonas* spp. (Borges et al. 2016).

## **6. Aplicação de aprendizado de máquina no processamento de dados hiperespectrais**

O volume de dados de reflectância espectral gerados por sensores ópticos, associados com a sua complexidade e necessidade de aquisição de informações em tempo hábil abriram espaço para a utilização de algoritmos de Aprendizado de Máquina (do inglês *Machine*

*Learning*) no processo de reconhecimento, estudo e classificação de plantas doentes. A aplicação de novas tecnologias digitais baseadas em aprendizado de máquina pode automatizar essas análise, tornando-as mais rápidas e eficientes.

Diferentes trabalhos têm aplicado dados espectrais associados com aprendizado de máquina na detecção de alterações fisiológicas causadas por fitopatógenos em patossistemas distintos. Dentre eles, pode-se citar a mancha bacteriana do tomateiro (Abdulridha et al. 2020), a murcha bacteriana do amendoim (Chen et al. 2020), o fogo bacteriano da macieira (Skoneczny et al. 2020) e a pinta-preta da batata (Van De Vijver et al. 2020). Adicionalmente, a junção dessas abordagens, imagens hiperespectrais e aprendizado de máquina, têm permitido atingir uma precisão de 90% na diagnose de doenças consideradas difíceis devido à complexidade de sintomas existentes (Li et al. 2012; Nagasubramanian et al. 2019).

De maneira mais ampla, comprehende-se o aprendizado de máquina como o campo de estudo que possibilita aos computadores a habilidade de aprender com as experiências sem a necessidade do esforço de programação detalhado (Samuel 1959). O aprendizado de máquina é uma área crucial dentro da inteligência artificial, a qual utiliza algoritmos computacionais para realizar diferentes tarefas, tais como classificação e agrupamento, a partir de dados de entrada. Essas características tornam o aprendizado de máquina uma ferramenta valiosa para identificar as tendências e padrões em dados hiperespectrais (Dhakal et al. 2023).

As técnicas de aprendizado de máquina são divididas em três categorias principais: aprendizado supervisionado, não supervisionado e semi-supervisionado. O aprendizado supervisionado utiliza dados rotulados para construir modelos preditivos. Nesse processo, um especialista atribui rótulos aos dados, associando-os a características específicas e às classes de interesse, o que permite ao modelo discriminar diferentes tipos de dados. Por outro lado, o aprendizado não supervisionado busca identificar padrões ou agrupamentos em dados que não possuem rótulos pré-definidos (Greener et al. 2022; Asnicar et al. 2024). O aprendizado semi-supervisionado combina dados rotulados e não rotulados, permitindo otimizar o processo de

classificação, especialmente em situações em que a rotulagem de dados é custosa ou demorada (Greener et al. 2022).

Diversos algoritmos de aprendizado de máquina têm sido utilizados para construir modelos de previsão de doenças em plantas (Ahmad et al. 2023; Omaye et al. 2024). O desempenho desses algoritmos de aprendizado de máquina pode ser influenciado pela natureza dos dados e pela interação entre o patógeno e o hospedeiro, como já foi observado em trabalhos anteriores. Abdulridha et al. (2020) observaram que o desempenho de algoritmos de aprendizado de máquina variou ao comparar dados hiperespectrais de duas doenças em tomateiro: uma fúngica, causada por *Corynespora cassiicola*, e outra bacteriana, causada por *Xanthomonas perforans*, analisadas tanto em condições de bancada quanto de campo. Em um estudo mais recente, (Javidan et al. 2024) demonstraram a capacidade de distinguir assinaturas espectrais de quatro doenças fúngicas em tomateiro, causadas por *Botrytis cinerea*, *Fusarium oxysporum*, *Alternaria alternata* e *Alternaria solani*, utilizando imagens hiperespectrais associadas à técnica de aprendizado de máquina Random Forest.

Diante disso, a integração de técnicas de aprendizado de máquina com dados hiperespectrais é uma abordagem promissora para detectar alterações fisiológicas resultantes de infecções por fitopatógenos, auxiliando no diagnóstico de doenças em plantas. Essa estratégia é especialmente relevante na agricultura, seja no uso de sensores acoplados a veículos aéreos não tripulados (VANT) e sensores proximais, seja na avaliação de material propagativo, como manivas e sementes, durante a triagem.

## REFERÊNCIAS

Abdulridha J, Ampatzidis Y, Kakarla SC, Roberts P (2020) Detection of target spot and bacterial spot diseases in tomato using UAV-based and benchtop-based hyperspectral imaging techniques. *Precision Agriculture* 21:955–978

Ahmad A, Saraswat D, El Gamal A (2023) A survey on using deep learning techniques for plant disease diagnosis and recommendations for development of appropriate tools. *Smart Agricultural Technology* 3:1-13

Ang MCY, Lew TTS (2022) Non-destructive technologies for plant health diagnosis. *Frontiers in Plant Science* 13:1-9

Aquiles KR, Marques E, Malaquias JV, Mattos JKA, Fialho JF, Vieira EA, Uesugi CH (2021) Reaction of sweet cassava genotypes to *Xanthomonas phaseoli* pv. *manihotis* from three regions of Brazil. *Journal of Agricultural Science* 13:1-9

Arrieta-Ortiz ML, Rodríguez-R LM, Pérez-Quintero ÁL, Poulin L, Díaz AC, Rojas NA, Trujillo C, Benavides MR, Bart R, Boch J, Boureau T, Darrasse A, David P, De Bernonville TD, Fontanilla P, Gagnevin L, Guérin F, Jacques MA, Lauber E, Lefevre P, Medina C, Medina E, Montenegro N, Bodnar AM, Noël LD, Ortiz Quiñones JF, Osorio D, Pardo C, Patil PB, Poussier S, Pruvost O, Robèn-Soustrade I, Ryan RP, Tabima J, Urrego Morales OG, Vernière C, Carrere S, Verdier V, Szurek B, Restrepo S, López C, Koebnik R, Bernal A (2013) Genomic survey of pathogenicity determinants and VNTR markers in the cassava bacterial pathogen *Xanthomonas axonopodis* pv. *manihotis* strain CIO151. *PLoS One* 8:1-18

Asnicar F, Thomas AM, Passerini A, Waldron L, Segata N (2024) Machine learning for microbiologists. *Nature Reviews Microbiology* 22:191–205

Bart R, Cohn M, Kassen A, McCallum EJ, Shybut M, Petriello A, Krasileva K, Dahlbeck D, Medina C, Alicai T, Kumar L, Moreira LM, Rodrigues Neto J, Verdier V, Santana MA, Kositcharoenkul N, Vanderschuren H, Gruisse W, Bernal A, Staskawicz BJ (2012) High-throughput genomic sequencing of cassava bacterial blight strains identifies conserved effectors to target for durable resistance. *Proceedings of the National Academy of Sciences* 109: E1972–E1979.

Bernal-Galeano V, Ochoa JC, Trujillo C, Rache L, Bernal A, López CA (2018) Development of a multiplex nested PCR method for detection of *Xanthomonas axonopodis* pv. *manihotis* in cassava. *Tropical Plant Pathology* 43:341–350

Berhet A, Bondar G (1915) Molestia bacteriana da mandioca. *Boletim de Agricultura* 16:513-524.

Bhakta, I, Phadikar, S, Majumder, K (2018). Importance of thermal features in the evaluation of bacterial blight in rice plant. In: Mandal, J., Sinha, D. (eds) Social Transformation – Digital

Way. CSI 2018. *Communications in Computer and Information Science*, vol 836. Springer, Singapore.

Bondar G (1912) Una nova molestia bacteriana das hastas da mandioca. *Chacaras e Quintaes* 5:15-18.

Borges DL, Guedes STC de M, Nascimento AR, Melo-Pinto P (2016) Detecting and grading severity of bacterial spot caused by *Xanthomonas* spp. in tomato (*Solanum lycopersicon*) fields using visible spectrum images. *Computers and Electronics in Agriculture* 125:149–159

Burns A, Gleadow R, Cliff J, Zacarias A, Cavagnaro T (2010) Cassava: the drought, war and famine crop in a changing world. *Sustainability* 2:3572–3607

CABI (2023) *Xanthomonas axonopodis* pv. *manihotis* (cassava bacterial blight). Disponível em: <https://plantwiseplusknowledgebank.org/doi/full/10.1079/pwkb.species.56952#sec-3>. Acesso em: 20 de novembro de 2024.

Cerqueira-Melo RC, Bragança CAD, Pestana KN, da Silva HSA, Ferreira CF, de Oliveira SAS (2019) Improvement of the specific detection of *Xanthomonas phaseoli* pv. *manihotis* based on the *pthB* gene. *Acta Scientiarum Agronomy* 41:1-9

Chege MN, Wamunyokoli F, Kamau J, Nyaboga EN (2017) Phenotypic and genotypic diversity of *Xanthomonas axonopodis* pv. *manihotis* causing bacterial blight disease of cassava in Kenya. *Journal of Applied Biology and Biotechnology* 5:38–44

Chen T, Yang W, Zhang H, Zhu B, Zeng R, Wang X, Wang S, Wang L, Qi H, Lan Y, Zhang L (2020) Early detection of bacterial wilt in peanut plants through leaf-level hyperspectral and unmanned aerial vehicle data. *Computers and Electronics in Agriculture* 177:1-10

Constantin EC, Cleenwerck I, Maes M, Baeyen S, Van Malderghem C, De Vos P, Cottyn B (2016) Genetic characterization of strains named as *Xanthomonas axonopodis* pv. *dieffenbachiae* leads to a taxonomic revision of the *X. axonopodis* species complex. *Plant Pathology* 65:792–806

Daniel JF, Boher B, N'dongo P, Makoundou L (1985) Etude des modes de survie de l'agent causal de la bactériose vasculaire du manioc, *Xanthomonas campestris* pathovar *manihotis*. *Agronomie* 5:339–346

Dhakal K, Sivaramakrishnan U, Zhang X, Belay K, Oakes J, Wei X, Li S (2023) Machine learning analysis of hyperspectral images of damaged wheat kernels. *Sensors* 23:1-13

Elango F, Lozano JC (1980) Transmission of *Xanthomonas manihotis* in seed of cassava (*Manihot esculenta*). *Plant Disease* 64:784-786

Elango FN, Lozano JC (1981) Epiphytic survival of *Xanthomonas manihotis* on common weeds in Colombia. *Proceedings of the 5th International Conference on Plant Pathogenic Bacteria* 203–209

Fanou AA, Zinsou AV, Wydra K (2017) Survival of *Xanthomonas axonopodis* pv. *manihotis* in weed species and in cassava debris: Implication in the epidemiology of cassava bacterial blight. *International Journal of Advanced Research* 5:2098–2112

Fanou AA, Zinsou VA, Wydra K (2018) Cassava bacterial blight: A devastating disease of cassava. In: Waisundara VY (ed) *Cassava*. InTech, London, pp 13–36

Felipe FI, Alves LRA, Camargo SGC (2010) Panorama e perspectivas para a indústria de fécula de mandioca no Brasil. *Revista Raízes e Amidos Tropicais* 6:134-146

Flores C, Zarate C, Triplett L, Maillot-Lebon V, Moufid Y, Kanté M, Bragard C, Verdier V, Gagnevin L, Szurek B, Robène I (2019) Development of a duplex-PCR for differential diagnosis of *Xanthomonas phaseoli* pv. *manihotis* and *Xanthomonas cassavae* in cassava (*Manihot esculenta*). *Physiological and Molecular Plant Pathology* 105:34–46

Food And Agriculture Organization – FAO (2017) Food Outlook: biannual report on global food market. Disponível em: < <http://www.fao.org/3/a-I8080e.pdf> >. Acesso em: 28 de dezembro de 2023.

Food And Agriculture Organization – FAO (2023) FAOSTAT. Disponível em: <<https://www.fao.org/faostat/en/#data/QCL>>. Acesso em: 12 de novembro de 2024.

Fukuta S, Kato S, Yoshida K, Mizukami Y, Ishida A, Ueda J, Kanbe M, Ishimoto Y (2003) Detection of tomato yellow leaf curl virus by loop-mediated isothermal amplification reaction. *Journal of Virological Methods* 112:35–40

Gétaz M, Bühlmann A, Schneeberger PHH, Van Malderghem C, Duffy B, Maes M, Pothier JF, Cottyn B (2017) A diagnostic tool for improved detection of *Xanthomonas fragariae* using a rapid and highly specific LAMP assay designed with comparative genomics. *Plant Pathology* 66:1094-1102

Goel AK, Rajagopal L, Nagesh N, Sonti RV (2002) Genetic locus encoding functions involved in biosynthesis and outer membrane localization of xanthomonadin in *Xanthomonas oryzae* pv. *oryzae*. *Journal of Bacteriology* 184:3539–3548

Goto M, Honda E, Ogura A, Nomoto A, Hanaki KI (2009) Colorimetric detection of loop-mediated isothermal amplification reaction by using hydroxy naphthol blue. *BioTechniques* 46:167–172

Greener JG, Kandathil SM, Moffat L, Jones DT (2022) A guide to machine learning for biologists. *Nature Reviews Molecular Cell Biology* 23:40–55

He YW, Cao XQ, Poplawsky AR (2020) Chemical structure, biological roles, biosynthesis and regulation of the yellow xanthomonadin pigments in the phytopathogenic genus *Xanthomonas*. *Molecular Plant-Microbe Interactions* 33:705–714

Hill J, Beriwal S, Chandra I, Paul VK, Kapil A, Singh T, Wadowsky RM, Singh V, Goyal A, Jahnukainen T, Johnson JR, Tarr PI, Vats A (2008) Loop-mediated isothermal amplification assay for rapid detection of common strains of *Escherichia coli*. *Journal of Clinical Microbiology* 46:2800–2804

IBGE (2023) Levantamento Sistemático da Produção Agrícola. Disponível em: <<https://sidra.ibge.gov.br/tabela/6588>>. Acesso em: 12 de novembro de 2024.

Javidan SM, Banakar A, Vakilian KA, Ampatzidis Y, Rahnama K (2024) Early detection and spectral signature identification of tomato fungal diseases (*Alternaria alternata*, *Alternaria solani*, *Botrytis cinerea*, and *Fusarium oxysporum*) by RGB and hyperspectral image analysis and machine learning. *Heliyon* 10:1-19

Kante M, Flores C, Moufid Y, Wonni I, Hutin M, Thomas E, Fabre S, Gagnevin L, Dagné K, Verdier V, Koita O, Szurek B (2020) First report of *Xanthomonas phaseoli* pv. *manihotis*, the causal agent of cassava bacterial blight, in Mali. *Plant Disease* 104:1852

Kubota R, Vine BG, Alvarez AM, Jenkins DM (2008) Detection of *Ralstonia solanacearum* by loop-mediated isothermal amplification. *Phytopathology* 98:1045–1051

Kumar S, Bansal K, Patil PP, Patil PB (2019) Phylogenomics insights into order and families of *Lysobacterales*. *Access Microbiology* 1:1-9

Kushalappa AC, Yogendra KN, Karre S (2016) Plant innate immune response: Qualitative and quantitative resistance. *CRC Critical Reviews in Plant Science* 35:38–55

Larrea-Sarmiento A, Dhakal U, Boluk G, Fatdal L, Alvarez A, Strayer-Scherer A, Wang J, Latorre F, Levesque C, McMullen M (2018) Development of a genome-informed loop-mediated isothermal amplification assay for rapid and specific detection of *Xanthomonas euvesicatoria*. *Plant Disease* 102(8):1457-1464

- Li X, Lee WS, Li M, Ehsani R, Mishra AR, Yang C, Mangan RL (2012) Spectral difference analysis and airborne imaging classification for citrus greening infected trees. *Computers and Electronics in Agriculture* 83:32–46
- Lozano JC (1986) Cassava bacterial blight: a manageable disease. *Plant Disease* 70:1089–1093
- Lozano JC, Booth RH (1974) Diseases of cassava (*Manihot esculenta* Crantz). *PANS Pest Articles and News Summaries* 20:30–54
- Manicom BQ, Becker MM, Deschodt DCN (1981) First report of cassava bacterial blight in South Africa. *Phytophylactica* 1981:195–196
- Mansfield J, Genin S, Magori S, Citovsky V, Sriariyanum M, Ronald P, Dow M, Verdier V, Beer SV, Machado MA, Toth I, Salmond G, Foster GD (2012) Top 10 plant pathogenic bacteria in molecular plant pathology. *Molecular Plant Pathology* 13:614–629
- MAPA (2017) Lista de pragas quarentenárias ausentes e presentes. Disponível em: <<https://www.gov.br/agricultura/pt-br/assuntos/sanidade-animal-e-vegetal/sanidade-vegetal/arquivos-quarentena/lista-de-pragas-quarentenarias-ausentes-e-presentes.pdf/view>>. Acesso em: 12 de fevereiro de 2025.
- Maraite H, Meyer JA (1975) *Xanthomonas manihotis* (Arthaud-Berthet) Starr, causal agent of bacterial wilt, blight, and leaf spots of cassava in Zaire. *PANS Pest Articles and News Summaries* 21:27–37
- Nagamine K, Hase T, Notomi T (2002) Accelerated reaction by loop-mediated isothermal amplification using loop primers. *Molecular and Cellular Probes* 16:223–229
- Nagasubramanian K, Jones S, Singh AK, Sarkar S, Singh A, Ganapathysubramanian B (2019) Plant disease identification using explainable 3D deep learning on hyperspectral images. *Plant Methods* 15:1–10
- Nassar N, Junior O, Sousa M, Ortiz R (2012) Improving carotenoids and amino acids in cassava. *Recent Patents on Food, Nutrition & Agriculture* 1:32–38
- Nie X (2005) Reverse transcription loop-mediated isothermal amplification of DNA for detection of potato virus Y. *Plant Disease* 89:605–610
- Notomi T, Okayama H, Masubuchi H, Yonekawa T, Watanabe K, Amino N, Hase T (2000) Loop-mediated isothermal amplification of DNA. *Nucleic Acids Research* 28:e63
- Oerke EC (2020) Remote sensing of diseases. *Annual Review of Phytopathology* 58:225–252

- Ogunjobi AA, Dixon AGO, Fagade OE (2007) Molecular genetic study of cassava bacterial blight causal agent in Nigeria using random amplified polymorphic DNA. *Electronic Journal of Environmental, Agricultural and Food Chemistry* 6:2364–2376
- Ogunjobi AA, Fagade OE, Dixon AGO (2006) Molecular variation in population structure of *Xanthomonas axonopodis* pv. *manihotis* in southeastern Nigeria. *African Journal of Biotechnology* 5:1868–1872
- Ogunjobi AA, Fagade OE, Dixon AGO (2008) Physiological studies on *Xanthomonas axonopodis* pv. *manihotis* (Xam) strains isolated in Nigeria. *Advances in Biological Research* 2:90–96
- Ogunjobi AA, Fagade OE, Dixon AGO (2010) Comparative analysis of genetic variation among *Xanthomonas axonopodis* pv. *manihotis* isolated from the western states of Nigeria using RAPD and AFLP. *Indian Journal of Microbiology* 50:132–138
- Ojeda S, Verdier V (2000) Detecting *Xanthomonas axonopodis* pv. *manihotis* in cassava true seeds by nested polymerase chain reaction assay. *Canadian Journal of Plant Pathology* 22:241–247
- Olarinde LO, Abass AB, Abdoulaye T, Adepoju AA, Adio MO, Fanifosi EG, Wasiu A (2020) The influence of social networking on food security status of cassava farming households in Nigeria. *Sustainability* 12:1–35
- Olsen KM, Schaal BA (1999) Evidence on the origin of cassava: Phylogeography of *Manihot esculenta*. *Proceedings of the National Academy of Sciences of the United States of America (PNAS)* 96:5586–5591
- Omaye JD, Ogbuju E, Ataguba G, Jaiyeoba O, Aneke J, Oladipo F (2024) Cross-comparative review of machine learning for plant disease detection: apple, cassava, cotton, and potato plants. *Artificial Intelligence in Agriculture* 12:127–151
- Paiva BAR, Wendland A, Teixeira NC, Ferreira MASV (2019) Rapid detection of *Xanthomonas citri* pv. *fuscans* and *Xanthomonas phaseoli* pv. *phaseoli* in common bean by loop-mediated isothermal amplification. *Plant Disease* 103(11):2916-2922
- Panno S, Matić S, Tiberini A, Caruso AG, Bella P, Torta L, Stassi R, Davino S (2020) Loop-mediated isothermal amplification: Principles and applications in plant virology. *Plants* 9:1–28
- Parida M, Horioke K, Ishida H, Dash PK, Saxena P, Jana AM, Islam MA, Inoue S, Hosaka N, Morita K (2005) Rapid detection and differentiation of dengue virus serotypes by a real-time

reverse transcription-loop-mediated isothermal amplification assay. *Journal of Clinical Microbiology* 43:2895–2903

Parmar A, Sturm B, Hensel O (2017) Crops that feed the world: Production and improvement of cassava for food, feed, and industrial uses. *Food Security* 9:907–927

Pereira FMV, Milori DMBP, Pereira-Filho ER, Venâncio AL, Russo M de ST, Cardinali MC do B, Martins PK, Freitas-Astúa J (2011) Laser-induced fluorescence imaging method to monitor citrus greening disease. *Computers and Electronics in Agriculture* 79:90–93

Pérez-Bueno ML, Pineda M, Barón M (2019) Phenotyping plant responses to biotic stress by chlorophyll fluorescence imaging. *Frontiers in Plant Science* 10:1–15

Persley GJ (1979) Studies on the survival and transmission of *Xanthomonas manihotis* on cassava seed. *Annals of Applied Biology* 93:159–166

Pilet-Nayel ML, Moury B, Caffier V, Montarry J, Kerlan MC, Fournet S, Durel CE, Delourme R (2017) Quantitative resistance to plant pathogens in pyramiding strategies for durable crop protection. *Frontiers in Plant Science* 8:1–9

Rache L, Blondin L, Flores C, Trujillo C, Szurek B, Restrepo S, Koebnik R, Bernal A, Vernière C (2019) An optimized microsatellite scheme for assessing populations of *Xanthomonas phaseoli* pv. *manihotis*. *Phytopathology* 109:859–869

Raza SEA, Prince G, Clarkson JP, Rajpoot NM (2015) Automatic detection of diseased tomato plants using thermal and stereo visible light images. *PLOS ONE* 10:1–20

Restrepo S, Duque M, Tohme J, Verdier V (1999) AFLP fingerprinting: An efficient technique for detecting genetic variation of *Xanthomonas axonopodis* pv. *manihotis*. *Microbiology (New York)* 145:107–114

Restrepo S, Velez CM, Duque MC, Verdier V (2004) Genetic structure and population dynamics of *Xanthomonas axonopodis* pv. *manihotis* in Colombia from 1995 to 1999. *Applied and Environmental Microbiology* 70:255–261

Restrepo S, Vélez CM, Verdier V (2000) Measuring the genetic diversity of *Xanthomonas axonopodis* pv. *Manihotis* within different fields in Colombia. *Phytopathology* 90:683–690

Restrepo S, Verdier V (1997) Geographical differentiation of the population of *Xanthomonas axonopodis* pv. *manihotis* in Colombia. *Applied and Environmental Microbiology* 63:4427–4434

Rolfe SA, Scholes JD (2010) Chlorophyll fluorescence imaging of plant-pathogen interactions. *Protoplasma* 247:163–175

Rubio R, Shocke J, Carrascal L, Ernesto C, Melgarejo LM (2017) Physiological behavior of cassava plants (*Manihot esculenta* Crantz) in response to infection by *Xanthomonas axonopodis* pv. *manihotis* under greenhouse conditions. *Physiological and Molecular Plant Pathology* 100:136–141

Samuel AL (1959) Some studies in machine learning. *IBM Journal of Research and Development* 3:210–229

Sandino T, López-Kleine L, López C, Marquínez X (2015) Caracterización de la respuesta morfológica de variedades susceptibles y resistentes de yuca (*Manihot esculenta* Crantz) a la bacteriosis vascular causada por *Xanthomonas axonopodis* pv. *manihotis*. *Summa Phytopathologica* 41:94–100

Santos MN, Zárate-Salazar JR, de Carvalho R, Albuquerque UP (2020) Intraspecific variation, knowledge, and local management of cassava (*Manihot esculenta* Crantz) in the semiarid region of Pernambuco, Northeast Brazil. *Environmental Development and Sustainability* 22:2881–2903

Silva IRC, Cardoso RCV, Góes JWA, Druzian JI, Vidal Júnior PO, Andrade ACB (2016) Food safety in cassava “flour houses” of Copioba Valley, Bahia, Brazil: Diagnosis and contribution to geographical indication. *Food Control* 1-8

Silveira PR, Nascimento KJT, Andrade CCL, Bispo WMS, Oliveira JR, Rodrigues FA (2015) Physiological changes in tomato leaves arising from *Xanthomonas Gardneri* infection. *Physiological and Molecular Plant Pathology* 92:130–138

Skoneczny H, Kubiak K, Spiralski M, Kotlarz J (2020) Fire blight disease detection for apple trees: Hyperspectral analysis of healthy, infected, and dry leaves. *Remote Sensing (Basel)* 12:1-16

Sundin GW, Castiblanco LF, Yuan X, Zeng Q, Yang CH (2016) Bacterial disease management: challenges, experience, innovation, and future prospects: Challenges in bacterial molecular plant pathology. *Molecular Plant Pathology* 17:1506–1518

Tanner NA, Zhang Y, Evans TC (2015) Visual detection of isothermal nucleic acid amplification using pH-sensitive dyes. *Biotechniques* 58:59–68

Taylor RK, Griffin RL, Jones LM, Pease B, Tsatsia F, Fanai C, Macfarlane B, Dale CJ, Davis RI (2017) First record of *Xanthomonas axonopodis* pv. *manihotis* in Solomon Islands. *Australasian Plant Disease Notes* 12:1-4

Teixeira JHS, Guimarães MAS, Cardoso SC, Brito A dos S, Diniz RP, Oliveira EJ, Oliveira SAS (2021) Evaluation of resistance to bacterial blight in Brazilian cassava germoplasm and disease-yield relationships. *Tropical Plant Pathology* 46:324–335

Tomita N, Mori Y, Kanda H, Notomi T (2008) Loop-mediated isothermal amplification (LAMP) of gene sequences and simple visual detection of products. *Nature Protocols* 3:877–882

Trujillo CA, Ochoa JC, Mideros MF, Restrepo S, López C, Bernal A (2014) A Complex Population Structure of the Cassava Pathogen *Xanthomonas axonopodis* pv. *manihotis* in Recent Years in the Caribbean Region of Colombia. *Microbial Ecology* 68:155–167

Van De Vijver R, Mertens K, Heungens K, Somers B, Nuyttens D, Borra-Serrano I, Lootens P, Roldán-Ruiz I, Vangeyte J, Saeys W (2020) In-field detection of *Alternaria solani* in potato crops using hyperspectral imaging. *Computers and Electronics in Agriculture* 168:1-11

Van Den Mooter M, Maraite H, Meiresonne L, Swings J, Gillis M, Kersters K, De Ley J (1987) Comparison between *Xanthomonas campestris* pv. *manihotis* (ISPP List 1980) and *X. campestris* pv. *cassavae* (ISPP List 1980) by means of phenotypic, protein electrophoretic, DNA hybridization and phytopathological techniques. *Journal of General Microbiology* 133:57–71

Vauterin L, Hoste B, Kersters K, Swings J (1995) Reclassification of *Xanthomonas*. *International Journal of Systematic Bacteriology* 45:472–489

Verdier V, Boher B, Maraite H, Geiger J-P (1994) Pathological and Molecular Characterization of *Xanthomonas campestris* Strains Causing Diseases of Cassava (*Manihot esculenta*). *Applied and Environmental Microbiology* 60:4478–4486

Verdier V, Dongo P, Boher B (1993) Assessment of genetic diversity among strains of *Xanthomonas campestris* pv. *manihotis*. *Journal of General Microbiology* 139:2591–2601

Verdier V, López C, Bernal A (2012) Cassava Bacterial Blight, Caused by *Xanthomonas axonopodis* pv. *manihotis*. In: Ospina Patiño B, Ceballos H (eds) *Cassava in the third millennium: modern production, processing, use, and marketing systems*. Centro Internacional de Agricultura Tropical (CIAT), Cali, CO, pp 200–212

Verdier V, Mosquera G, Assigbetsé K (1998) Detection of the Cassava Bacterial Blight Pathogen, *Xanthomonas axonopodis* pv. *manihotis*, by Polymerase Chain Reaction. *Plant Disease* 82:79–83

Wang W, Feng B, Xiao J, Xia Z, Zhou X, Li P, Zhang W, Wang Y, Møller BL, Zhang P, Luo MC, Xiao G, Liu J, Yang J, Chen S, Rabinowicz PD, Chen X, Zhang H Bin, Ceballos H, Lou Q, Zou M, Carvalho LJC B, Zeng C, Xia J, Sun S, Fu Y, Wang H, Lu C, Ruan M, Zhou S, Wu Z, Liu H, Kannangara RM, Jørgensen K, Neale RL, Bonde M, Heinz N, Zhu W, Wang S, Zhang Y, Pan K, Wen M, Ma PA, Li Z, Hu M, Liao W, Hu W, Zhang S, Pei J, Guo A, Guo J, Zhang J, Zhang Z, Ye J, Ou W, Ma Y, Liu X, Tallon LJ, Galens K, Ott S, Huang J, Xue J, An F, Yao Q, Lu X, Fregene M, López-Lavalle LAB, Wu J, You FM, Chen M, Hu S, Wu G, Zhong S, Ling P, Chen Y, Wang Q, Liu G, Liu B, Li K, Peng M (2014) Cassava genome from a wild ancestor to cultivated varieties. *Nature Communications* 5:1-9

Wonni I, Ouedraogo L, Dao S, Tekete C, Koita O, Taghouti G, Portier P, Szurek B, Verdier V (2015) First Report of Cassava Bacterial Blight Caused by *Xanthomonas axonopodis* pv. *manihotis* in Burkina Faso. *Plant Disease* 99:551

Woźniakowski G, Kozdruń W, Samorek-Salamonowicz E (2012) Loop-mediated isothermal amplification for the detection of goose circovirus. *Molecular Biology Reports* 9:1–11

Yameogo F, Wonni I, Sanou A, Sere I, Somda I, Szurek B, Gagnevin L (2023) Evaluation of Weeds as Alternative Hosts of *Xanthomonas phaseoli* pv. *manihotis*, the Causal Agent of Cassava Bacterial Blight in Burkina Faso. *PhytoFrontiers* 3:420–429

Yang CM (2010) Assessment of the severity of bacterial leaf blight in rice using canopy hyperspectral reflectance. *Precision Agriculture* 11:61–81

Zandjanakou-Tachin M, Fanou A, Le Gall P, Wydra K (2007) Detection, survival and transmission of *Xanthomonas axonopodis* pv. *manihotis* and *X. axonopodis* pv. *vignicola*, causal agents of cassava and cowpea bacterial blight, respectively, in/by insect vectors. *Journal of Phytopathology* 155:159–169

Zárate-Chaves CA, Moufid Y, López CE, Bernal A, Szurek B, Yáñez JM (2024) First Report of Cassava Bacterial Blight Caused by *Xanthomonas phaseoli* pv. *manihotis* in the Amazonian Forest of Ecuador. *Plant Disease* 108:1879

Zárate-Chaves CA, Osorio-Rodríguez D, Mora RE, Pérez-Quintero ÁL, Dereeper A, Restrepo S, López CE, Szurek B, Bernal A (2021) TAL effector repertoires of strains of *Xanthomonas*

*phaseoli* pv. *manihotis* in commercial cassava crops reveal high diversity at the country scale.  
*Microorganisms* 9:1–26

Zhang J, Huang Y, Pu R, Gonzalez-Moreno P, Yuan L, Wu K, Huang W (2019) Monitoring plant diseases and pests through remote sensing technology: A review. *Computers and Electronics in Agriculture* 165:1-14

Zoheir KMA, Allam AA (2010) A rapid method for sexing the bovine embryo. *Animal Reproduction Science* 119:92–96

## CAPÍTULO 2

---

---

**Colorimetric lamp assay for detection of *Xanthomonas phaseoli* pv. *manihotis* in cassava through genomics: a new approach to an old problem**

**Colorimetric LAMP assay for detection of *Xanthomonas phaseoli* pv. *manihotis* in cassava through genomics: a new approach to an old problem**

Ian C. Bispo Carvalho<sup>1</sup>, Alice Maria Silva Carvalho<sup>1</sup>, Adriane Wendland<sup>2</sup>, Maurício Rossato<sup>1\*</sup>

<sup>1</sup>Universidade de Brasília, Brasília, Distrito Federal, Brazil

<sup>2</sup>Embrapa Arroz e Feijão, Goiânia, Goiás, Brazil

\*Corresponding Author: M. Rossato; E-mail: mauricio.rossato@unb.br

Funding: FAP-DF Grant Number: 00193-00000868/2021-96

## **Abstract**

Bacterial spot caused by *Xanthomonas phaseoli* pv. *manihotis* (Xpm) is considered the main bacterial disease that affects cassava, causing significant losses when not properly managed. In the present study, a fast, sensitive, and easy-to-apply method to detect Xpm via colorimetric loop-mediated isothermal amplification (LAMP) was developed. In order to ensure the use of a unique to the target pathovar core region for primer design, 74 complete genomic sequences of Xpm together with different bacterial species and pathovars were used for comparative genomics. A total of 42 unique genes were used to design 27 LAMP primer sets, from which nine primers were synthesized and only one (Xpm\_Lp1 primer set) showed sufficient efficiency in preliminary tests. The sensitivity, assessed by a serial dilution of the pathotype strain (IBSBF 278) DNA, yielded high sensitivity, detecting up to 100 fg. The LAMP primers showed high specificity, not cross-reacting with other bacterial species or other pathovars tested and amplifying only the Xpm isolates. Tests confirmed the high efficiency of the protocol using infected or inoculated macerated cassava leaves, without the need for additional sample treatment. The LAMP test developed in this study was able to detect Xpm in a fast, simple, and sensitive way, and it can be used to monitor the disease under laboratory and field conditions.

**Keywords:** Bacterial blight, comparative genomics, loop-mediated isothermal amplification

## **Introduction**

Cassava is a crop of great economic and social value. Its cultivation is mostly carried out by small farmers, and plants are characterized for being robust, drought tolerant, and requiring less agricultural input resources compared to other cultivated species (Parmar et al. 2017; Santos et al. 2020; Olarinde et al. 2020). However, cassava bacterial blight caused by *Xanthomonas phaseoli* pv. *manihotis* (Xpm) can severely reduce production. The impact of the disease can vary depending on environmental conditions, with production losses ranging from 30% to 90%, reaching 100% after two or three crop cycles if adequate management measures are not adopted (Mansfield et al. 2012; Zárate-Chaves et al. 2021).

Over the past 25 years, several publications have reported Xpm detection methods using molecular techniques. Most of these techniques are PCR-based, such as a PCR protocol proposed by Verdier, Mosquera, and Assigbésé (1998); a nested-PCR assay to detect Xpm in infected seeds by Ojeda and Verdier (2000); a multiplex nested-PCR technique using *Cterm* and *rpoB* regions by Bernal-Galeano et al. (2018); and, lastly, Cerqueira-Melo et al. (2019) developed an improved PCR with a redesigned set of primers previously published by Verdier, Mosquera, and Assigbésé (1998). In addition to these methods, a duplex-PCR assay was designed for the differential diagnosis of Xpm and *Xanthomonas cassavae* (Flores et al. 2019). However, there is still no specific loop-mediated isothermal amplification (LAMP) assay for Xpm detection. It is worth noting that, according to estimates, a LAMP reaction costs around US\$ 3, which makes this test inexpensive compared to a conventional PCR reaction, which requires at least US\$ 12 as it requires nucleic acid extraction, a PCR assay, and electrophoresis (Panno et al. 2020).

LAMP also has the advantage of providing methods other than agarose gel electrophoresis to visualize the products. Several studies have reported the successful use of colorimetric LAMP with pH indicator dyes for the detection of a variety of plant pathogens

(Choudhary et al. 2020; Omer et al. 2022; Çelik 2022; Amoia et al. 2023), including plant pathogenic bacteria of the genus *Xanthomonas* (Stehlíková et al. 2020; Buddhachat et al. 2021).

For high specificity of a successful LAMP assay, it is priority to select an exclusive region conserved in the target species or pathovar in this case (Larrea-Sarmiento et al. 2018; Dobhal et al. 2019). Comparative genomics is a valuable tool to search for unique ORFs or regions when designing specific set of primers, including the use of software programs such as ROARY (Page et al. 2015) or RUCS (Thomsen et al. 2017) to search for unique ORFs or regions. These methods may also help assess whether the region chosen for primer design is also present in all available sequenced genomes of the target species or pathovars, while not present in non-target ones.

We developed a molecular detection assay by isothermal amplification (LAMP) with a pH indicator dye, using the comparative genomics approach for a fast, easy to apply, sensitive and specific detection of Xpm in cassava. Another advantage of this new assay is that it can be performed without expensive equipment and under field conditions.

## Material and Methods

### Genomic region selection and LAMP primer design

For the selection of potential regions for the design of LAMP primers, a total of 92 complete genomic sequences available at GenBank (NCBI) were used: 74 Xpm of 14 different countries, 3 different pathovars of *Xanthomonas phaseoli* (*X. phaseoli* pv. *phaseoli*, *X. phaseoli* pv. *syngonii*, and *X. phaseoli* pv. *dieffenbachiae*), 1 *Xanthomonas cassavae*, and 14 other *Xanthomonas* (Supplementary table S1). All genomes used were re-annotated using the Prokka software v.1.14.0 (Seemann 2014), and comparative genomic analysis was performed using Roary software v.3.13.0 (Page et al. 2015) with default parameters. Based on this information, 42 genomic regions longer than 200 bp present exclusively in all Xpm isolates, were selected for the design of 27 LAMP primer sets (not shown). Sets were generated using the NEB LAMP

Primer Design Tool platform (<https://lamp.neb.com/#/>) with default settings. Nine primer sets (not shown) were synthesized after being assessed for the following parameters: melting temperature of external primers F3, B3, and internal primers F2, B2 (Figure 1) from 59 °C to 61 °C; for internal primers F1c and B1c (Figure 1), 64 °C to 66 °C; the  $\Delta G \leq -4$ ; and GC content between 50 - 60%. Primer BLAST (NCBI) was used to verify the LAMP external primers (F3/B3) against the NCBI database. Primer set Xpm\_Lp1 (Table 1/Figure 1) was selected for all assays because was the set that best complied with most of the criteria described above.

**Table 1.** Set of Xpm\_Lp1 LAMP primers designed for *Xanthomonas phaseoli* pv. *manihotis* and their sequences.

<b>Primers</b>	<b>Sequence (5' - 3')</b>	<b>Primer length</b>
Xpm_Lp1_F3	TGCGTTGCATTGCTTTGG	19
Xpm_Lp1_B3	GAAGAGCTGAGATCCATCGG	20
	(F1c) CAGTTGATCCAGCATGCGCAC	21
Xpm_Lp1_FIP*	(F2) TGCTACGGTTGCTCACGT	18
	(B1c) GCGGGATCCAAGCCCTATGC	20
Xpm_Lp1_BIP*	(B2) CGCCAGGATGTGCTAACCC	18
Xpm_Lp1_LF	AGTGATAGAGCACCTTCGGA	20
Xpm_Lp1_LB	GCATCATGCAGGTCGTCT	18

\*The FIP primer consists of sequences F1c and F2, whereas primer BIP consists of sequences B2 and B1c.

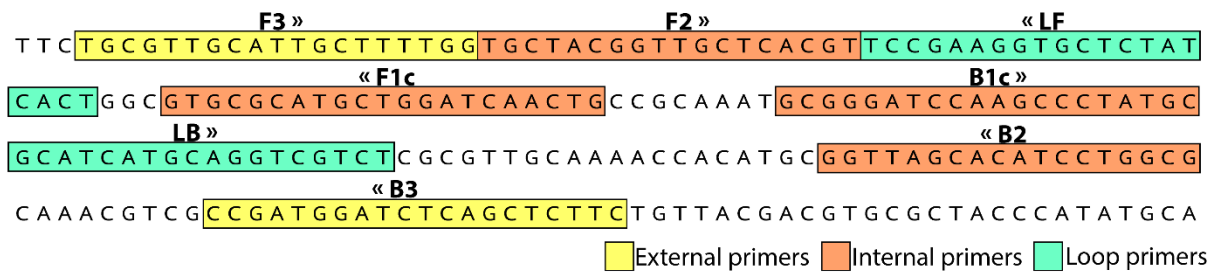


**Figure 1.** Schematic representation of the position and sequence of the designed LAMP primer set Xpm\_Lp1 within the nucleotide sequence.

### Bacterial isolates, culture conditions, and DNA extraction

The bacterial isolates used in this study (Table 2) consisted of the type strain of Xpm (IBSBF 278 = ICMP 5741 = LMG 784), six Xpm isolates from different edaphoclimatic zones of Brazil, additionally, there were eight isolates obtained from various species or pathovars within the genera *Xanthomonas*, as well as from *Pseudomonas*, *Curtobacterium*, and *Ralstonia*. Bacterial isolates were cultured in the 523 medium (10 g of sucrose, 8 g of hydrolyzed casein, 4 g of yeast extract, 2 g of K<sub>2</sub>HPO<sub>4</sub>, 0,3 g of MgSO<sub>4</sub> 7H<sub>2</sub>O, 15 g of agar) established by Kado and Heskett (1970) and incubated at 28°C for 48 hours to promote the growth of colonies. DNA was extracted using Mahuku's protocol (2004), First, 200 µL of TE (0.2 M Tris-HCl [pH 8], 10 mM EDTA [pH 8]), 30 µL of SDS (20%), and 10 µL of proteinase K were added to the bacterial pellet. Next, 250 µL of 7.5 M ammonium acetate was added. The samples were incubated at -20°C for 10 minutes and then centrifuged at 13000 RPM for 20 minutes. The supernatant (400 µL) was transferred to a new tube. Then, 400 µL of chilled isopropanol was added to the sample and incubated at -20°C for 1 hour. Subsequently, the samples were centrifuged at 13000 RPM for 20 minutes, and the supernatant was discarded. Next, 800 µL of chilled 70% ethanol was added to the sample and centrifuged at 13000 RPM for 5 minutes. Finally, the DNA pellets were resuspended in 50 µL of TE with RNase (50 µg/mL). All DNA samples were quantified using a NanoDrop (Thermo Scientific), and the concentration was adjusted to 25 ng µL<sup>-1</sup>. All *Xanthomonas* isolates were confirmed as belonging to this genus by

PCR using Xgum-D F7/R7 primers (Adriko et al. 2014) (data not shown). All “UnB” isolates were obtained from the plant bacteriology collection of the Plant Pathology Department of the University of Brasilia.

**Table 2.** Bacterial isolates used to validate the specificity and sensitivity of the LAMP assay for detection of *Xanthomonas phaseoli* pv. *manihotis*.

Bacterial species	Isolate	Host	Origin
<i>Xanthomonas phaseoli</i> pv. <i>manihotis</i> (Xpm)	IBSBF 278	Cassava	Brazil
	UnB 8	Cassava	Castanhal – PA
	UnB 17	Cassava	Acará - PA
	UnB 1111	Cassava	Paranavaí - PR
	UnB 1115	Cassava	Rolândia - PR
	UnB 1152	Cassava	Manaus - AM
	UnB 1163	Cassava	Brasília - DF
<i>X. citri</i> pv. <i>malvacearum</i> (Xcm)	IBSBF 2003	Cotton	Brazil
<i>X. citri</i>	UnB-XtecFFT02	Teak	Brazil
<i>X. euvesicatoria</i> pv. <i>alli</i> (Xea)	UnB 1430	Onion	Brazil
<i>X. euvesicatoria</i> pv. <i>perforans</i> (Xep)	UnB 1431	Tomato	Brazil
<i>X. hortorum</i> pv. <i>gardneri</i> (Xhg)	UnB 1432	Tomato	Brazil
<i>Ralstonia solanacearum</i> (Rsol)	UnB 1273	Tomato	Brasília - DF
<i>Curtobacterium flaccumfaciens</i> pv. <i>flaccumfaciens</i> (Cff)	UnB 1377	Bean	Alto Paraíso - GO
<i>Pseudomonas syringae</i> pv. <i>tomato</i> (Pto)	UnB 1045	Tomato	Brasília - DF

## **LAMP assay**

The volume reaction for the assays was set to 25 µl, 12.5 µl of WarmStart Colorimetric LAMP 2X Master Mix (New England Biolabs Inc., Ipswich, MA, USA), 2.5 µl of primer mix (2 µM F3 and B3 / 16 µM FIP and BIP / 4 µM LF and LB), 1 µl of DNA (25 ng µl<sup>-1</sup>) and 9 µl of ultrapure water. Water and the DNA of Xpm IBSBF 278 isolate were used as negative and positive controls, respectively. To optimize conditions for the reaction, the LAMP assays were carried out with the proportions between internal to external primer quantities of 4:1 and 8:1 at 65 °C for 0, 20, 30, 40, 50, and 60 minutes. These tests were performed in duplicate to confirm the results. Positive amplification was determined by the color change of the LAMP reaction from pink to yellow, thanks to the presence of the phenol red pH indicator dye. The reaction was also visualized by electrophoresis on a 2% agarose gel stained with GelRed (Biotium Inc., Fremont, CA, USA) in a UV transilluminator Loccus (Loccus, São Paulo, SP, Brazil) with 302 to 312 nm UV wavelength and photographed.

## **Specificity and sensitivity tests**

The specificity of the LAMP primer sets was verified using DNA samples extracted from seven Xpm isolates, eight different species of the genus *Xanthomonas* and other genera of plant pathogenic bacteria (Table 2). In order to evaluate the sensitivity of the LAMP primer set, the genomic DNA of the Xpm type strain (isolate IBSBF 278) was adjusted to 10 ng µl<sup>-1</sup> and then seven 1:10 serial dilutions were performed, with the concentration ranging from 10 ng µl<sup>-1</sup> to 1 fg µl<sup>-1</sup>. The number of genomic copies of Xpm was predicted using the equation below, considering the genome size of 5.15 Mb (Arrieta-Ortiz et al. 2013).

$$\text{Genomic copies} = \frac{\text{ng of double stranded DNA} \times \text{Avogadro's constant } (6.022 \times 10^{23})}{\text{Length in base pairs} \times 10^9 \times 650 \text{ Daltons}}$$

Both assays (sensitivity and specificity) were performed at least twice as described above, at 65 °C for 0, 30, 45, and 60 minutes. Positive amplification was visualized with the naked eye by the color change of the LAMP reaction.

The same diluted DNA samples used for the LAMP assay were used to compare the sensitivity of the proposed LAMP with a multiplex nested-PCR developed by Berna-Galeano et al. (2018). The reaction was visualized by electrophoresis on a 1% agarose gel stained with GelRed and photographed.

### **Detection in cassava leaves with Xpm by LAMP assay and sample preheating**

Tests with plant samples were performed to assess limiting factors for the LAMP protocol developed, i.e., whether there are inhibitors such as phenolic compounds in cassava leaves or whether bacteria could be present at low concentrations. Healthy and artificially inoculated cassava leaves (cv. BGMC 962) were tested with the Xpm\_Lp1 primer set. A total of four cassava seedlings were inoculated by spraying with the isolate UnB 17, using a bacterial suspension at a concentration of  $1 \times 10^8$  CFU ml<sup>-1</sup>. All plants inoculated and mock-inoculated were kept in a moist chamber for three days, after which they were transferred to a greenhouse until the manifestation of symptoms, approximately 15 days after inoculation.

Leaf disks measuring 1 cm in diameter were sectioned and macerated with pestles in 1.5 ml tubes containing 200 µl of ultrapure water. Each sample consisted of a single disk of inoculated or non-inoculated plants. In addition, in order to verify whether there was the need to heat the samples to promote the lysis of bacterial cells and release genetic material before the LAMP assay, tests were performed with and without prior heating of the samples at 95 °C for 5 minutes. The LAMP reactions used 1 µl of each sample as a template. The tests were performed in duplicates to confirm the results at 65 °C for 60 minutes. Positive reactions were determined by the color change of the LAMP reaction.

To test whether naturally infected plant material could interfere with the LAMP reaction due to pesticides or other contaminants, cassava leaves collected from fields with suspected Xpm presence were used as a template. Samples were collected from four locations in Brazil,

three of which from different locations in the South and one from the Central West region of the country. The leaves were processed as previously described.

## Results

### Genomic region selection and LAMP primer design

A total of 27 primer sets were designed, and nine were synthesized to be tested. Only one primer set (Xpm\_Lp1) could generate the multiple-band pattern typical of a LAMP reaction (Figure 2). Therefore, it was selected to be used for all sequential tests. The target for Xpm\_Lp1 LAMP primer set was identified as being the partial gene sequence of a glycosyltransferase (Figure 1), with a sequence unique to Xpm while present in all evaluated genomes of this pathovar.

### LAMP assay optimization

The temperature adopted in the tests was that indicated by the manufacturer of the colorimetric kit (65 °C), achieving good amplification and color change. The results for the ratio of internal to external primers, 4:1 and 8:1, indicate that there is no difference between them, with color change occurring within 30 minutes in both primer proportions (Figure 2). Furthermore, the low-cost 8:1 proportion achieved the same result, thus constituting a better choice. All subsequent tests used the standard time of 60 minutes and a primer ratio of 8:1.

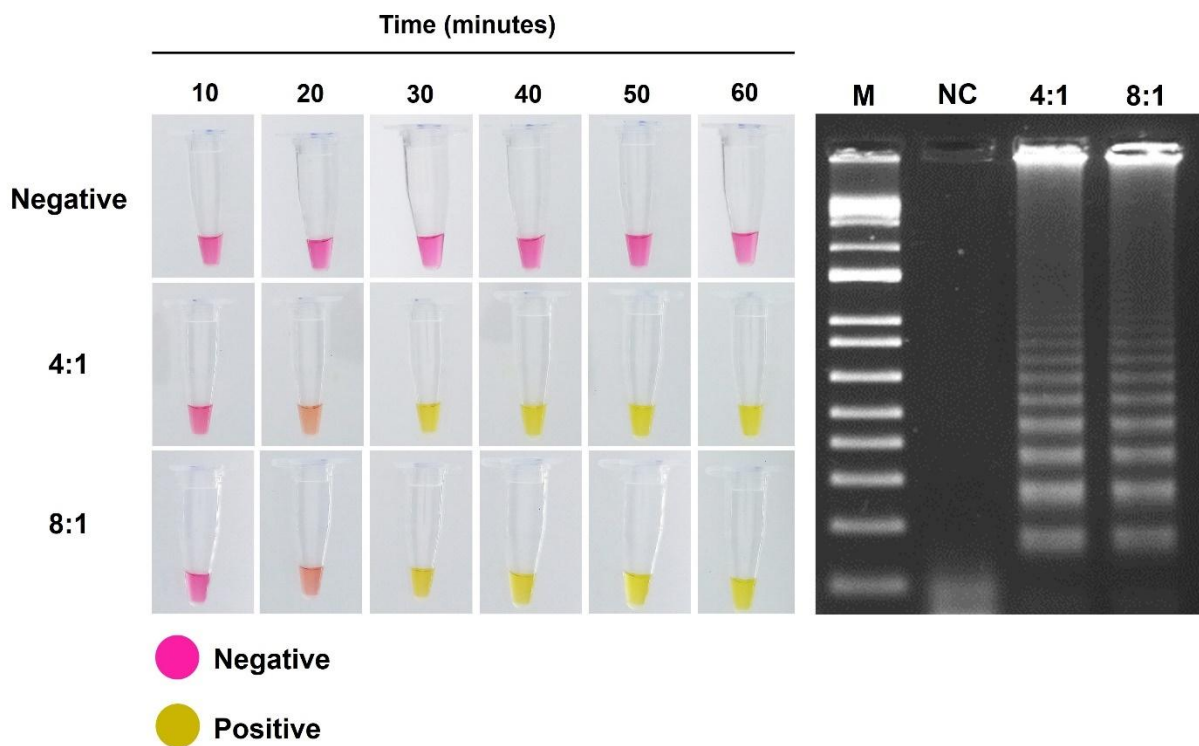


**Figure 2.** LAMP assay using different primer proportions (4:1 / 8:1) of primer set Xpm\_Lp1 at different time intervals with the DNA of the type strain of *Xanthomonas phaseoli* pv. *manihotis*, IBSBF 278. The DNA amplification product was visualized by color change of the pH indicator dye (left) and by agarose gel electrophoresis (right). M: DNA Ladder 1 kb Plus (Invitrogen), NC: Negative control.

### Sensitivity and specificity of LAMP assay

After 30 minutes incubation, only reactions with DNA quantities per reaction higher than  $10^4$  fg displayed a salmon color, indicating partial positivity compared to the standards set by this specific master mix. After 45 minutes, the test was positive for reactions above  $10^3$  fg of DNA per reaction. It was only after 60 minutes that there was amplification and consequent change in the color of the LAMP reaction at DNA quantities as low as 100 fg, corresponding to approximately 18 copies of bacterial DNA (Figure 3). Reactions with DNA quantities of 10 fg ( $\geq 1.8$  copies) and 1 fg (approximately less than one copy) could not be detected.

The sensitivity of the multiplex nested-PCR for the *Cterm* and *RpoB* regions (Bernal-Galeano et al. 2018) had a detection limit of up to 100 fg (Supplementary figure S1). Only one band was present for 1 fg of DNA, which was considered a negative result by the original author. The proposed LAMP with Xpm\_Lp1 primers had the same sensitivity as the multiplex nested-PCR assay.

The specificity test of the Xpm\_Lp1 primer set resulted in the amplification of all Xpm, while the other species and pathovars tested did not amplify or change color (Figure 4). These results confirmed that the LAMP assay with the set of primers developed in this study is specific to detect Xpm.

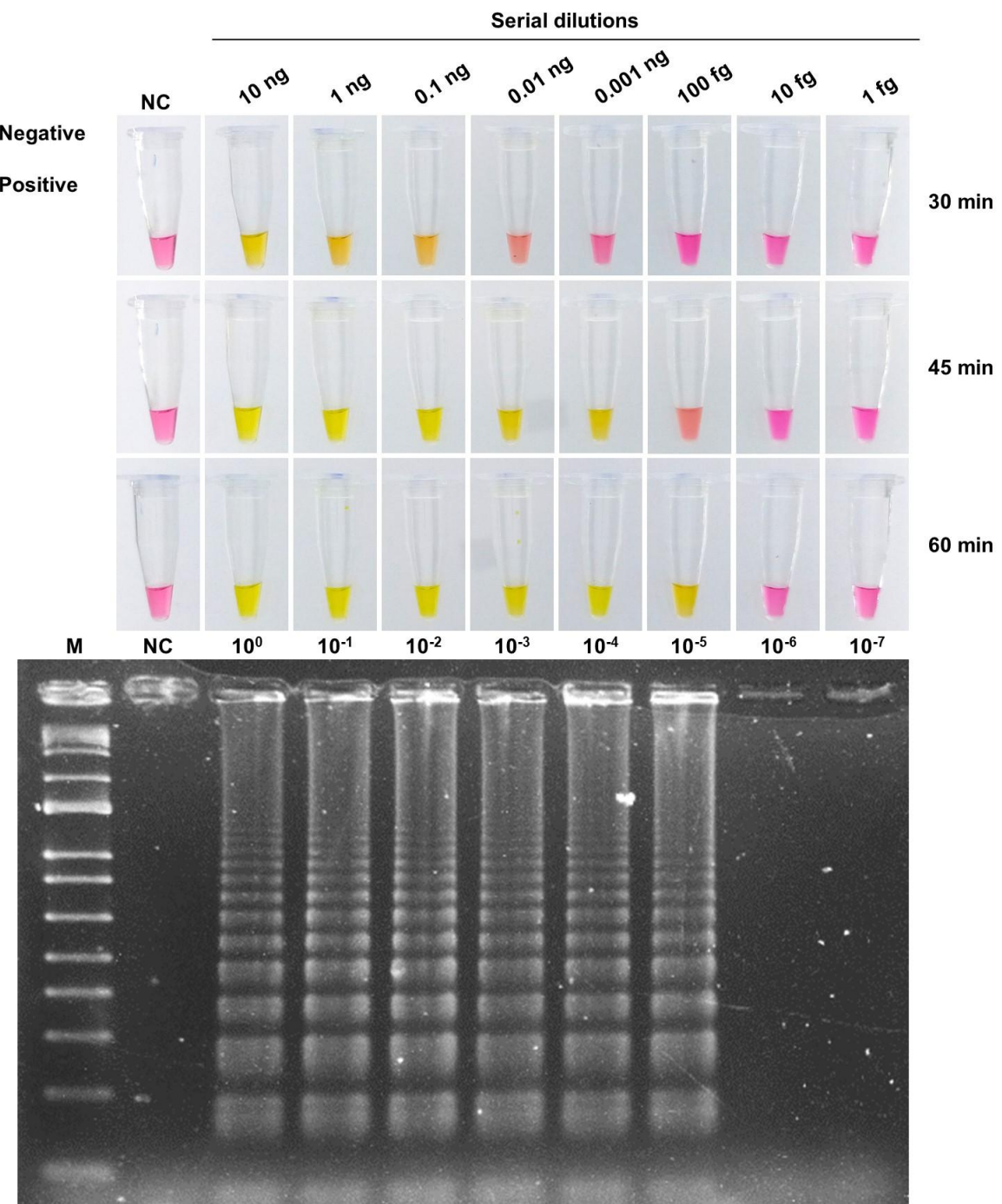


**Figure 3.** Sensitivity of the LAMP primer set Xpm\_Lp1 using different dilutions of the genomic DNA of the type strain of *Xanthomonas phaseoli* pv. *manihotis*, IBSBF 278, ranging from 10 ng ( $10^7$  fg) to 1 fg. The DNA amplification product was visualized by color change of the pH indicator dye (top) and by agarose gel electrophoresis (bottom). M: DNA Ladder 1 kb Plus (Invitrogen), NC: Negative control.

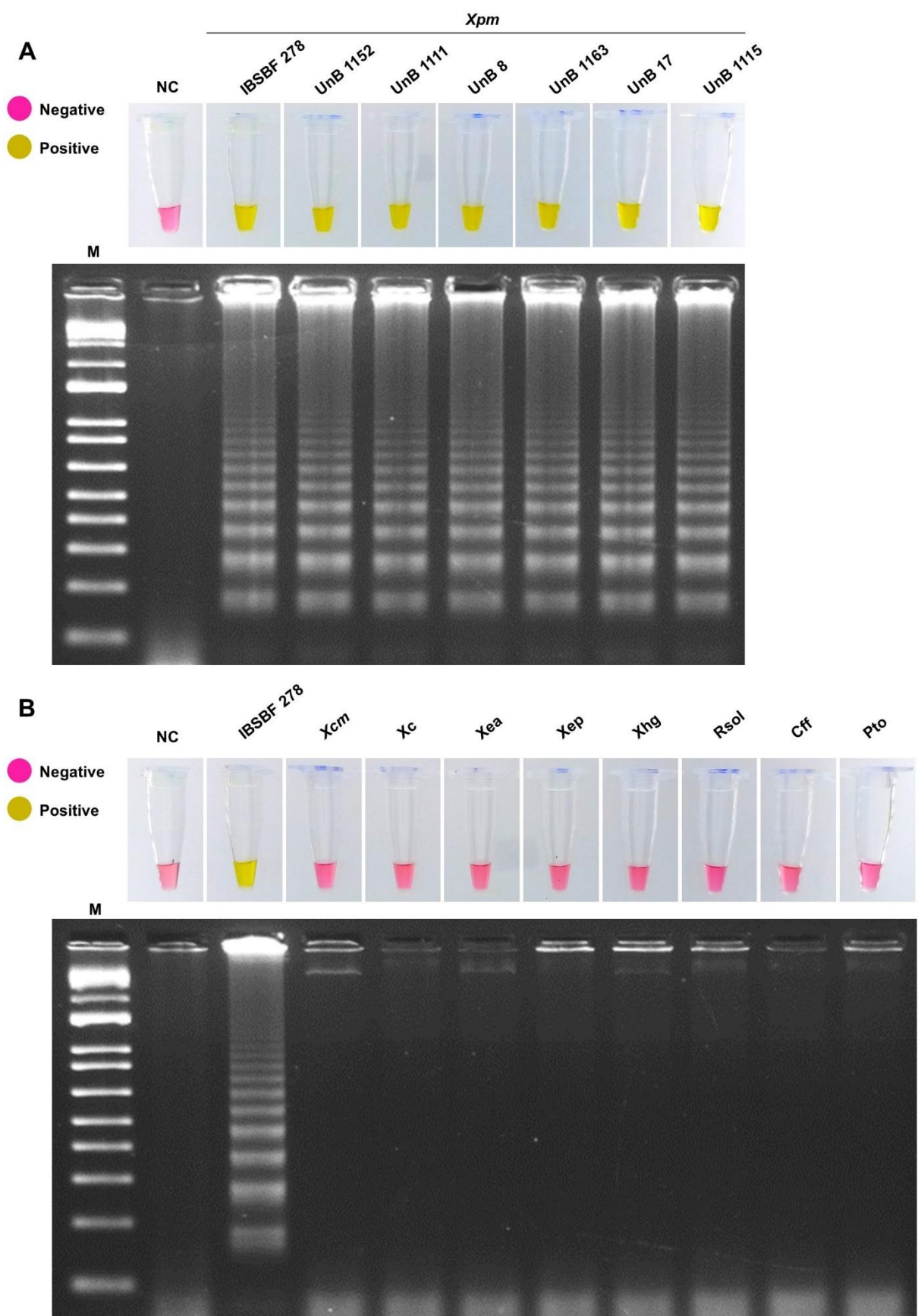


**Figure 4.** Evaluation of the LAMP assays specificity with the primer set Xpm\_Lp1. A) LAMP assays are able to detect *Xpm* isolates from the plant bacteriology collection at UnB. B) LAMP

assays do not detect other pathovars or species. Xcm: *Xanthomonas citri* pv. *malvacearum*, Xc: *Xanthomonas citri*, Xea: *Xanthomonas euvesicatoria* pv. *allii*, Xep: *Xanthomonas euvesicatoria* pv. *perforans*, Xhg: *Xanthomonas hortorum* pv. *gardneri*, Rsol: *Ralstonia solanacearum*, Cff: *Curtobacterium flaccumfaciens* pv. *flaccumfaciens*, Pto: *Pseudomonas syringae* pv. *tomato*. Type strain (IBSBF 278) was used as a positive control. The DNA amplification product was visualized by observing the change in color of the pH indicator dye (top) and by agarose gel electrophoresis (bottom). M: DNA Ladder 1 kb Plus (Invitrogen), NC: Negative control.

### **Detection in cassava leaves infected with Xpm by LAMP assay**

An assay was carried out with leaf discs of inoculated and non-inoculated plants with and without prior heating of the samples, to test the need for cell lysis and DNA release. In both cases, with and without preheating, the color changes were clear, revealing the amplification of the Xpm bacterial DNA (Figure 5). This finding demonstrated that there is no need to pre-treat the leaf samples to perform a successful test, or to extract DNA.

The test to assess whether the factors within field plants, e.g., pesticides, plant phenolic compounds, or other contaminants could interfere with Xpm detection using the LAMP assay revealed the target bacteria was present in three of the four fields screened (Figure 6). Positive results were corroborated by bacterial isolation from the same samples used for the LAMP assay. Non-inoculated plants did not present any kind of symptoms, also, the negative control for the LAMP assay was negative for all tests, confirming the absence of contaminants or other cross detection with non-target microorganisms.

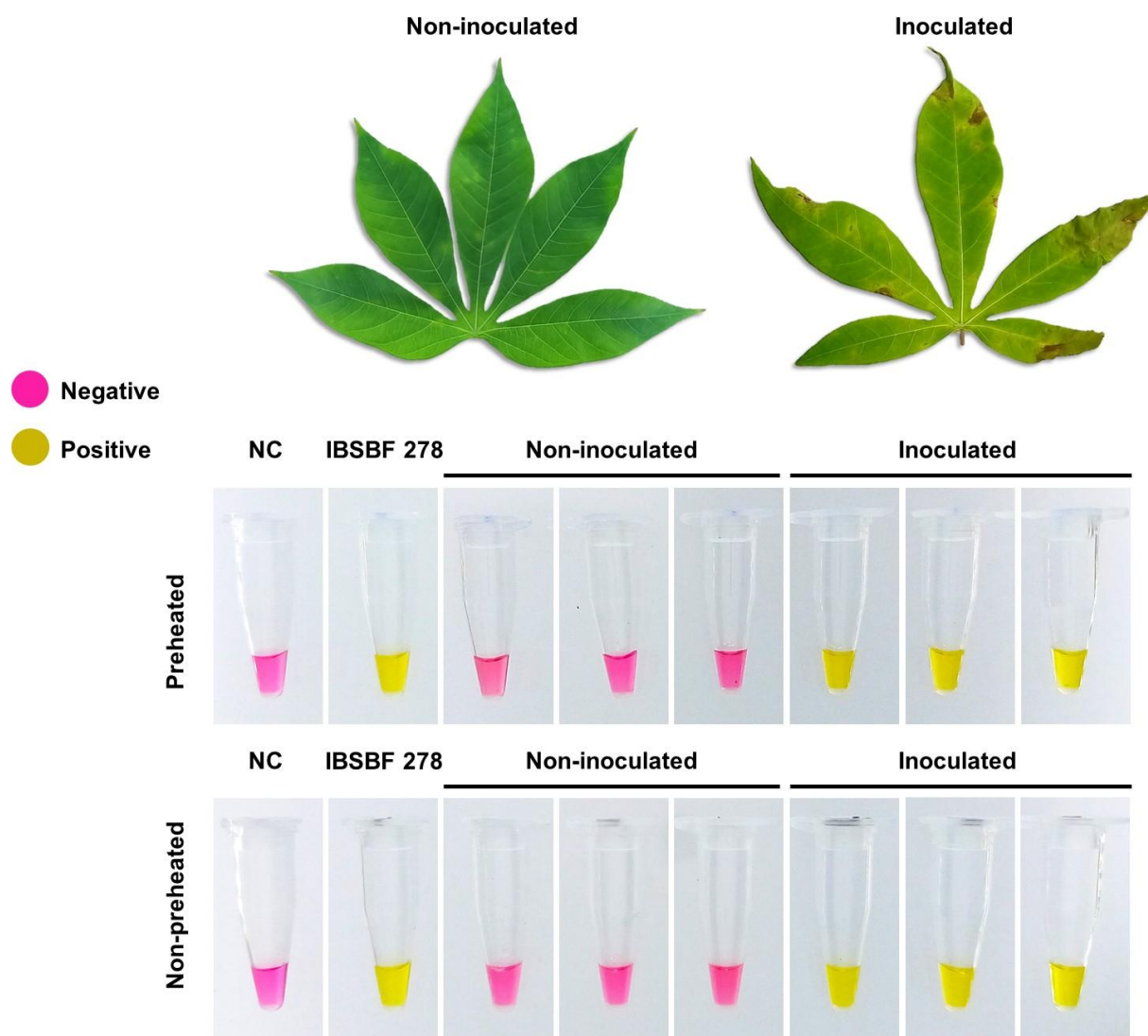


**Figure 5.** Effect of pre-heating treatment for LAMP assay with primers Xpm\_Lp1 for detection of *Xanthomonas phaseoli* pv. *manihotis* (Xpm) in inoculated with strain UnB 17 and non-inoculated cassava leaves. The DNA amplification product was visualized by observing the change in color of the pH indicator dye. Xpm type strain (IBSBF\_278) was used as positive control. NC: Negative control.

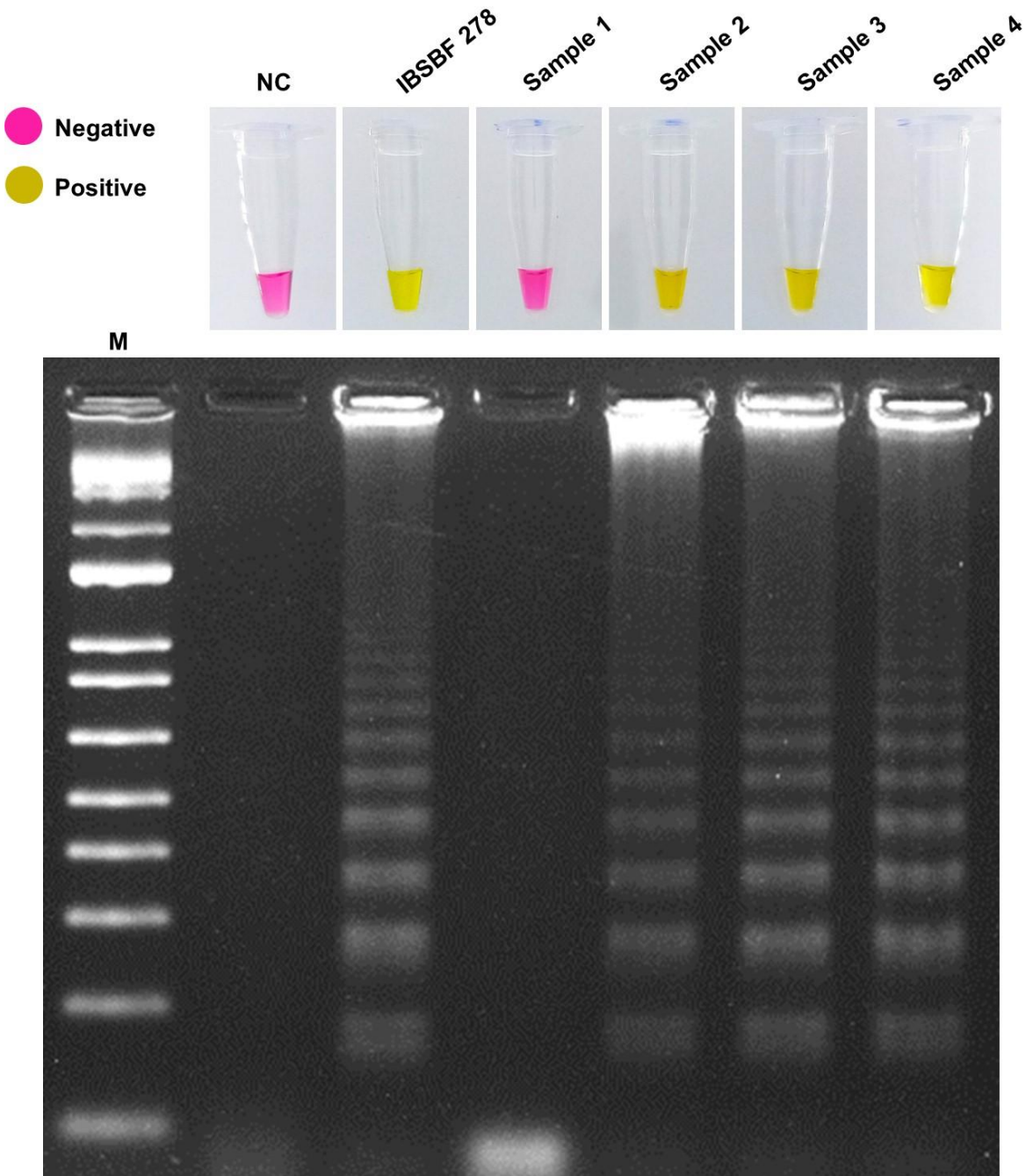


**Figure 6.** LAMP assay with primer set Xpm\_Lp1 for detection of *Xanthomonas phaseoli* pv. *manihotis* (Xpm) in naturally infected cassava leaves collected from four cassava production fields. DNA from Xpm type strain (IBSBF 278) was used as positive control. The DNA amplification product was visualized by observing the change in color of the pH indicator dye (top) and by agarose gel electrophoresis (bottom). M: DNA Ladder 1 kb Plus (Invitrogen), NC: Negative control.

## Discussion

LAMP offers key benefits such as consistent temperature operation, affordability, high sensitivity, and rapid reaction times, often completing in under an hour or within 30 minutes with loop primers. This study marks the first successful development of a LAMP test for the rapid, straightforward, stable, and highly sensitive detection of Xpm. It is well-suited to monitor the disease in both laboratory and field settings.

The detection limit of our method, at 100 fg, markedly improves its sensitivity over other two molecular techniques employed to detect Xpm. The detection limit is comparable to or more sensitive than other previously developed LAMP assays. For instance, the limit of 51 fg for *Xanthomonas campestris* pv. *musacearum* (Hodgetts et al. 2015), 100 fg for *Xanthomonas fragariae* and *Xanthomonas euvesicatoria* (Gétaz et al. 2016; Larrea-Sarmiento et al. 2018), and  $1.61 \times 10^3$  fg for *Pseudomonas syringae* pv. *tomato* (Chen et al. 2010). In comparison, Cerqueira-Melo et al.'s (2019) conventional PCR protocol, using Verdier et al. (1998) primers, reached a maximum sensitivity of  $2.5 \times 10^7$  fg. In contrast, Bernal-Galeano et al. (2018) multiplex nested-PCR strategy, focusing on the cterm and rpoB regions, could detect Xpm DNA at levels as low as  $1.84 \times 10^3$  fg. This nested-PCR method achieves comparable results, but with one order of magnitude less sensitivity compared to our LAMP assay. However, nested-PCR assays require two rounds of amplification for the target fragments, rendering it more labor-intensive and time-consuming (Wang et al. 2019; Demeuse et al. 2016). In contrast, our LAMP method is simpler and faster, as it doesn't require a thermal cycler, involves only one step, and eliminates the need for prior DNA extraction, characteristic of LAMP assays (Feng et al. 2019). This streamlined process highlights the LAMP technique's advantage as a quick and efficient method for detecting Xpm.

Our study used a comparative genomics approach to assess diversity and identify specific targets in conserved regions for Xpm, which improved the effectiveness of our LAMP primer set. We adopted a similar methodology to that employed by Shang et al. (2021) for

*Salmonella* and Domingo et al. (2021) for *Pectobacterium parmentieri*. Using RUCS software, we identified unique core regions, expanding the target sequence pool, especially when targets and non-targets are genetically similar (Alič et al. 2022). The genomic approach is crucial to ensure accurate detection of a target pathogen with significant genetic variations between haplotypes, as seen in the case of Xpm. For instance, Verdier et al. (1998) used a conventional PCR protocol to detect 10 fg of the pathogen's DNA, but the test was limited to specific Xpm isolates. Many studies detect phytobacteria using the species' pathogenicity genes (Verdier et al. 1998; Cerqueira-Melo et al. 2019; Ojeda and Verdier 2000). However, this approach has drawbacks, such as false negatives (Flores et al. 2019), due to some Xpm strains lacking the target genes (Cohn et al. 2014). Therefore, using conserved regions, as done in this experiment, can mitigate the adverse effects of genetic variability among Xpm populations.

This methodology allows rapid detection of Xpm in infected cassava leaves without prior sample treatment to reduce or eliminate inhibitory components for subsequent molecular testing. This is important given the inhibitory compounds found in cassava leaves (Xu et al. 2010; Behnam et al. 2019). Conventional PCR reactions are significantly affected by secondary metabolites (Russell and Paterson 2004; Schori et al. 2013). Although, the LAMP test is more tolerant due to the Bst polymerase's greater tolerance to inhibitory substances (Tomlinson et al. 2010; Francois et al. 2011; Yang et al. 2014). The test with field plants confirmed the absence of non-specific amplifications attributable to the endophytic populations present within those plants. Although the present work did not assess the genera or species of endophytic microorganisms, prior publications have demonstrated a substantial diversity of bacteria on cassava plants. Hong et al. (2020), using high-throughput sequencing, identified up to 405 different operational taxonomic units among cassava plants. Additionally, Melo et al. (2009), employing culture media to assess diversity, identified up to 67 isolates in 19 genera of bacteria within a limited number of plant samples (6).

This work demonstrated a sensitive, user-friendly technique that can be used in the field without expensive equipment, complex procedures, DNA extraction or preliminary treatment to eliminate inhibitory chemical compounds from the sample.

## References

- Adriko, J., Mbega, E. R., Mortensen, C. N., Wulff, E. G., Tushemereirwe, W. K., Kubiriba, J., et al. 2014. Improved PCR for identification of members of the genus *Xanthomonas*. Eur J Plant Pathol. 138:293–306.
- Alič, Š., Dermastia, M., Burger, J., Dickinson, M., Pietersen, G., Pietersen, G., et al. 2022. Genome-Informed Design of a LAMP Assay for the Specific Detection of the Strain of ‘*Candidatus Phytoplasma asteris*’ Phytoplasma Occurring in Grapevines in South Africa. Plant Dis. 106:2927–2939.
- Amoia, S. S., Loconsole, G., Ligorio, A., Pantazis, A. K., Papadakis, G., Gizeli, E., et al. 2023. A Colorimetric LAMP Detection of *Xylella fastidiosa* in Crude Alkaline Sap of Olive Trees in Apulia as a Field-Based Tool for Disease Containment. Agriculture (Switzerland). 13.
- Arrieta-Ortiz, M. L., Rodríguez-R, L. M., Pérez-Quintero, Á. L., Poulin, L., Díaz, A. C., Rojas, N. A., et al. 2013. Genomic survey of pathogenicity determinants and VNTR markers in the cassava bacterial pathogen *Xanthomonas axonopodis* pv. *manihotis* strain CIO151. PLoS One. 8.
- Behnam, B., Bohorquez-Chaux, A., Castaneda-Mendez, O. F., Tsuji, H., Ishitani, M., and Becerra Lopez-Lavalle, L. A. 2019. An optimized isolation protocol yields high-quality RNA from cassava tissues (*Manihot esculenta* Crantz). FEBS Open Bio. 9:814–825.
- Bernal-Galeano, V., Ochoa, J. C., Trujillo, C., Rache, L., Bernal, A., and López, C. A. 2018. Development of a multiplex nested PCR method for detection of *Xanthomonas axonopodis* pv. *manihotis* in Cassava. Trop Plant Pathol. 43:341–350.
- Buddhachat, K., Ritbamrung, O., Sripairoj, N., Inthima, P., Ratanasut, K., Boonsrangsom, T., et al. 2021. One-step colorimetric LAMP (cLAMP) assay for visual detection of *Xanthomonas oryzae* pv. *oryzae* in rice. Crop Protection. 150.

- Çelik, A. 2022. A novel technology for the one-step detection of *prune dwarf virus*: Colorimetric reverse transcription loop-mediated isothermal amplification assay. Crop Prot. 155.
- Cerqueira-Melo, R. de C., Bragança, C. A. D., Pestana, K. N., da Silva, H. S. A., Ferreira, C. F., and de Oliveira, S. A. S. 2019. Improvement of the specific detection of *Xanthomonas phaseoli* pv. *manihotis* based on the *pthb* gene. Acta Sci Agron. 41.
- Chen, Z. D., Kang, H. J., Chai, A. L., Shi, Y. X., Xie, X. W., Li, L. and Li, B. J. 2020. Development of a loop-mediated isothermal amplification (LAMP) assay for rapid detection of *Pseudomonas syringae* pv. *tomato* in planta. Eur. J. Plant Pathol. 156: 739–750.
- Choudhary, P., Rai, P., Yadav, J., Verma, S., Chakdar, H., Goswami, S. K., et al. 2020. A rapid colorimetric LAMP assay for detection of *Rhizoctonia solani* AG-1 IA causing sheath blight of rice. Sci Rep. 10.
- Cohn, M., Bart, R. S., Shybut, M., Dahlbeck, D., Gomez, M., Morbitzer, R., et al. 2014. *Xanthomonas axonopodis* virulence is promoted by a transcription activator-like effector - Mediated induction of a SWEET sugar transporter in Cassava. Mol Plant Microbe In. 27:1186–1198.
- Dobhal, S., Larrea-Sarmiento, A., Alvarez, A. M., and Arif, M. 2019. Development of a loop-mediated isothermal amplification assay for specific detection of all known subspecies of *Clavibacter michiganensis*. J Appl Microbiol. 126:388–401.
- Demeuse, K. L., Grode, A. S., and Szendrei, Z. 2016. Comparing qPCR and nested PCR diagnostic methods for aster yellows phytoplasma in aster leafhoppers. Plant Dis. 100:2513–2519.
- Domingo, R., Perez, C., Klair, D., Vu, H., Candelario-Tochiki, A., Wang, X., et al. 2021. Genome-informed loop-mediated isothermal amplification assay for specific detection of *Pectobacterium parmentieri* in infected potato tissues and soil. Sci Rep. 11.
- Feng W., Hieno A., Kusunoki M., Suga H., and Kageyama K. 2019. LAMP Detection of Four Plant-Pathogenic Oomycetes and Its Application in Lettuce Fields. Plant Dis. 103:298-307.
- Flores, C., Zarate, C., Triplett, L., Maillot-Lebon, V., Moufid, Y., Kanté, M., et al. 2019. Development of a duplex-PCR for differential diagnosis of *Xanthomonas phaseoli* pv. *manihotis* and *Xanthomonas cassavae* in cassava (*Manihot esculenta*). Physiol Mol Plant Pathol. 105:34–46.

- Francois, P., Tangomo, M., Hibbs, J., Bonetti, E. J., Boehme, C. C., Notomi, T., et al. 2011. Robustness of a loop-mediated isothermal amplification reaction for diagnostic applications. FEMS Immunol Med Microbiol. 62:41–48.
- Gétaz, M., Bühlmann, A., Schneeberger, P. H. H., Van Malderghem, C., Duffy, B., Maes, M., Pothier, J. F. and Cottyn, B. 2017. A diagnostic tool for improved detection of *Xanthomonas fragariae* using a rapid and highly specific LAMP assay designed with comparative genomics. Plant Pathol. 66: 1094-1102.
- Hodgetts, J., Hall J., Karamura, G., Grant, M., Studholme, D. J., Boonham, N., Karamura, E. and Smith, J.J. 2015. Rapid, specific, simple, in-field detection of *Xanthomonas campestris* pathovar *musacearum* by loop-mediated isothermal amplification. J. Appl. Microbiol. 119: 1651–1658.
- Kado, C. I., and Heskett, M. G. 1970. Selective media for isolation of *Agrobacterium*, *Corynebacterium*, *Erwinia*, *Pseudomonas*, and *Xanthomonas*. Phytopathology. 60:969–976.
- Larrea-Sarmiento, A., Dhakal, U., Boluk, G., Fatdal, L., Alvarez, A., Strayer-Scherer, A., et al. 2018. Development of a genome-informed loop-mediated isothermal amplification assay for rapid and specific detection of *Xanthomonas euvesicatoria*. Sci Rep. 8.
- Li, H., Yan, C., Tang, Y., Ma, X., Chen, Y., Chen, S., & Liu, Z. 2020. Endophytic bacterial and fungal microbiota in different cultivars of cassava (*Manihot esculenta* Crantz). J. Microbiol 58:614-623.
- Mahuku, G. S. 2004. A Simple Extraction Method Suitable for PCRBased Analysis of Plant, Fungal, and Bacterial DNA. Plant Mol Biol Report. 22:71–81.
- Mansfield, J., Genin, S., Magori, S., Citovsky, V., Sriariyanum, M., Ronald, P., et al. 2012. Top 10 plant pathogenic bacteria in molecular plant pathology. Mol Plant Pathol. 13:614–629.
- Melo, F.M., Fiore, M.F., Moraes, L.A., Silva-Stenico, M.E., Scramin, S., Teixeira, M.D., Melo, I.S. 2009. Antifungal compound produced by the cassava endophyte *Bacillus pumilus* MAIIIM4A. Sci Agric. 66:583-592.
- Ojeda, S., and Verdier, V. 2000. Detecting *Xanthomonas axonopodis* pv. *manihotis* in cassava true seeds by nested polymerase chain reaction assay. Can J Plant Pathol. 22:241–247.
- Olarinde, L. O., Abass, A. B., Abdoulaye, T., Adepoju, A. A., Adio, M. O., Fanifosi, E. G., et al. 2020. The influence of social networking on food security status of cassava farming households in Nigeria. Sustainability (Switzerland). 12.

- Omer, Z. S., Wallenhammar, A. C., and Viketoft, M. 2022. Development of Loop-Mediated Isothermal Amplification Assay for Rapid Detection and Analysis of the Root-Knot Nematode *Meloidogyne hapla* in Soil. Horticulturae. 8.
- Page, A. J., Cummins, C. A., Hunt, M., Wong, V. K., Reuter, S., Holden, M. T. G., et al. 2015. Roary: Rapid large-scale prokaryote pan genome analysis. Bioinformatics. 31:3691–3693.
- Panno, S., Matić, S., Tiberini, A., Caruso, A. G., Bella, P., Torta, L., et al. 2020. Loop mediated isothermal amplification: Principles and applications in plant virology. Plants. 9.
- Parmar, A., Sturm, B., and Hensel, O. 2017. Crops that feed the world: Production and improvement of cassava for food, feed, and industrial uses. Food Secur. 9:907–927.
- Russell, R., and Paterson, M. 2004. The isoepoxydon dehydrogenase gene of patulin biosynthesis in cultures and secondary metabolites as candidate PCR inhibitors. Mycol Res. 108:1431–1437.
- Santos, M. N., Zárate-Salazar, J. R., de Carvalho, R., and Albuquerque, U. P. 2020. Intraspecific variation, knowledge and local management of cassava (*Manihot esculenta* Crantz) in the semiarid region of Pernambuco, Northeast Brazil. Environ Dev Sustain. 22:2881–2903.
- Schori, M., Appel, M., Kitko, A., and Showalter, A. M. 2013. Engineered DNA Polymerase Improves PCR Results for Plastid DNA. Appl Plant Sci. 1:1200519.
- Seemann, T. 2014. Prokka: Rapid prokaryotic genome annotation. Bioinformatics. 30:2068–2069.
- Shang, Y., Ye, Q., Cai, S., Wu, Q., Pang, R., Yang, S., et al. 2021. Loop-mediated isothermal amplification (LAMP) for rapid detection of *Salmonella* in foods based on new molecular targets. LWT. 142.
- Stehlíková, D., Beran, P., Cohen, S. P., and Čurn, V. 2020. Development of real-time and colorimetric loop mediated isothermal amplification assay for detection of *Xanthomonas gardneri*. Microorganisms. 8:1–12.
- Thomsen, M. C. F., Hasman, H., Westh, H., Kaya, H., and Lund, O. 2017. RUCS: Rapid identification of PCR primers for unique core sequences. Bioinformatics. 33:3917–3921.
- Tomlinson, J. A., Dickinson, M. J., and Boonham, N. 2010. Detection of *Botrytis cinerea* by loop-mediated isothermal amplification. Lett Appl Microbiol. 51:650–657.

Verdier, V., Mosquera, G., and Assigbésé, K. 1998. Detection of the Cassava Bacterial Blight Pathogen, *Xanthomonas axonopodis* pv. *manihotis*, by Polymerase Chain Reaction. Plant Dis. 82:79–83.

Wang Z., Zhu Y., Li Z., Yang X., Zhang T., and Zhou G. 2019. Development of a Specific Polymerase Chain Reaction System for the Detection of Rice Orange Leaf Phytoplasma. Plant Dis. 104:521-526.

Xu, J., Aileni, M., Abbagani, S., and Zhang, P. 2010. A reliable and efficient method for total RNA isolation from various members of spurge family (Euphorbiaceae). Phytochem Anal. 21:395–398.

Yang, Q., Wang, F., Prinyawiwatkul, W., and Ge, B. 2014. Robustness of *Salmonella* loop-mediated isothermal amplification assays for food applications. J Appl Microbiol. 116:81–88.

Zárate-Chaves, C. A., Osorio-Rodríguez, D., Mora, R. E., Pérez-Quintero, Á. L., Dereeper, A., Restrepo, S., et al. 2021. TAL Effector Repertoires of Strains of *Xanthomonas phaseoli* pv. *manihotis* in Commercial Cassava Crops Reveal High Diversity at the Country Scale. Microorganisms. 9:1–26 Available at: <https://doi.org/10.3390/microorganisms>.

## Supplementary material

**Table S1.** List of bacterial species, pathovars and isolate names used on the comparative genomics for the selection of regions for LAMP primer design.

Bacterial species and pathovar	Isolate	Accession	Country of origin
<i>Xanthomonas arboricola</i>	17	CP011256.1	-
<i>Xanthomonas campestris</i> pv. <i>campestris</i>	ATCC33913	AE008922.1	United Kingdom
<i>Xanthomonas cassavae</i>	CFBP4642	GCA_020783895.1	Malawi
<i>Xanthomonas citri</i> pv. <i>phaseoli</i>	CFBP4885	CP020992.2	France
<i>Xanthomonas euvesicatoria</i>	LMG930	CP018467.1	USA
<i>Xanthomonas euvesicatoria</i> pv. <i>alfafae</i>	CM002261	CM002261.1	Sudan
<i>Xanthomonas euvesicatoria</i> pv. <i>allii</i>	CFBP6369	CM002866.1	Reunion
<i>Xanthomonas euvesicatoria</i> pv. <i>citrumelo</i>	F1	CP002914.1	-
<i>Xanthomonas euvesicatoria</i> pv. <i>perforans</i>	LH3	CP018475.1	Mauritius
<i>Xanthomonas euvesicatoria</i> pv. <i>perforans</i>	91-118	CP019725.1	-
<i>Xanthomonas fragariae</i>	Fap21	CP016830.1	USA
<i>Xanthomonas oryzae</i> pv. <i>oryzae</i>	AUST2013	CP033196.1	Australia
<i>Xanthomonas phaseoli</i> pv. <i>dieffenbachiae</i>	NCPPB1833	GCA_017746675.1	Brazil
<i>Xanthomonas phaseoli</i> pv. <i>manihotis</i>	AFNC1360	GCA_000265785.1	Nigeria
<i>Xanthomonas phaseoli</i> pv. <i>manihotis</i>	LMG784	GCA_001482665.1	Brazil
<i>Xanthomonas phaseoli</i> pv. <i>manihotis</i>	KHM01	GCA_015352415.1	Cambodia
<i>Xanthomonas phaseoli</i> pv. <i>manihotis</i>	GX08	NZ_JADKPW000000000.1	China
<i>Xanthomonas phaseoli</i> pv. <i>manihotis</i>	CFBP7153= IBSBF 278	GCA_017745335.1	-
<i>Xanthomonas phaseoli</i> pv. <i>manihotis</i>	NBC1264	GCA_017745415.1	-
<i>Xanthomonas phaseoli</i> pv. <i>manihotis</i>	NBC1265	GCA_017745455.1	-

<i>Xanthomonas phaseoli</i> pv. <i>manihotis</i>	NBC1192	GCA_017745475.1	Malaysia
<i>Xanthomonas phaseoli</i> pv. <i>manihotis</i>	NBC1194	GCA_017745505.1	Zaire
<i>Xanthomonas phaseoli</i> pv. <i>manihotis</i>	IBSBF2818	GCA_000266105.2	Brazil
<i>Xanthomonas phaseoli</i> pv. <i>manihotis</i>	CIO151	GCA_000265845.1	Colombia
<i>Xanthomonas phaseoli</i> pv. <i>manihotis</i>	AT6B	GCA_000265765.1	Venezuela
<i>Xanthomonas phaseoli</i> pv. <i>manihotis</i>	CFBP1851	GCA_000265805.1	Colombia
<i>Xanthomonas phaseoli</i> pv. <i>manihotis</i>	CIO151	GCA_004025275.1	Colombia
<i>Xanthomonas phaseoli</i> pv. <i>manihotis</i>	CIO1	GCA_000265825.1	Colombia
<i>Xanthomonas phaseoli</i> pv. <i>manihotis</i>	IBSBF1182	GCA_000265865.1	Brazil
<i>Xanthomonas phaseoli</i> pv. <i>manihotis</i>	IBSBF1411	GCA_000265885.1	Brazil
<i>Xanthomonas phaseoli</i> pv. <i>manihotis</i>	IBSBF1994	GCA_000265905.1	Brazil
<i>Xanthomonas phaseoli</i> pv. <i>manihotis</i>	IBSBF2345	GCA_000265925.1	Brazil
<i>Xanthomonas phaseoli</i> pv. <i>manihotis</i>	IBSBF2346	GCA_000265925.1	Brazil
<i>Xanthomonas phaseoli</i> pv. <i>manihotis</i>	IBSBF2538	GCA_000265965.1	Brazil
<i>Xanthomonas phaseoli</i> pv. <i>manihotis</i>	IBSBF2539	GCA_000265985.1	Brazil
<i>Xanthomonas phaseoli</i> pv. <i>manihotis</i>	IBSBF2665	GCA_000265645.1	Brazil
<i>Xanthomonas phaseoli</i> pv. <i>manihotis</i>	IBSBF2666	GCA_000265625.1	Brazil
<i>Xanthomonas phaseoli</i> pv. <i>manihotis</i>	IBSBF2667	GCA_000266745.1	Brazil
<i>Xanthomonas phaseoli</i> pv. <i>manihotis</i>	IBSBF2670	GCA_000266765.1	Brazil
<i>Xanthomonas phaseoli</i> pv. <i>manihotis</i>	IBSBF2672	GCA_000266005.1	Brazil
<i>Xanthomonas phaseoli</i> pv. <i>manihotis</i>	IBSBF2673	GCA_000266025.1	Brazil
<i>Xanthomonas phaseoli</i> pv. <i>manihotis</i>	IBSBF278	GCA_000266045.1	Brazil
<i>Xanthomonas phaseoli</i> pv. <i>manihotis</i>	IBSBF280	GCA_000266065.1	Brazil
<i>Xanthomonas phaseoli</i> pv. <i>manihotis</i>	IBSBF2816	GCA_000266085.1	Brazil
<i>Xanthomonas phaseoli</i> pv. <i>manihotis</i>	IBSBF2819	GCA_000266125.1	Brazil

<i>Xanthomonas phaseoli</i> pv. <i>manihotis</i>	IBSBF2820	GCA_000266145.1	Brazil
<i>Xanthomonas phaseoli</i> pv. <i>manihotis</i>	IBSBF2821	GCA_000266165.1	Brazil
<i>Xanthomonas phaseoli</i> pv. <i>manihotis</i>	IBSBF2822	GCA_000266185.1	Brazil
<i>Xanthomonas phaseoli</i> pv. <i>manihotis</i>	IBSBF285	GCA_000266205.1	Nigeria
<i>Xanthomonas phaseoli</i> pv. <i>manihotis</i>	IBSBF289	GCA_000266225.1	Brazil
<i>Xanthomonas phaseoli</i> pv. <i>manihotis</i>	IBSBF320	GCA_000265745.1	Brazil
<i>Xanthomonas phaseoli</i> pv. <i>manihotis</i>	IBSBF321	GCA_000265665.1	Brazil
<i>Xanthomonas phaseoli</i> pv. <i>manihotis</i>	IBSBF356	GCA_000265725.1	Brazil
<i>Xanthomonas phaseoli</i> pv. <i>manihotis</i>	IBSBF436	GCA_000265685.1	Brazil
<i>Xanthomonas phaseoli</i> pv. <i>manihotis</i>	IBSBF614	GCA_000266785.1	Brazil
<i>Xanthomonas phaseoli</i> pv. <i>manihotis</i>	IBSBF725	GCA_000266245.1	Brazil
<i>Xanthomonas phaseoli</i> pv. <i>manihotis</i>	IBSBF726	GCA_000266265.1	Brazil
<i>Xanthomonas phaseoli</i> pv. <i>manihotis</i>	NCPPB1159	GCA_000266285.1	Brazil
<i>Xanthomonas phaseoli</i> pv. <i>manihotis</i>	NG1	GCA_000266285.1	Nigeria
<i>Xanthomonas phaseoli</i> pv. <i>manihotis</i>	ORST17	GCA_000265605.1	Republic of the Congo
<i>Xanthomonas phaseoli</i> pv. <i>manihotis</i>	ORST4	GCA_000266305.1	Colombia
<i>Xanthomonas phaseoli</i> pv. <i>manihotis</i>	ORSTX27	GCA_000266325.1	Togo
<i>Xanthomonas phaseoli</i> pv. <i>manihotis</i>	ThaiXam	GCA_000266345.1	Thailand
<i>Xanthomonas phaseoli</i> pv. <i>manihotis</i>	UA226	GCA_000265585.1	Colombia
<i>Xanthomonas phaseoli</i> pv. <i>manihotis</i>	UA303	GCA_000265565.1	Colombia
<i>Xanthomonas phaseoli</i> pv. <i>manihotis</i>	UA306	GCA_000266825.1	Colombia
<i>Xanthomonas phaseoli</i> pv. <i>manihotis</i>	UA323	GCA_000266805.1	Colombia
<i>Xanthomonas phaseoli</i> pv. <i>manihotis</i>	UA324	GCA_000266845.1	Colombia
<i>Xanthomonas phaseoli</i> pv. <i>manihotis</i>	UA536	GCA_000266365.1	Colombia
<i>Xanthomonas phaseoli</i> pv. <i>manihotis</i>	UA556	GCA_000266385.1	Colombia

<i>Xanthomonas phaseoli</i> pv. <i>manihotis</i>	UA560	GCA_000266405.1	Colombia
<i>Xanthomonas phaseoli</i> pv. <i>manihotis</i>	UA686	GCA_000266425.1	Colombia
<i>Xanthomonas phaseoli</i> pv. <i>manihotis</i>	UG21	GCA_000266445.1	Uganda
<i>Xanthomonas phaseoli</i> pv. <i>manihotis</i>	UG23	GCA_000266465.1	Uganda
<i>Xanthomonas phaseoli</i> pv. <i>manihotis</i>	UG24	GCA_000266485.1	Uganda
<i>Xanthomonas phaseoli</i> pv. <i>manihotis</i>	UG27	GCA_000266505.1	Uganda
<i>Xanthomonas phaseoli</i> pv. <i>manihotis</i>	UG28	GCA_000266525.1	Uganda
<i>Xanthomonas phaseoli</i> pv. <i>manihotis</i>	UG39	GCA_000266545.1	Uganda
<i>Xanthomonas phaseoli</i> pv. <i>manihotis</i>	UG43	GCA_000266565.1	Uganda
<i>Xanthomonas phaseoli</i> pv. <i>manihotis</i>	UG44	GCA_000266585.1	Uganda
<i>Xanthomonas phaseoli</i> pv. <i>manihotis</i>	UG45	GCA_000266605.1	Uganda
<i>Xanthomonas phaseoli</i> pv. <i>manihotis</i>	UG51	GCA_000266625.1	Uganda
<i>Xanthomonas phaseoli</i> pv. <i>manihotis</i>	Xam1134	GCA_000266645.1	-
<i>Xanthomonas phaseoli</i> pv. <i>manihotis</i>	Xam668	GCA_000266665.1	Indonesia
<i>Xanthomonas phaseoli</i> pv. <i>manihotis</i>	Xam669	GCA_000266685.1	Brazil
<i>Xanthomonas phaseoli</i> pv. <i>manihotis</i>	Xam672	GCA_000266705.1	Cameroon
<i>Xanthomonas phaseoli</i> pv. <i>manihotis</i>	Xam678	GCA_000266725.1	Republic of the Congo
<i>Xanthomonas phaseoli</i> pv. <i>phaseoli</i>	Xcp25	CP029284.1	USA
<i>Xanthomonas phaseoli</i> pv. <i>syngonii</i>	LMG9055	GCA_001412025.2	USA
<i>Xanthomonas sacchari</i>	R1	CP010409.1	China
<i>Xanthomonas translucens</i> pv. <i>undulosa</i>	Xtu4699	CP008714.1	USA
<i>Xanthomonas vesicatoria</i>	LMG911	CP018725.1	New Zealand

**1:50 dilution from multiplex-PCR product**

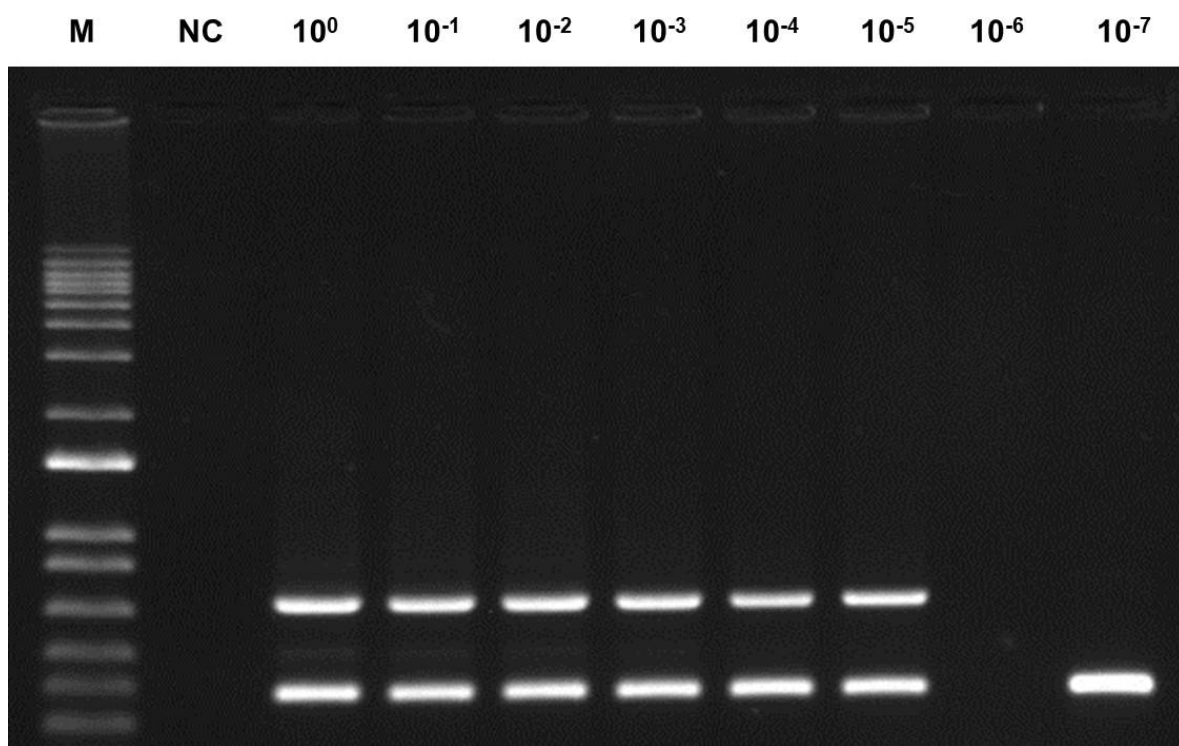


**Figure S1.** Multiplex nested-PCR with primers by Bernal-Galeano et al. (2018) to assess the concentration limit of detection using a genomic DNA dilution of *Xanthomonas phaseoli* pv. *manihotis* type strain IBSBF 278 ranging from 10 ng ( $10^7$  fg) to 1 fg. M: DNA Ladder 1 kb Plus (Invitrogen), NC: Negative control.

## **CAPÍTULO 3**

---

---

**Resistance classification to bacterial blight (*Xanthomonas phaseoli* pv. *manihotis*) in cultivars, clones and accessions of Brazilian cassava (*Manihot esculenta*) based on a new qualitative ordinal scale**

**Resistance classification to bacterial blight (*Xanthomonas phaseoli* pv. *manihotis*) in cultivars, clones and accessions of Brazilian cassava (*Manihot esculenta*) based on a new qualitative ordinal scale**

Ian Carlos Bispo Carvalho<sup>1</sup>, Henrique Povoa Rodrigues Lima<sup>1</sup>, Alice Maria Silva Carvalho<sup>1</sup>, Eduardo Alano Vieira<sup>2</sup>, Valdir Lourenço Jr.<sup>3</sup>, Maurício Rossato<sup>1\*</sup>

<sup>1</sup>Universidade de Brasília, Brasília, Distrito Federal, Brazil

<sup>2</sup>Embrapa Cerrados, Planaltina, Distrito Federal, Brazil

<sup>3</sup>Embrapa Hortaliças, Brasília, Distrito Federal, Brazil

\*Corresponding Author: Maurício Rossato; E-mail: mauricio.rossato@unb.br

Funding: FAP-DF Grant Number: 00193-00000868/2021-96

## **Abstract**

Cassava (*Manihot esculenta* Crantz) is a staple food for over 800 million people. However, its production can be severely impacted by various diseases caused by viruses, fungi, and bacteria. One major bacterial disease is cassava bacterial blight (CBB), caused by *Xanthomonas phaseoli* pv. *manihotis* (Xpm). The objective of this study was to classify 11 cassava genotypes (cultivars, clones and accessions) according to resistance types using a new ordinal qualitative scale. Isolate UnB 17 of Xpm, from Pará state (Brazil) and highly virulent to cassava variety BGMC 962, was cultivated and inoculated by spraying  $10^8$  CFU mL<sup>-1</sup> into plants. All inoculated and mock-inoculated plants were kept in moist chamber for three days, followed by greenhouse conditions for the rest of the experiment/evaluations. Evaluations were conducted at a 5-day interval after inoculation. Visual symptomatology criterion was adopted based on the intensity of symptoms. The data obtained from the rating scale were used to calculate the Area Under the Disease Progress Curve (AUDPC). From the hierarchical clustering and the Elbow method, three distinct groups were identified: moderately resistant, moderately susceptible, and susceptible to the disease. No genotype exhibited complete resistance, as all evaluated genotype showed typical symptoms of bacterial blight. This study highlights the need for multiple trials under different periods and environmental conditions to gain a more comprehensive understanding of genotype's behavior regarding resistance and susceptibility.

**Keywords:** Bacterial blight, *Manihot esculenta*, plant pathogen

## **Introduction**

Cassava (*Manihot esculenta* Crantz) is one of the world's primary sources of carbohydrates, serving as a staple food for over 800 million people (Nassar et al. 2009; Burns et al. 2010). Belonging to the Euphorbiaceae family, cassava's center of origin is in South America, specifically in the tropical lowlands along the southern edge of the Amazon basin (Olsen and Schaal 1999; Wang et al. 2014). This crop stands out for its good drought tolerance, low input requirements, and resilience, especially when compared to other agricultural species, and is predominantly cultivated by small-scale farmers (Parmar et al. 2017; Santos et al. 2020; Olarinde et al. 2020).

Brazil is the sixth-largest producer of cassava globally, with a total production estimated at approximately 17.64 million tons, surpassed only by Nigeria, the Democratic Republic of the Congo, Thailand, Ghana, and Cambodia (FAO, 2022). Despite the global significance of this crop, its production can be threatened by the presence of diseases. Cassava bacterial blight (CBB), caused by *Xanthomonas phaseoli* pv. *manihotis* (Xpm), is one of the major diseases affecting the crop, leading to significant losses if not properly managed (Mansfield et al. 2012; Zárate-Chaves et al. 2021). Xpm has been considered one of the most important plant-pathogenic bacteria worldwide due to its economic and scientific relevance (Mansfield et al. 2012).

Effective management of CBB is challenging due to pathogen's genetic diversity, which allows it to adapt to different environmental conditions and develop resistance to copper (Trujillo et al. 2014; Shi et al. 2023). As a result, genetic host resistance emerges as a crucial approach for controlling this disease. Resistant plants possess mechanisms that inhibit or delay the pathogen's development within plant tissues, which is essential for minimizing the negative impacts of the disease on crops (Jones and Dangl 2006; Andersen et al. 2018). This resistance can be either quantitative or qualitative, depending on the genes involved and their interaction with the pathogen (Jorge and Verdier 2002; Mora et al. 2019; Díaz-Tatis et al. 2022).

In Brazil, it was identified only one cassava genotype resistant to CBB (BGMC 434) in two separate trials (Teixeira et al. 2021; Aquiles et al. 2021). These results highlight the ongoing need for CBB-resistant varieties and underscore the importance of understanding the ability of cassava cultivars to prevent or suppress infection and colonization of the plant by the pathogen.

The evaluation of plant resistance to pathogens can be conducted in two ways: greenhouse or field trials. While field tests are considered the ultimate measure of resistance, greenhouse screenings provide reliable data for a quick screening. The use of specific strains is particularly valuable for investigating distinct interactions within the cassava-Xpm pathosystem. (Jorge et al. 2000).

Therefore, the objective of this study was to evaluate different cassava genotypes (cultivars, clones and accessions) according to resistance types using a new ordinal qualitative scale. The goal is to identify promising accessions for use in future cassava breeding programs.

## **Material and methods**

The experiment was conducted in the greenhouse at the Experimental Station of the Institute of Biological Sciences at the University of Brasília. For the resistance study, seven sweet cassava cultivars (Vieira et al. 2011, 2018, 2019, 2022), two cassava elite clones from Embrapa Cerrados cassava breeding program, and two accessions of sweet cassava conserved in the regional cassava germplasm collection of the Cerrado biome (BGMC) were used (Table 1). The propagation material consisted of mini-cuttings with two buds and a length of four to six centimeters. The propagation materials for each selected genotype were sanitized in a 5% sodium hypochlorite solution and water for 5 minutes to eliminate potential surface contaminants. The cassava cuttings were planted in 2 L aluminum pots (one cutting per pot) with autoclaved red latosol and N-P-K fertilizer, following the recommended guidelines for cassava cultivation (Fialho et al., 2017).

**Table 1.** Cassava genotypes evaluated for resistance to *Xanthomonas phaseoli* pv. *manihotis*.

Nº	Genotypes	Cassava type	Pulp color
1	BRS 398	Sweet	Cream
2	BRS 399	Sweet	Yellow
3	Clone 54/10	Sweet	Yellow
4	Clone 1097/13	Industry flour and/or starch	White
5	BRS 400	Sweet	Pink
6	BRS 401	Sweet	Pink
7	BRS 418	Industry flour and/or starch	White
8	BRS 429	Sweet	Yellow
9	BRS Japonesa	Sweet	Yellow
10	BGMC 434	Sweet	White
11	BGMC 962	Sweet	White

Two independent experiments were conducted at different times. A randomized block design was used, with 11 cassava genotypes and three replicates, totaling 33 plots. Each plot consisted of four plants, resulting in 132 plants per experiment.

Isolate UnB 17 of Xpm, highly virulent to cassava variety BGMC 962 and collected in Pará State was identified due its typical morphology and by multiplex nested PCR technique using Cterm and rpoB regions by Bernal-Galeano et al. (2018). The inoculum was prepared using 523 culture medium (Kado and Heskett 1970) and incubated at 28°C for 48 hours in a growth chamber. A bacterial suspension was then prepared in distilled water. An absorbance of 0.350 (550 nm) corresponded to a bacterial concentration of  $10^8$  CFU mL<sup>-1</sup> (Aquiles et al. 2021).

Six weeks after planting the cuttings, the plants were inoculated by spraying the aerial parts with the bacterial suspension using a manual sprayer. The inoculated plants were kept in a moist chamber for three days and then transferred to a greenhouse, where they were monitored throughout the study period. Mock-inoculated plants (BGMC 962) treated with sterile distilled water were also maintained under the same conditions.

Evaluations were conducted at 5-day intervals following inoculation, with plants assessed 35 days post-inoculation. An ordinal qualitative scale with nine scores (0 to 8) was proposed based on the progress of the symptoms on the plant. The severity of leaf symptoms was assessed using a rating scale adapted to greenhouse from the field scale proposed by Teixeira et al. (2021), with the following categories: 0 = no symptoms; 1 = angular water-soaked lesion/spot on one-third or less of the leaves; 2 = angular water-soaked lesion/spot on more than one-third of the leaves; 3 = necrotic spots/scorch symptoms on one-third or less of the leaves; 4 = necrotic spots/scorch symptoms on more than one-third of the leaves; 5 = necrotic lesions on the stem or petiole; 6 = necrotic lesions on the stem or petiole associated with exudation; 7 = wilting associated with exudation or death of one-third or less of the plant; 8 = wilting associated with exudation or death of more than one-third of the plant.

For the AUDPC calculation, the Disease Index (DI) was determined, where the observed values assigned to the evaluated plants were converted according to McKinney (1923), using the following expression:

$$DI(\%) = 100 \times \sum \left[ \frac{(f \times v)}{(n \times x)} \right] \quad (2)$$

where f is the number of plants with the same score, v is the observed score, n is the total number of plants evaluated, and x is the maximum score on the scale. This allows for comparison between the estimated Disease Index (DI) and the resistance of the accessions.

The data obtained from DI were used to calculate the Area Under the Disease Progress Curve (AUDPC), following the methodology of Madden et al. (2007) for each genotype evaluated, according to the expression:

$$A_k = \sum_{i=1}^{N_i-1} \frac{(Y_i + Y_{i-1})}{2} (t_{i+1} - t_i) \quad (1)$$

where  $y_i$  and  $y_{i-1}$  represent the ordinal scores corresponding to the affected leaf area observed in assessments  $i$  and  $(i+1)$ , respectively;  $t_i$  and  $t_{i+1}$  represent the time considered in days  $i$  and  $(i+1)$ , respectively; and N is the total number of assessments.

## Results

Based on the AUDPC data, genotype clustering was performed using the Ward method with Euclidean distance as the dissimilarity measure. The analyses were conducted in R version 4.3.0 (R Development Core Team, 2008). The packages used were factoextra (Kassambara, 2020), readxl (Wickham and Bryan, 2023), and dendextend (Galili et al., 2023). To determine the optimal number of clusters, the Elbow method was applied by calculating the total within-cluster sum of squares (WCSS) for different values of K (number of clusters) and identifying the inflection point in the corresponding graph.

From the hierarchical clustering and the Elbow method, three distinct groups were identified: moderately resistant, moderately susceptible, and susceptible to CBB. No genotype exhibited complete resistance to the disease, as all evaluated genotypes showed typical symptoms of bacterial blight. Mock-inoculated plants showed no symptom development. Variation in the response of some genotypes was observed over the assessment periods, while others maintained stable resistance or susceptibility levels (Figure 1; Table 1). The comparison between the final score (ranging from 0 to 8), the disease index, and the AUDPC is presented in Figure 2.

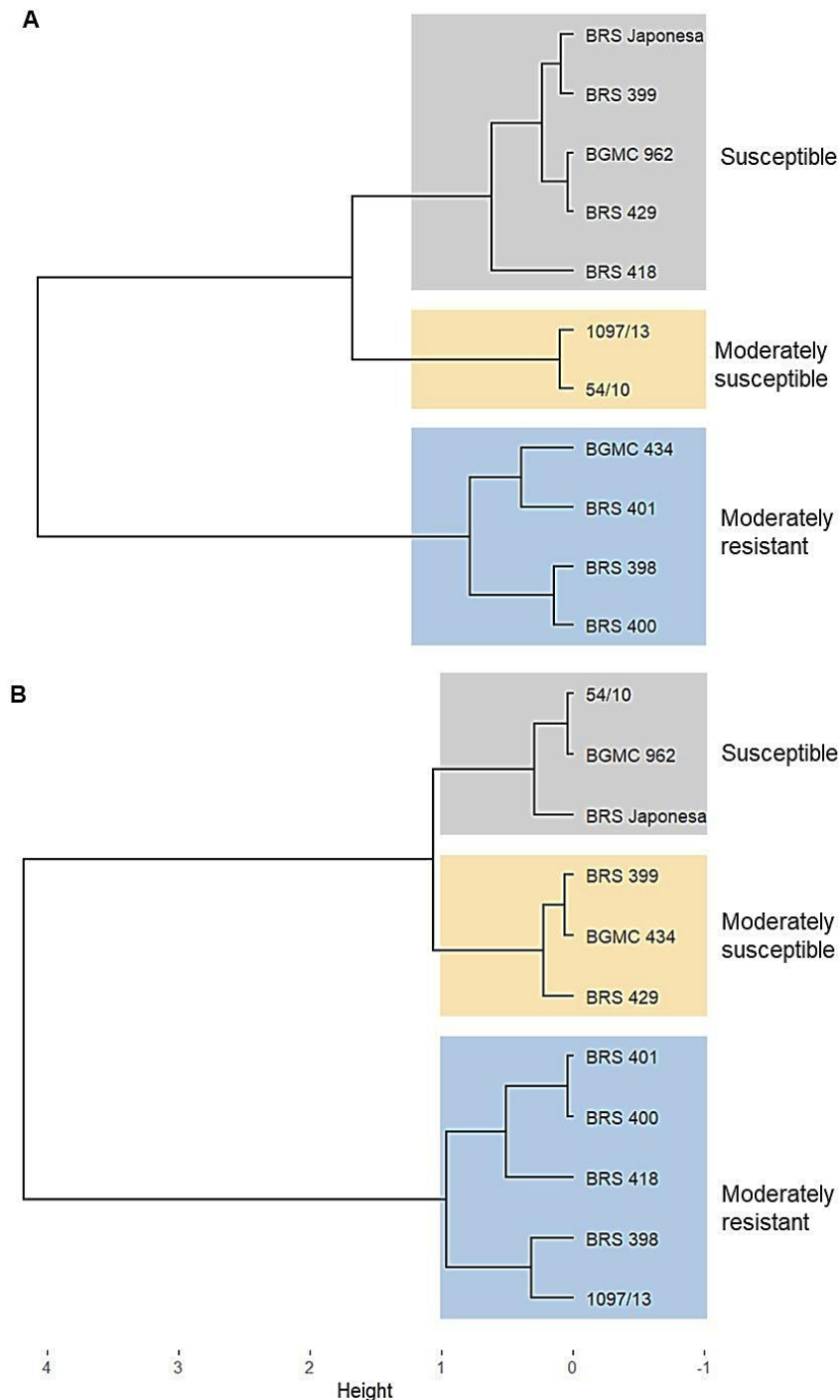


**Figure 1.** Clustering of cassava genotypes assessed for resistance to CBB in the first (A) and second (B) trials using the area under the disease progress curve.

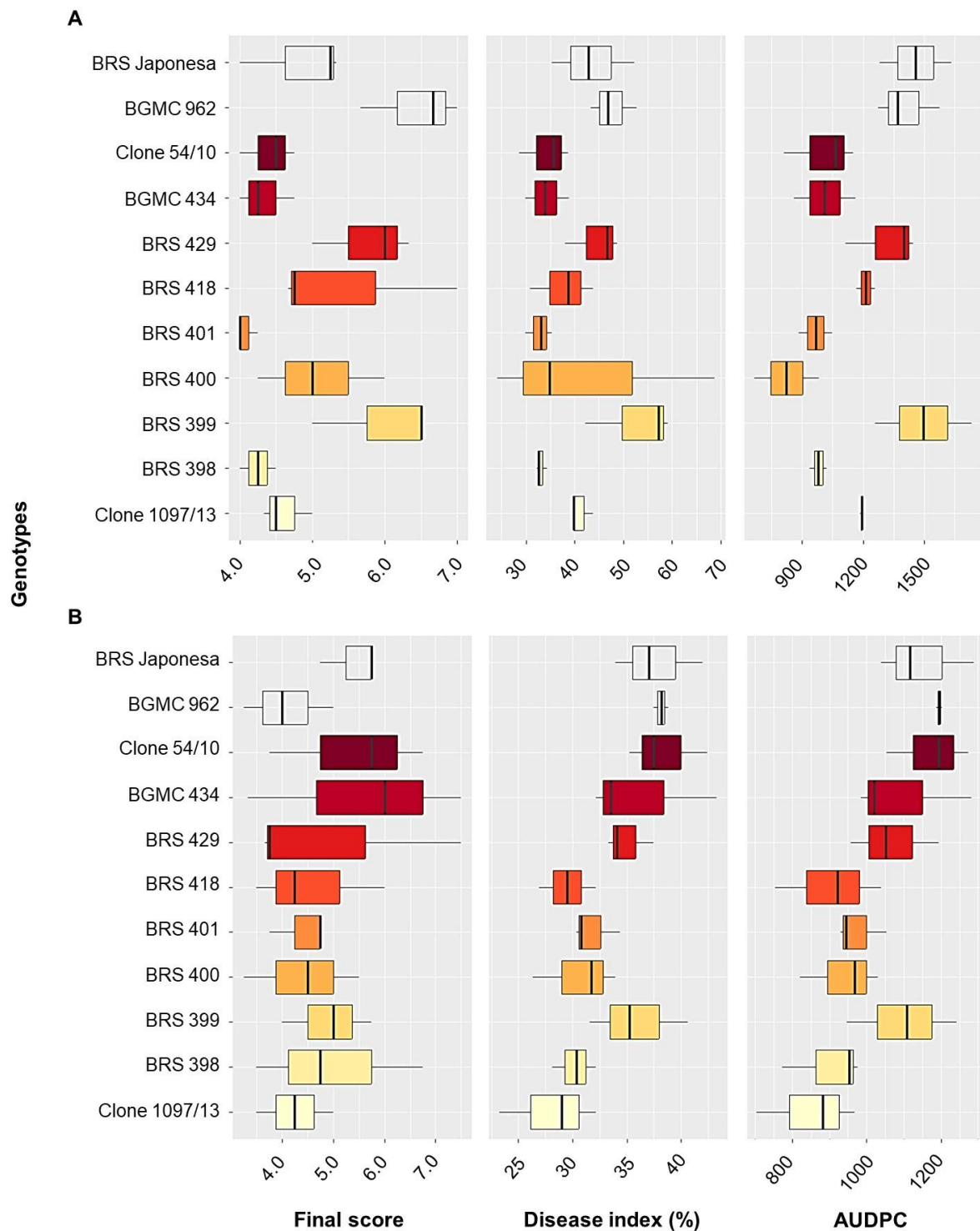


**Figure 2.** Response of different cassava genotypes to CBB in the first (A) and second (B) trials, assessed using three parameters: final score, disease index (%), and AUDPC (Area Under the Disease Progress Curve).

In the first trial, out of the 11 genotypes evaluated, four were classified as moderately resistant (BGMC 434, BRS 401, BRS 398, and BRS 400), two as moderately susceptible (clone

1097/13 and clone 54/10), and five as susceptible (BRS Japonesa, BRS 399, BRS 962, BRS 429, and BRS 418). In the second trial, five genotypes were considered moderately resistant (BRS 401, BRS 400, BRS 418, BRS 398, and clone 1097/13), three as moderately susceptible (BRS 399, BGMC 434, and BRS 429), and three as susceptible (clone 54/10, BGMC 962, and BRS Japonesa). Thus, 45.45% of the genotypes maintained their resistance classifications across both trials. Specifically, BRS 400, BRS 401, and BRS 398 were consistently classified as moderately resistant in both trials, while BGMC 962 and BRS Japonesa were susceptible in both periods. The cultivar BGMC 962 was used as a standard for susceptibility to CBB.

The AUDPC values ranged from 851.57 to 989.36 for moderately resistant genotypes, from 1008.68 to 1170.35 for moderately susceptible ones, and from 1148.43 to 1504.58 for susceptible ones.

**Table 2.** Classification of resistance levels of cassava genotypes in the first and second trials.

Genotypes	Trial	
	First	Second
BRS 400	MR	MR
BRS 401	MR	MR
BRS 398	MR	MR
BGMC 434	MR	MS
Clone 1097/13	MS	MR
Clone 54/10	MS	S
BRS 418	S	MR
BRS 429	S	MS
BRS 399	S	MS
BGMC 962	S	S
BRS Japonesa	S	S

S – Susceptible

MS – Moderately susceptible

MR – Moderately resistant

In the first trial, the average temperature was 25.23°C, and the average relative humidity was 65.11%. In the second trial, the average temperature increased to 30.22°C, relative humidity decreased to 56.70%. The average Disease Index (DI) at the first trial in susceptible

plants at 35 days was over 70% while at the second trial the average DI at 35 days was around 60%.

In the first trial (Figure 3A), the first disease symptoms were observed between 0 and 5 days after inoculation, with continuous and similar progression among the three groups [Moderately Resistant (MR), Moderately Susceptible (MS), and Susceptible (S)] until 10 days post-inoculation. After ten days, the behavior among the groups diverged, making the differences more pronounced. MR plants exhibited the lowest increase in severity values, followed by MS plants. Susceptible plants had the highest DI values.

In the second trial (Figure 3B), the results were similar across the three groups but differed from those observed in the first trial. The first symptoms appeared later, between five- and ten-days post-inoculation. Susceptible and moderately susceptible cultivars showed higher severity during this period compared to moderately resistant cultivars. Between days 20 and 30 after inoculation, susceptible plants had the highest DI values.

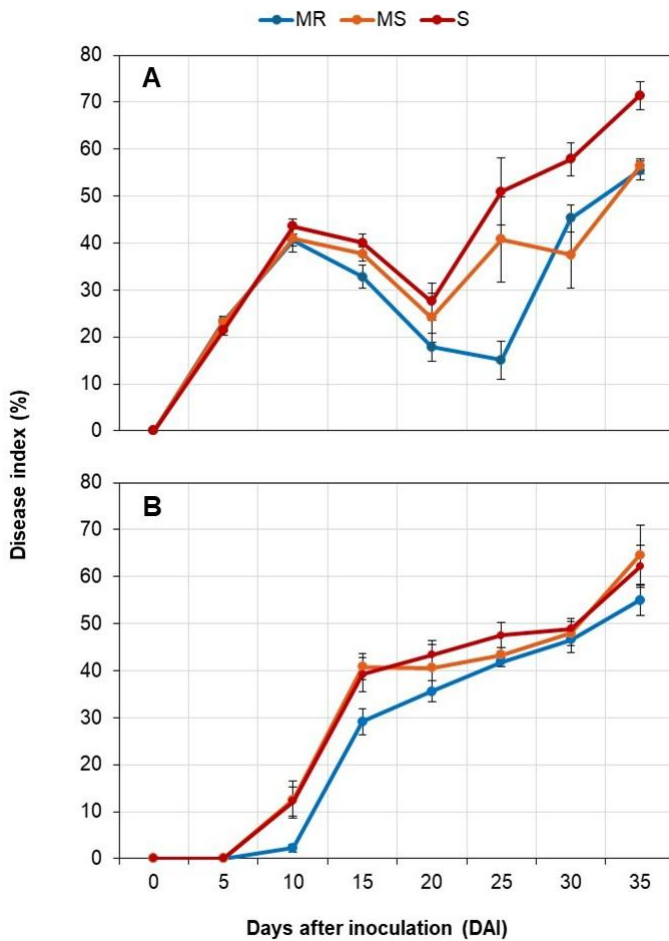


**Figure 3.** Disease progress curve of CBB in the first (A) and second (B) trials. MR, moderately resistant; MS, moderately susceptible; S, susceptible.

## Discussion

All evaluated genotypes demonstrated some level of disease severity, indicating that none of them have complete resistance to CBB. In Brazil, two independent trials were conducted to identify cassava genotypes with potential resistance to this disease. In the first study, conducted in the field, none of the tested genotypes showed complete resistance to CBB (Teixeira et al. 2021). In the second study, conducted in a greenhouse, only one of the 12 tested accessions was classified as resistant based on the average reaction to three different Xpm isolates (Aquiles et al. 2021).

The inoculation method did not seem as a limiting factor to find or not a resistant genotype, as on the present experiment, plants were inoculated by spraying bacterial suspension

into leaves, while Aquiles et al. (2021) used a far more severe method and still could identify a resistant genotype.

In pathosystems, the relationship between environment, host, and pathogen is complex and interdependent, and may or may not result in disease emergence (Velásquez et al. 2018; Singh et al. 2023; Caballol et al. 2024). Previous experiments have shown that during the vegetative period of cassava, average temperatures between 25 and 29°C and relative humidity between 59 and 85% favored rapid pathogen multiplication (Fanou et al. 2018).

In the first trial, the temperature and humidity conditions were considered ideal for bacterial development, which may have contributed to the high disease severity observed. In contrast, there was an increase in the average temperature and a decrease in average relative humidity, moving away from the ideal conditions for bacterial growth in the second trial. This resulted in a lower disease severity index at 35 days compared to the first trial.

The variation in genotype behavior over time in this experiment reveals that environmental conditions play a crucial role in disease development. However, little is known about how environmental conditions affect host response when exposed to a pathogen. Although resistance to CBB is determined by multiple genes, suggesting quantitative inheritance, there is evidence that it is strongly influenced by environmental conditions (Jorge et al. 2000; Díaz Tatis et al. 2018; Toure et al. 2020; Díaz-Tatis et al. 2022). In a study examining the transcriptional response of *Oryza sativa* infected with *Xanthomonas oryzae* pv. *oryzae*, alterations in gene expression were observed in rice plants exposed to different temperatures. As temperature increased, there was a reduction in the expression of pathogen-specific genes and pathways, while there was an increased focus on plant growth and development, including seed formation (Sahu et al. 2020).

Moreover, variations in physiological responses can occur among varieties subjected to the same environmental conditions. Based on this principle, notable differences in physiological responses were observed between a susceptible and a resistant cassava variety inoculated with

Xpm. The susceptible variety exhibited greater stomatal resistance, reduced leaf water potential, and increased proline levels compared to the resistant variety (Rubio et al. 2017a).

The lack of resistant genotypes for the breeding of resistant cassava plants to bacterial blight, highlight the need of use of other methods, as CRISPR/Cas9 to reduce the effects of Transcription activator-like (TAL) effectors of the pathogen (Elliott et al. 2024) or other disease management methods as biological control with endophytic bacteria, which was proven as effective (Ferreira et al. 2024). Additionally, this lack of resistance in cassava genotypes would lead to reliance on other disease management methods, such as copper applications. However, the discovery of copper-resistant clusters in Xpm isolates may hinder the effectiveness of this approach (Shi et al. 2023).

These results highlight the need for multiple trials under different periods and environmental conditions to gain a more comprehensive understanding of cassava genotypes' behavior regarding resistance and susceptibility.

### **Conflict of interest/competing interest statement**

The authors declare no conflict of interest.

### **Funding**

This work was funded by FAP-DF under the project number 00193-00000868/2021-96

Ian Carlos Bispo Carvalho was supported by a scholarship from CAPES

### **Authors' contribution statement**

Conceptualization: Maurício Rossato; Methodology: Ian Carlos Bispo Carvalho, Henrique Povoa Rodrigues Lima, Alice Maria Silva Carvalho; Formal analysis and investigation: Ian Carlos Bispo Carvalho, Eduardo Alano Vieira; Writing - original draft preparation: Ian Carlos Bispo Carvalho, Maurício Rossato; Writing - review and editing: Eduardo Alano Vieira, Valdir

Lourenço Jr.; Funding acquisition: Maurício Rossato; Resources: Eduardo Alano Vieira; Supervision: Maurício Rossato.

## Data availability statement

The datasets generated during and/or analysed during the current study are available from the corresponding author on reasonable request.

## References

- Andersen EJ, Ali S, Byamukama E, Yen Y, Nepal MP (2018) Disease resistance mechanisms in plants. *Genes* 9:1–27
- Aquiles KR, Marques E, Malaquias JV, Mattos JKA, Fialho JF, Vieira EA, Uesugi CH (2021) Reaction of Sweet Cassava Genotypes to *Xanthomonas phaseoli* pv. *manihotis* From Three Regions of Brazil. *Journal of Agricultural Science* 13:64–75
- Bernal-Galeano V, Ochoa JC, Trujillo C, Rache L, Bernal A, López, CA (2018) Development of a multiplex nested PCR method for detection of *Xanthomonas axonopodis* pv. *manihotis* in Cassava. *Tropical Plant Pathology* 43:341–350
- Burns A, Gleadow R, Cliff J, Zacarias A, Cavagnaro T (2010) Cassava: The drought, war and famine crop in a changing world. *Sustainability* 2:3572–3607
- Caballol M, Redondo MÁ, Catalán N, Corcobado T, Jung T, Marçais B, Milenković I, Nemesio-Gorriz M, Stenlid J, Oliva J (2024) Climate acts as an environmental filter to plant pathogens. *ISME Journal* 18:1–14
- Díaz-Tatis PA, Corzo M H, Cabezas JCO, Cipagauta A M, Prías MA, Verdier V, Aguirre PC, Carrascal CEL (2018) The overexpression of RXam1, a cassava gene coding for an RLK, confers disease resistance to *Xanthomonas axonopodis* pv. *manihotis*. *Planta* 247:1031–1042
- Díaz-Tatis PA, Ochoa JC, Rico EM, Rodríguez C, Medina A, Szurek B, Chavarriaga P, López CE (2022) RXam2, a NLR from cassava (*Manihot esculenta*) contributes partially to the quantitative resistance to *Xanthomonas phaseoli* pv. *manihotis*. *Plant Molecular Biology* 109:313–324

Elliott K, Veley KM, Jensen G, Gilbert KB, Norton J, Kambic L, Yoder M, Weil A, Motomura-Wages S, Bart RS (2024) CRISPR/Cas9-generated mutations in a sugar transporter gene reduce cassava susceptibility to bacterial blight. *Plant Physiology* 195:2566–2578

Fanou AA, Zinsou VA, Wydra K (2018) Cassava Bacterial Blight: A Devastating Disease of Cassava. In: Waisundara VY (Ed.) *Cassava*. InTech, London, pp 13–36

FAO. FAOSTAT: Crops and livestock products, 2024. Available at: <https://www.fao.org/faostat/en/#data/QCL>. Accessed on August 11, 2024

Ferreira SC, Nakasone AK, Cunha EFM, Serrão CP, Souza CRB (2024) Klebsiella endophytic bacteria control cassava bacterial blight in the eastern Amazon. *Acta Amazonica* 54

Fialho JF, Vieira EA, Borges AL (2017) Cultivo da mandioca para região do Cerrado. Embrapa Cerrados, Brasília

Galili T, O'Callaghan R, Sidi J (2023) dendextend: Extend 'dendrogram' Functionality. R package version 1.17.3. Available at: <https://cran.r-project.org/package=dendextend>. Accessed on June 02, 2024

Jones J, Dangl J (2006) The plant immune system. *Nature* 444:323–329

Jorge V, Fregene MA, Duque MC, Bonierbale MW, Tohme J, Verdier V (2000) Genetic mapping of resistance to bacterial blight disease in cassava (*Manihot esculenta* Crantz). *Theoretical and Applied Genetics* 101:865–872

Jorge V, Verdier V (2002) Qualitative and quantitative evaluation of cassava bacterial blight resistance in F1 progeny of a cross between elite cassava clones. *Euphytica* 123:41–48

Kado CI, Heskett MG (1970) Selective media for isolation of *Agrobacterium*, *Corynebacterium*, *Erwinia*, *Pseudomonas*, and *Xanthomonas*. *Phytopathology* 60:969–976

Kassambara A (2020) factoextra: Extract and Visualize the Results of Multivariate Data Analyses. R package version 1.0.7. Available at: <https://cran.r-project.org/package=factoextra>. Accessed on June 02, 2024

Madden LV, Hughes G, Van den Bosch F (2007) *The Study of Plant Disease Epidemics*. APS Press, St. Paul, Minnesota

Mansfield J, Genin S, Magori S, Citovsky V, Sriariyanum M, Ronald P, Dow M, Verdier V, Beer SV, Machado MA, Toth I, Salmond G, Foster GD (2012) Top 10 plant pathogenic bacteria in molecular plant pathology. *Molecular Plant Pathology* 13:614–629

McKinney HH (1923) Influence of soil temperature and moisture on infection of wheat seedlings by *Helminthosporium sativum*. Journal of Agricultural Research 26:195–217

Mora RE, Rodriguez MA, Gayoso LY, López CE (2019) Using in vitro plants to study the cassava response to *Xanthomonas phaseoli* pv. *manihotis* infection. Tropical Plant Pathology 44:423–429

Nassar NMA, Junior OP, Sousa MV, Ortiz R (2009) Improving Carotenoids and Amino-Acids in Cassava. Recent Patents on Food, Nutrition & Agriculture 1:32–38

Olarinde LO, Abass AB, Abdoulaye T, Adepoju AA, Adio MO, Fanifosi EG, Wasiu A (2020) The influence of social networking on food security status of cassava farming households in Nigeria. Sustainability 12:1–13

Olsen KM, Schaal BA (1999) Evidence on the origin of cassava: Phylogeography of *Manihot esculenta*. Proceedings of the National Academy of Sciences of the United States of America 96:5586–5591

Parmar A, Sturm B, Hensel O (2017) Crops that feed the world: Production and improvement of cassava for food, feed, and industrial uses. Food Security 9:907–927

R Development Core Team. R: A Language and Environment for Statistical Computing. R Foundation for Statistical Computing. Available at: <https://www.R-project.org>. Accessed on June 02, 2024

Rubio JSR, López Carrascal CE, Melgarejo LM (2017) Physiological behavior of cassava plants (*Manihot esculenta* Crantz) in response to infection by *Xanthomonas axonopodis* pv. *manihotis* under greenhouse conditions. Physiological and Molecular Plant Pathology 100:136–141

Sahu A, Das A, Saikia K, Barah P (2020) Temperature differentially modulates the transcriptome response in *Oryza sativa* to *Xanthomonas oryzae* pv. *oryzae* infection. Genomics 112:4842–4852

Santos MN, Zárate-Salazar JR, de Carvalho R, Albuquerque UP (2020) Intraspecific variation, knowledge and local management of cassava (*Manihot esculenta* Crantz) in the semiarid region of Pernambuco, Northeast Brazil. Environment, Development and Sustainability 22:2881–2903

Shi T, Li C, Wang G, Huang G (2023) Multilocus Sequence Analysis and Detection of Copper Ion Resistance of *Xanthomonas phaseoli* pv. *manihotis* Causing Bacterial Blight in Cassava. Current Issues in Molecular Biology 45:5389–5402

Singh BK, Delgado-Baquerizo M, Egidi E, Guirado E, Leach JE, Liu H, Trivedi P (2023) Climate change impacts on plant pathogens, food security and paths forward. *Nature Reviews Microbiology* 21:640–656

Teixeira JHS, Guimarães MAS, Cardoso SC, Brito AS, Diniz RP, Oliveira EJ, Oliveira SAS (2021) Evaluation of resistance to bacterial blight in Brazilian cassava germoplasm and disease-yield relationships. *Tropical Plant Pathology* 46:324–335

Toure HMAC, Ehui KJN, Abo K, Kone D (2020) Four years assessment of Cassava Bacterial Blight expression according to weather conditions in Côte d'Ivoire. *SN Applied Sciences* 2:1–13

Trujillo CA, Ochoa JC, Mideros MF, Restrepo S, López C, Bernal A (2014) A Complex Population Structure of the Cassava Pathogen *Xanthomonas axonopodis* pv. *manihotis* in Recent Years in the Caribbean Region of Colombia. *Microbial Ecology* 68:155–167

Velásquez AC, Castroverde CDM, He SY (2018) Plant–Pathogen Warfare under Changing Climate Conditions. *Current Biology* 28: 619–634

Vieira EA, Fialho JF, Julio L, Carvalho LJC, Corte JLD, Rinaldi MM, Oliveira CM, Fernandes FD, Anjos JRN (2019) BRS 400 and BRS 401, sweet cassava cultivars with pink roots developed by participatory breeding. *Crop Breeding and Applied Biotechnology* 19:501–504

Vieira EA, Fialho JF, Julio L, Carvalho LJCB, Corte JLD, Rinaldi MM, Oliveira CM, Fernandes FD, Anjos JRN (2018). Sweet cassava cultivars with yellow or cream root pulp developed by participatory breeding. *Crop Breeding and Applied Biotechnology* 18:450–454.

Vieira EA, Fialho JF, Silva MS, Paula-Moraes SV, Oliveira CM, Anjos JRN, Rinaidi MM, Fernandes FD, Guimarães JR (2011) BRS Japonesa: new sweet cassava cultivar for the Distrito Federal region. *Crop Breeding and Applied Biotechnology* 11:193–196

Vieira EA, Rangel MAS, Fialho JF, Ringenberg R, Romano MR, Rinaldi MM, Oliveira CM, Antonini JCA (2022) BRS 429: Sweet cassava with yellow pulp and high technological and sensory qualities. *Crop Breeding and Applied Biotechnology* 22:434–443

Wickham H, Bryan J (2023) *readxl*: Read Excel Files. R package version 1.4.2. Available at: <https://cran.r-project.org/package=readxl>. Accessed on June 02, 2024

Zárate-Chaves CA, Osorio-Rodríguez D, Mora RE, Pérez-Quintero AL, Dereeper A, Restrepo S, López CE, Szurek B, Bernal A (2021) TAL effector repertoires of strains of *Xanthomonas*

*phaseoli* pv. *manihotis* in commercial cassava crops reveal high diversity at the country scale.  
Microorganisms 9:1–26

## Supplementary material

0	1 or 2	3 or 4	5	6	7	8
0 = no symptoms.	1 = angular water-soaked lesion/spot on one-third or less of the leaves. 2 = angular water-soaked lesion/spot on more than one-third of the leaves.	3 = necrotic spots/scorch symptoms on one-third or less of the leaves. 4 = necrotic spots/scorch symptoms on more than one-third of the leaves.	5 = necrotic lesions on the stem or petiole.	6 = necrotic lesions on the stem or petiole associated with exudation.	7 = wilting associated with exudation or death of one-third or less of the plant.	8 = wilting associated with exudation or death of more than one-third of the plant.

## CAPÍTULO 4

---

---

**Hyperspectral imaging and machine learning for detecting  
physiological changes in cassava caused by *Xanthomonas*  
*phaseoli* pv. *manihotis***

**Hyperspectral Imaging and Machine Learning for Detecting Physiological Changes in  
Cassava Caused by *Xanthomonas phaseoli* pv. *manihotis***

Ian Carlos Bispo Carvalho<sup>1</sup>, Luciellen da Costa Ferreira<sup>1</sup>, Ana Régia de Mendonça Neves<sup>2</sup>,  
Alice Maria Silva Carvalho<sup>1</sup>, Henrique Póvoa Rodrigues Lima<sup>1</sup>, Maurício Rossato<sup>1\*</sup>

<sup>1</sup>Universidade de Brasília, Brasília, DF - Brazil

<sup>2</sup>Casa Civil da Presidência da República, Brasília, Distrito Federal, Brazil.

\*Corresponding Author: Maurício Rossato; E-mail: mauricio.rossato@unb.br

## **Abstract**

This study explores the use of hyperspectral imaging (HSI) combined with machine learning to detect physiological alterations in cassava leaves caused by *Xanthomonas phaseoli* pv. *manihotis* (Xpm), a bacterial plant disease that causes significant yield losses worldwide. Therefore, the use of hyperspectral images (HSI) associated with machine learning can provide information rapidly and accurately, aiming to support decision-making. HSI captures spectral data that reflects biochemical changes in infected plant tissues. Cassava leaves inoculated with Xpm were imaged using a hyperspectral camera across wavelengths from 400 to 1000 nm, with image calibration and spectral normalization to improve data quality. Spectral parameters, such as mean reflectance and spectral differences (healthy vs. infected), were analyzed. Six machine learning models were tested for classification: Decision Tree (DT), Random Forest (RF), Support Vector Machine (SVM), K-Nearest Neighbors (KNN), Extreme Gradient Boosting (XGBoost), and Multi-Layer Perceptron (MLP). SVM performed best with 91.21% accuracy and an AUC-ROC of 0.9684, followed by MLP (86.14%), RF (77.52%), and XGBoost (79.04%). KNN and DT had the lowest accuracy (70.44% and 71.62%, respectively). The results suggest that HSI, particularly when combined with SVM, offers a rapid and accurate method for diagnosing cassava bacterial blight, with potential for large-scale field applications.

**Key words:** HSI; bacterial blight; plant disease; plant physiology

## **Introduction**

Cassava bacterial blight, caused by *Xanthomonas phaseoli* pv. *manihotis* (Xpm), is a major phytosanitary challenge that threatens cassava production globally. The disease can lead to significant yield losses, with reductions ranging from 30% to 90%, and in severe cases, can result in a complete loss of the crop after two or three planting cycles if effective management strategies are not implemented (Mansfield et al. 2012; Zárate-Chaves et al. 2021).

In recent decades, considerable progress has been made in developing non-invasive techniques for plant disease diagnosis, such as fluorescence spectroscopy, VNIR spectroscopy, fluorescence imaging, and hyperspectral imaging (Sankaran et al. 2010; Golhani et al. 2018). Among these, hyperspectral sensors have gained prominence for their efficiency in extracting diverse types of information from plant tissues (Ortenberg, 2018). These techniques have found widespread application in agriculture, including seed quality analysis (Feng et al. 2019) and soil assessment (Demattê et al. 2010).

Recent studies have highlighted the potential of spectral data to understand the behavior of plants under pathogen infection across different pathosystems, such as tomato bacterial blight (Abdulridha et al. 2020), peanut bacterial wilt (Chen et al. 2020), apple blight (Skoneczny et al. 2020), and potato blight (Van De Vijver et al. 2020). Despite the promise of hyperspectral imaging, challenges remain in selecting optimal wavelengths and scaling this technology for practical use in large agricultural settings. Addressing these challenges often requires the application of machine learning algorithms to extract meaningful insights from the spectral data and develop effective disease management strategies (Zhang et al. 2020; Feng et al. 2021).

Machine learning, a key area within artificial intelligence, employs computational algorithms that learn from input data to perform various tasks, such as classification or clustering. This approach is particularly well-suited for identifying parameters and trends in hyperspectral data (Dhakal et al., 2023). Machine learning techniques can be broadly categorized into supervised and unsupervised learning. In supervised learning, predictive

models are trained using labeled data, where each data point is associated with a known "ground truth," either assigned by experts or verified experimentally. In contrast, unsupervised learning identifies patterns in unlabeled data, without predefined labels (Greener et al., 2022; Asnicar et al., 2024). Additionally, semi-supervised learning, which combines both labeled and unlabeled data, can optimize the process, especially when data labeling is costly (Greener et al., 2022).

Various machine learning algorithms, such as Support Vector Machines (SVM), Random Forest (RF), have been widely used to build plant disease prediction models, each offering different performances depending on the dataset and the application (Ahmad et al., 2023; Omaye et al., 2024).

Given these advances, this study aims to utilize hyperspectral imaging in combination with machine learning to identify cassava plants infected with *Xpm*, thereby improving the diagnosis and management of cassava bacterial blight.

## **Material and methods**

### ***Xpm* inoculation on cassava plants**

The bacterial inoculum (UnB 17 isolate) was prepared using 523 culture medium (Kado and Heskett 1970) and incubated at 28°C for 48 hours in a growth chamber. A bacterial suspension was subsequently prepared in distilled water and its concentration measured and adjusted with a Shimadzu UV-1203 spectrophotometer at a wavelength of 550 nm. An absorbance reading of 0.350 corresponded to a bacterial concentration of  $10^8$  CFU/mL.

Variety BGMC 962 of cassava, commonly used in Brazil, was chosen for the experiment and propagated by cuttings. Eight weeks cassava plants were inoculated by spraying the aerial parts with the bacterial suspension using a handheld sprayer until runoff. The inoculated plants were maintained in a moist chamber for three days and then transferred to a greenhouse with controlled temperature (26 °C), where they were monitored for disease development over the study period. Twenty days after inoculation, both healthy and symptomatic leaves from cassava

plants, exhibiting varying degrees of disease severity, were harvested for hyperspectral imaging. The collection process started 20 days after inoculation and extended over a 30-day period. By the end of this period, a total of 962 leaves were collected, comprising 402 healthy leaves and 450 symptomatic leaves.

### **Image capture**

The collection of hyperspectral imaging of cassava leaves was performed using an FX10e camera (Specim, Finland), capable of measuring reflectance in 224 bands within the 400–1000 nm spectral range, attached to a LabScanner (Specim, Finland) with six halogen lamps (Figure 1). Images were captured with Software Breeze v. 2024.1 (Prediktera, Sweden) also used for storage and initial processing of images. Each group of symptomatic leaves were distributed along the LabScanner tray for sample movement and proper hyperspectral image capture. An RGB image was also captured to serve as a reference for the normal appearance of the samples.

Before beginning the image capture, reference images for white and black were obtained with the camera shutter closed. The imaging was performed across all spectral bands within the capabilities of the equipment used for this project. To extract the true spectral response of each sample, the influence of the black and white reference images was removed, resulting in a calibrated image (IR) (Kim et al. 2001).

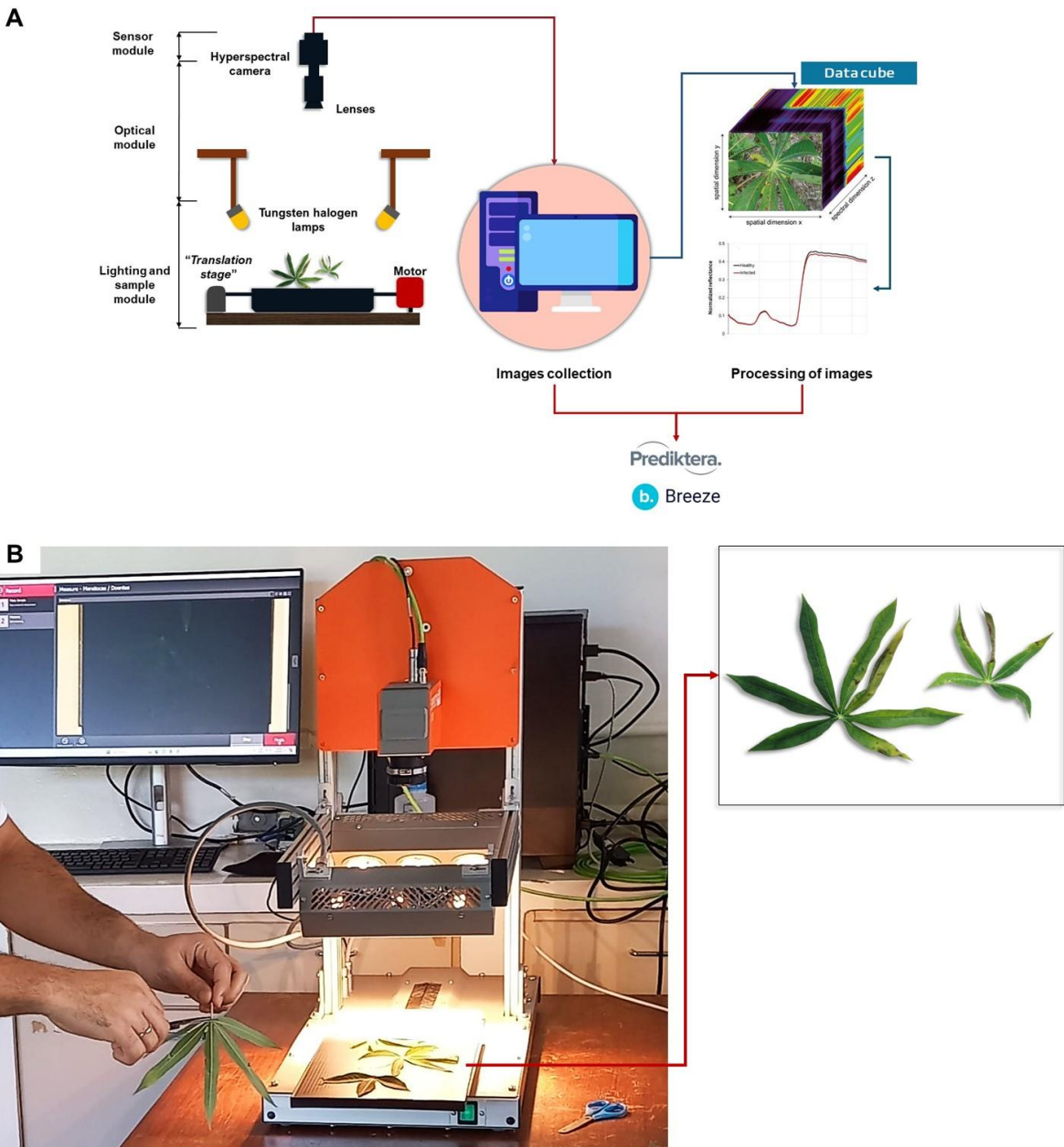


**Figure 1.** Schematic representation and setup of a benchtop hyperspectral imaging system for cassava leaf analysis. (A) Diagram of the hyperspectral imaging system components, including the FX10e camera, halogen lamps for illumination, and a motorized translation stage for sample movement. (B) Practical setup capturing cassava leaf samples under halogen lamp illumination.

### Hyperspectral image processing

Image segmentation and region of interest (ROI) selection were conducted using Breeze software. This process was designed to eliminate the background, enabling a clear view of the pixels representing cassava leaves (Baek et al. 2019). Following this, the spectral data were

normalized using the Standard Normal Variate (SNV) method, which adjusted for spectral variations in the numerical data.

## **Discriminant Spectral Parameters**

Three spectral parameters were used to identify wavelengths with significant differences between healthy and diseased leaves: (i) the mean reflectance values of cassava leaves infected with Xpm compared to healthy leaves; (ii) the spectral difference, calculated by subtracting the mean reflectance of healthy leaves from that of infected leaves at each wavelength; and (iii) sensitivity, determined by the ratio of the mean reflectance of diseased leaves to that of healthy leaves at each analyzed wavelength. These parameters provided additional information to support the analysis, complementing the interpretation of the spectral data, and were not directly used in the modeling process.

## **Data analysis**

The methodology for acquiring and analyzing the hyperspectral data followed a structured approach, encompassing data collection, image processing, model selection, data preprocessing, model optimization, training, testing, and performance evaluation. The workflow of the process is illustrated in Figure 2. The analyses were conducted using Python, utilizing the following libraries: Optuna (Optuna, 2024), Scikit-learn (Pedregosa et al., 2011), XGBoost (Chen and Guestrin 2016), Seaborn (Waskom et al., 2023), and Matplotlib (Hunter, 2007).

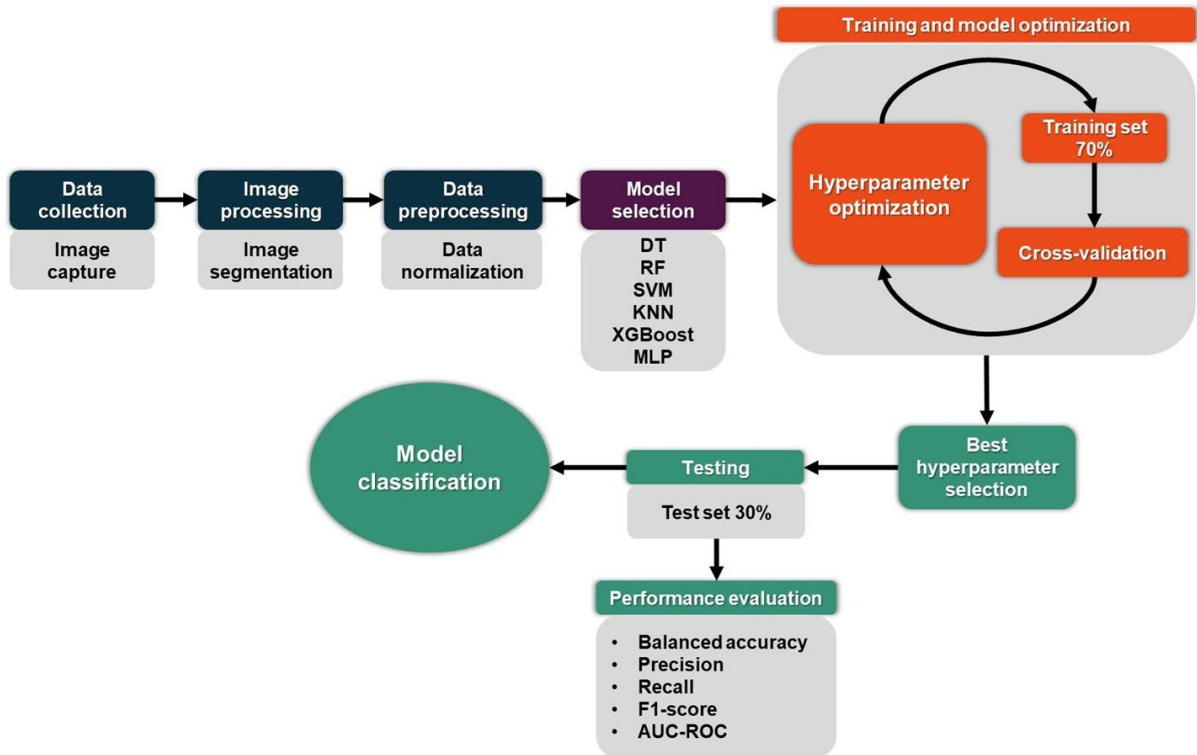


**Figure 2.** Workflow of the image classification process, including data collection, processing, hyperparameter optimization, training, testing, and performance evaluation.

## Classification Methods

Six classification methods were evaluated: Decision Tree (DT), Random Forest (RF), Support Vector Machine (SVM), K-Nearest Neighbors (KNN), Extreme Gradient Boosting (XGBoost), and Multi-Layer Perceptron (MLP).

A Decision Tree is a classification model that separate the feature space into distinct regions based on a sequence of binary decisions (Quinlan 1986; Rasoul Safavian and Landgrebe 1991; Costa and Pedreira 2023). The model constructs a tree by iteratively splitting the dataset based on specific features that minimize impurity. Decision Trees are intuitive and easy to interpret but can be prone to overfitting, especially when the tree becomes too deep (Bramer 2002).

Random Forest is an ensemble learning method that generates multiple decision trees during training. Each tree is trained on a randomly sampled subset of data (bootstrap sampling)

and on a random subset of features at each split. The final prediction is derived by combining the predictions from all individual trees. This approach increases model robustness and handles noisy and large datasets effectively (Breiman 2001; Nti et al. 2023).

Support Vector Machine is a classification algorithm that identifies an optimal hyperplane to separate classes in a high-dimensional feature space (Cortes and Vapnik 1995; Mountrakis et al. 2011). SVMs can also be extended to non-linear classification using kernel functions. Although primarily designed for binary classification, SVMs can be adapted to multiclass (Mammone et al. 2009; Pathak et al. 2022).

K-Nearest Neighbors is a non-parametric classification method that assigns a class to a new sample based on the majority class of its nearest neighbors in the feature space (Chirici et al. 2016; Uddin et al. 2022). The proximity is typically measured using a distance metric, such as Euclidean distance. The class label of the input sample is determined by the majority vote of its k-nearest neighbors (Hossain et al. 2019).

XGBoost is an ensemble learning method that builds a strong classifier by combining the predictions of multiple weak models using a boosting approach (Chen and Guestrin 2016; Nti et al. 2023). It minimizes a loss function using gradient descent and includes regularization terms to prevent overfitting, improving the model's generalization ability (Li et al. 2019; Bentéjac et al. 2020).

The MLP is a class of artificial neural network (ANN) that consists of multiple layers of interconnected perceptrons (neurons). Each neuron applies a weighted sum followed by a non-linear activation function to its input (Schmidhuber 2015; Rasamolina et al. 2020). The MLP is trained using backpropagation to minimize a cost function, such as cross-entropy for classification tasks (Pandian et al. 2022). MLPs are known for their capability to handle complex and high-dimensional data (Lecun et al. 2015; Golhani et al. 2018b).

## Hyperparameter optimization

For each machine learning method, hyperparameter optimization was conducted using the Optuna library to identify the optimal parameter settings. Following this, stratified cross-validation was performed, and the mean cross-validation scores for the various hyperparameter combinations were calculated. After optimization, the final model was trained using the best-found hyperparameters. Additionally, for each classification method, a pipeline was configured and trained on the training dataset.

## Model validation

The quality of the models was assessed using the test set and several performance metrics: balanced accuracy, precision, recall, and F1-score. Balanced accuracy was chosen due to the imbalance in the dataset, providing a more reliable measure of overall accuracy. These metrics are based on True Positive, False Negative, and True Negative values, and are mathematically represented by Equations (1), (2), (3), and (4):

$$Accuracy = \frac{TP+TN}{VP+VN+FP+FN} \quad (1)$$

$$Precision = \frac{TP}{(TP+FP)} \quad (2)$$

$$Recall = \frac{TP}{TP+FN} \quad (3)$$

$$F1\ score = 2 \frac{Precision \times Recall}{Precision + Recall} \quad (4)$$

Additionally, the ROC-AUC (Receiver Operating Characteristic - Area Under the Curve) metric was calculated to evaluate the models' ability to distinguish between classes. This

metric quantifies the probability that the model will assign a higher score to a positive class observation compared to a negative class observation.

$$AUC = P(f(x_{positive}) > f(x_{negative})) \quad (5)$$

where  $f(x_{positive})$  is the variable from the estimator  $f$  applied to positive observations  $x_{positive}$ ;  $f(x_{negative})$  comes from applying  $f$  applied to negative observations  $x_{negative}$ ; and  $P$  denotes the probability density function, representing the likelihood of these values.

## Results

Infected plants exhibit progressively evolving symptoms over time, ranging from initial water-soaked spots to advanced necrotic lesions, reflecting distinct stages of disease progression. A total of 450 infected leaves, representing various disease stages, were evaluated and divided into training and testing sets. A total of 448 bands of the visible and near infrared were captured with the hyperspectral camera for each leaf.

## Model performance

The accuracy of the machine learning models applied to the spectral data of healthy cassava leaves and those infected by *Xanthomonas phaseoli* pv. *manihotis* (Xpm) is presented in Figure 3. Among the evaluated models, SVM achieved the highest accuracy (91.41%), effectively distinguishing between healthy and infected leaf samples. The MLP model also yielded strong results (87.5%), highlighting the neural network's ability to detect subtle variations in the spectral data.

XGBoost and Random Forest (RF), both decision tree-based algorithms, attained accuracies of 80.08% and 76.56%, respectively. These models exhibited intermediate performance, demonstrating a moderate capacity to model the spectral data, though with lower

accuracy compared to SVM and MLP. Decision tree (DT) achieved an accuracy of 71.88%, reflecting reasonable discriminative power of the samples in the feature space. The K-Nearest Neighbors (KNN) model had the lowest accuracy at 70.31%, performing below the other models.

The model validation parameters indicate that the SVM demonstrated the best overall performance. It achieved the highest values for the F1 Score (0.9209), Recall (0.9481), and AUC-ROC (0.9684) metrics, suggesting that the SVM effectively balances precision and sensitivity, making it the most suitable choice for classifying spectral data from healthy and diseased plants. The MLP (Multilayer Perceptron) also performed well, particularly in Recall (0.8963) and AUC-ROC (0.9287), indicating its strong ability to detect the positive class.

In contrast, XGBoost yielded more balanced results, with Precision of 0.7891 and F1 Score of 0.7878, but an AUC-ROC of 0.8758, suggesting it does not achieve the same level of discrimination as the SVM and MLP. Random Forest (RF), while exhibiting a relatively high Recall (0.8148), underperformed compared to the more complex models, with an F1 Score of 0.7942 and an AUC-ROC of 0.8495.

The Decision Tree (DT) displayed limited performance, with lower metrics such as an AUC-ROC of 0.7638, indicating reduced generalization capability. Finally, the KNN (K-Nearest Neighbors) exhibited the weakest performance, with a Precision of 0.7360 and Recall of 0.6815, demonstrating its unsuitability for this dataset.

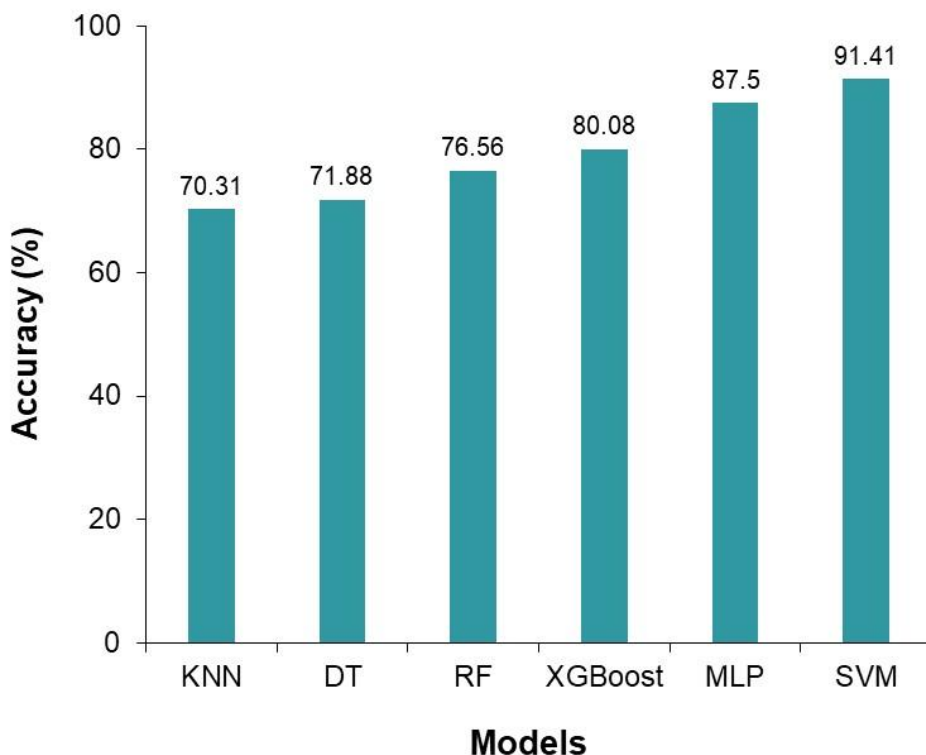


**Figure 3.** Accuracy results of classification methods differentiating healthy cassava leaves from those infected with *Xpm*. K-Nearest Neighbors (KNN); Decision Tree (DT); Random Forest (RF); Extreme Gradient Boosting (XGBoost); Multi-Layer Perceptron (MLP); Support Vector Machine (SVM).

**Table 1.** Result of the performance evaluation metrics of the models on the test set.

Classification Methods	Precision	Recall	F1 score	AUC-ROC
SVM	0.8951	0.9481	0.9209	0.9684
MLP	0.8521	0.8963	0.8736	0.9287
XGBoost	0.7891	0.7871	0.7878	0.8758
RF	0.7746	0.8148	0.7942	0.8495
DT	0.7203	0.7630	0.7410	0.7638
KNN	0.7360	0.6815	0.7077	0.7607

K-Nearest Neighbors (KNN); Decision Tree (DT); Random Forest (RF); Extreme Gradient Boosting (XGBoost); Multi-Layer Perceptron (MLP); Support Vector Machine (SVM).

## **Spectral reflectance characterization**

The spectral signature derived from the normalized reflectance of healthy and *Xanthomonas phaseoli* pv. *manihotis* (Xpm)-infected leaves is shown in Figure 4a. In the near-infrared (NIR) region (700-1000 nm), a pronounced difference was observed between healthy and infected leaves. Healthy leaves exhibited high reflectance in this range, which can be attributed to intact cellular structures and high-water content. Conversely, infected leaves showed a notable reduction in reflectance, indicating cell damage and water loss, both typical characteristics of bacterial infection.

The highest sensitivity was recorded in the 640-700 nm range, which encompasses the red region (640–680 nm), known for chlorophyll absorption (Figure 4b). This peak in sensitivity reflects the impact of infection on photosynthetic pigments, emphasizing the importance of this wavelength range for the early detection of pathogen infections. The largest spectral differences between healthy and infected leaves occurred around 760 nm in the NIR range (Figure 4c). In this region, the reflectance of infected leaves was significantly lower, confirming the presence of structural damage and turgor loss.

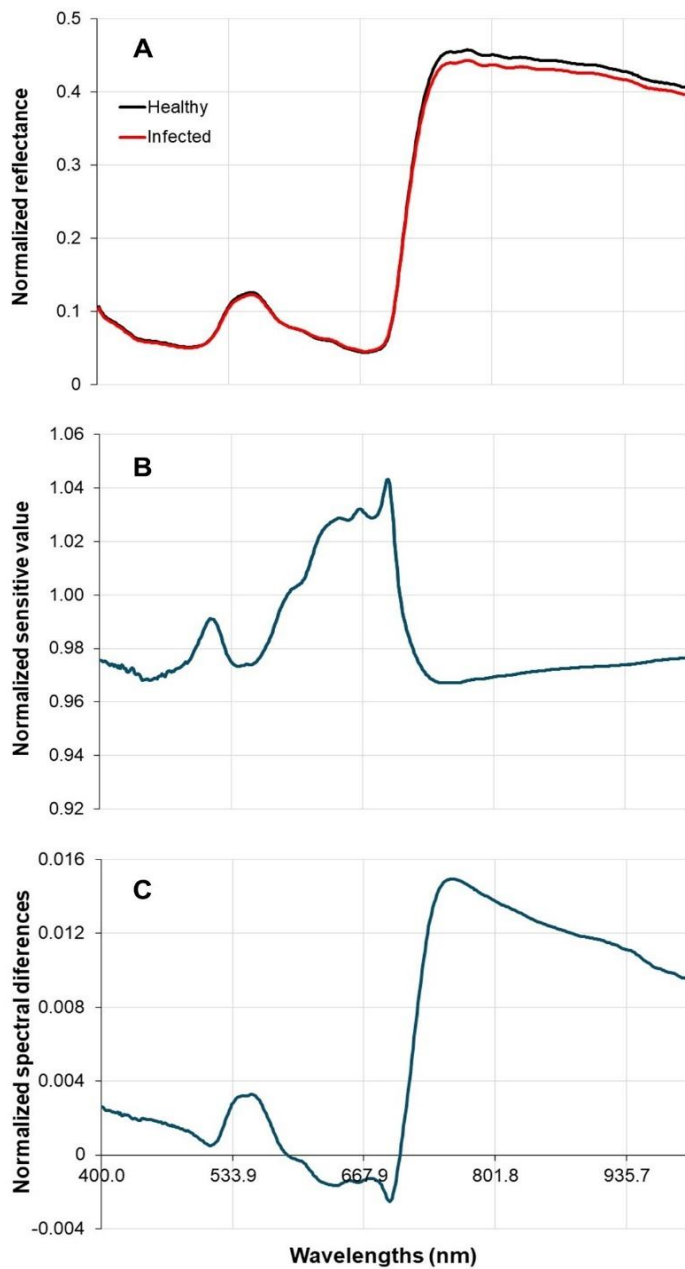


**Figure 4.** Cassava leaves spectral reflectance characterization: normalized spectral reflectance curves (a); normalized sensitivity value (b); normalized spectral difference (c).

## Discussion

The evaluation of prediction performance ensures that the model can generalize well to unseen data, not just the training dataset. However, the use of only one cultivar in this experiment may be a limiting factor in the generalization process. Additionally, the performance metrics used provided valuable insights into the behavior of the tested models.

Failing to apply these appropriate metrics can lead to significant issues, such as the model predominantly predicting the majority class when the data are imbalanced, which may result in overfitting to that class (Johnson and Khoshgoftaar 2019; López et al. 2022).

Therefore, in the comparative analysis of techniques for classifying healthy and infected plants, metrics developed were utilized. These include accuracy, area under the ROC curve (AUC-ROC), sensitivity (or recall), and precision. Accuracy, sensitivity, and precision rely on the confusion matrix, which compares the predictions of positive and negative classes. By examining the confusion matrix, it is possible to establish relationships between the true and predicted values, providing a comprehensive understanding of the model's performance (Wardhani et al. 2019; Johnson and Khoshgoftaar 2019).

The integration of machine learning techniques with hyperspectral data for diagnosing cassava bacterial blight has yielded promising results, particularly with the Support Vector Machine (SVM). SVM emerged as the most effective model for distinguishing between healthy leaves and those infected with *Xanthomonas phaseoli* pv. *manihotis*, based on all performance metrics. Following closely was the Multi-Layer Perceptron (MLP), which also demonstrated itself as a viable alternative. XGBoost and Random Forest exhibited intermediate performances, while Decision Tree and KNN were the least suitable for this task.

The effectiveness of SVM can be attributed to its capability to manage complex, high-dimensional data, a notable advantage highlighted in various plant disease classification studies (Nagasubramanian et al. 2018). The use of kernel functions in SVM enables the transformation of data into a higher-dimensional space, which facilitates class separation and mitigates the risk of overfitting (Pathak et al. 2022). The MLP achieved a balanced accuracy that was only 5.07% lower than that of the SVM, showcasing its strong performance in classifying healthy and infected cassava leaves based on hyperspectral data. Its proficiency in processing large volumes of complex hyperspectral data has been corroborated by other studies on plant diseases, which have reported significant results (Abdulridha et al. 2020b; Lee et al. 2022).

XGBoost and Random Forest are ensemble learning models based on decision trees, designed to combine the predictions of multiple decision trees to enhance accuracy, resulting in more robust and reliable outcomes (Breiman 2001; Chen and Guestrin 2016; Nti et al. 2023). The adoption of this strategy effectively mitigates overfitting, and despite the distinct characteristics of each model, both approaches yielded satisfactory results. These findings underscore the effectiveness of ensemble techniques in the analysis of spectral data.

Decision Tree and K-Nearest Neighbors (KNN) models were considered the least suitable for the classification task. Both models exhibit significant limitations regarding precision and generalization, rendering them less favorable compared to the other methods analyzed. While the simplicity of these methods can be advantageous in certain contexts, it was insufficient to meet the specific requirements of this analysis.

These variations in algorithm performance underscore the specific suitability of each method for processing hyperspectral data in the binary classification of healthy and diseased plants. In a previous study, differences were observed in machine learning algorithm performance when comparing hyperspectral data of a fungal disease (*Corynespora cassiicola*) and a bacterial disease (*Xanthomonas perforans*) causing leaf spots in tomato plants, under both benchtop and unmanned aerial vehicle conditions (Abdulridha et al. 2020b). Recent work analyzed four fungal diseases in tomatoes (*Botrytis cinerea*, *Fusarium oxysporum*, *Alternaria alternata*, and *Alternaria solani*) using hyperspectral and RGB images with a Random Forest model. Hyperspectral imaging proved more accurate, revealing distinct spectral signatures for effective disease differentiation (Javidan et al. 2024). Therefore, the effectiveness of each technique can be influenced by the nature of the data and the interaction between the plant pathogen and the host.

Spectral data are extensively employed to identify physiological and biochemical changes induced by phytopathogens, offering critical insights into the differences between healthy and diseased plants (Abdulridha et al. 2020b; Castro-Valdecantos et al. 2024). In this

study, reflectance in the near-infrared (NIR, 700–1000 nm) was higher in healthy leaves, indicating cellular integrity and elevated water content, which are essential for maintaining turgor and physiological functions. Conversely, the lower reflectance observed in infected leaves suggests structural damage and a loss of turgor, typical characteristics of bacterial infections.

These findings align with observations from research on the physiological changes induced by *Xanthomonas phaseoli* pv. *manihotis* (Xpm) in cassava leaves. Such investigations revealed a reduction in water potential associated with increased stomatal resistance, along with a rise in proline concentration, indicating the plant's response to disruptions in cellular homeostasis due to bacterial infection (Rubio et al. 2017a). Similarly, a study on *Xanthomonas citri* subsp. *citri* in Sugar Belle mandarins demonstrated that vegetation indices related to chlorophyll and water content effectively detected early-stage bacterial infections (Abdulridha et al. 2019). In a study utilizing hyperspectral data and vegetation indices to assess healthy and *Xanthomonas perforans*-infected tomato plants, significant physiological differences between the groups were detected as early as two hours post-inoculation. At this stage, spectral bands in the ranges of 740–750 nm and 1404 nm were identified as the most critical for distinguishing between healthy and infected plants (Zhang et al. 2024). Furthermore, the spectral data for the four fungal diseases in tomatoes were most effective in the 500–550 nm and 740–950 nm ranges, which encompass the infrared wavelengths, for early-stage identification and diagnosis (Javidan et al. 2024).

The integration of machine learning techniques with hyperspectral data has proven effective in detecting physiological alterations caused by cassava bacterial blight in cassava leaves, with Support Vector Machine (SVM) achieving the best overall performance. The Multi-Layer Perceptron (MLP) also exhibited strong performance, while XGBoost and Random Forest produced satisfactory results. The variations in algorithm performance highlight the importance of selecting appropriate methods for the specific pathosystem under evaluation. In

addition to that, spectral analysis demonstrated that physiological changes induced by *Xanthomonas phaseoli* pv. *manihotis* can be detected through near-infrared reflectance, reinforcing the significance of spectral techniques in diagnosing plant diseases. Furthermore, further research will be necessary to refine this technique for detecting infected propagative material, including cuttings for commercial cultivation and seeds for breeding programs.

## References

- Abdulridha, J., Ampatzidis, Y., Kakarla, S. C., and Roberts, P. (2020). Detection of target spot and bacterial spot diseases in tomato using UAV-based and benchtop-based hyperspectral imaging techniques. *Precis. Agric.* 21, 955–978. doi: 10.1007/s11119-019-09703-4
- Abdulridha, J., Batuman, O., and Ampatzidis, Y. (2019). UAV-based remote sensing technique to detect citrus canker disease utilizing hyperspectral imaging and machine learning. *Remote Sens. (Basel)* 11. doi: 10.3390/rs11111373
- Ahmad, A., Saraswat, D., and El Gamal, A. (2023). A survey on using deep learning techniques for plant disease diagnosis and recommendations for development of appropriate tools. *Smart Agric. Technol.* 3. doi: 10.1016/j.atech.2022.100083
- Akiba, T., Sano, S., Yanase, T., Ohta, T., Koyama, M. (2019). Optuna: A next-generation hyperparameter optimization framework. *Proc. 25th ACM SIGKDD Int. Conf. Knowl. Discov. Data Mining*, 2623-2631.
- Asnicar, F., Thomas, A. M., Passerini, A., Waldron, L., and Segata, N. (2024). Machine learning for microbiologists. *Nat. Rev. Microbiol.* 22, 191–205. doi: 10.1038/s41579-023-00984-1
- Baek, I., Kim, M. S., Cho, B. K., Mo, C., Barnaby, J. Y., McClung, A. M., et al. (2019). Selection of optimal hyperspectral wavebands for detection of discolored, diseased rice seeds. *Appl. Sci. (Switzerland)* 9. doi: 10.3390/app9051027
- Bramer, M. (2002). Using J-pruning to reduce overfitting in classification trees. *Knowl.-Based Syst.* 15, 301–308.
- Breiman, L. (2001). Random Forests. *Mach. Learn.* 45, 5–32.

Castro-Valdecantos, P., Egea, G., Borrero, C., Pérez-Ruiz, M., and Avilés, M. (2024). Detection of fusarium wilt-induced physiological impairment in strawberry plants using hyperspectral imaging and machine learning. *Precis Agric.* 25, 2958–2976. doi: 10.1007/s11119-024-10173-6

Chen, T., and Guestrin, C. (2016). XGBoost: A scalable tree boosting system. *Proc. ACM SIGKDD Int. Conf. Knowl. Discov. Data Min.* 785–794. doi: 10.1145/2939672.2939785

Chen, T., Yang, W., Zhang, H., Zhu, B., Zeng, R., Wang, X., et al. (2020). Early detection of bacterial wilt in peanut plants through leaf-level hyperspectral and unmanned aerial vehicle data. *Comput. Electron. Agric.* 177. doi: 10.1016/j.compag.2020.105708

Chirici, G., Mura, M., McInerney, D., Py, N., Tomppo, E. O., Waser, L. T., et al. (2016). A meta-analysis and review of the literature on the k-Nearest Neighbors technique for forestry applications that use remotely sensed data. *Remote Sens. Environ.* 176, 282–294. doi: 10.1016/j.rse.2016.02.001

Cortes, C., and Vapnik, V. (1995). Support-Vector Networks. *Mach. Learn.* 20, 273–297.

Costa, V. G., and Pedreira, C. E. (2023). Recent advances in decision trees: an updated survey. *Artif. Intell. Rev.* 56, 4765–4800. doi: 10.1007/s10462-022-10275-5

Demattê, J. A. M., Fiorio, P. R., and Araújo, S. R. (2010). Variation of routine soil analysis when compared with hyperspectral narrow band sensing method. *Remote Sens.* 2, 1998–2016. doi: 10.3390/rs2081998

Dhakal, K., Sivaramakrishnan, U., Zhang, X., Belay, K., Oakes, J., Wei, X., et al. (2023). Machine Learning Analysis of Hyperspectral Images of Damaged Wheat Kernels. *Sensors* 23. doi: 10.3390/s23073523

Feng, L., Wu, B., He, Y., and Zhang, C. (2021). Hyperspectral Imaging Combined With Deep Transfer Learning for Rice Disease Detection. *Front. Plant Sci.* 12. doi: 10.3389/fpls.2021.693521

Feng, L., Zhu, S., Liu, F., He, Y., Bao, Y., and Zhang, C. (2019). Hyperspectral imaging for seed quality and safety inspection: A review. *Plant Methods* 15, 1–25. doi: 10.1186/s13007-019-0476-y

Golhani, K., Balasundram, S. K., Vadmalai, G., and Pradhan, B. (2018). A review of neural networks in plant disease detection using hyperspectral data. *Inf. Process. Agric.* 5, 354–371. doi: 10.1016/j.inpa.2018.05.002

Greener, J. G., Kandathil, S. M., Moffat, L., and Jones, D. T. (2022). A guide to machine learning for biologists. *Nat. Rev. Mol. Cell Biol.* 23, 40–55. doi: 10.1038/s41580-021-00407-0

Hunter, J. D. (2007). Matplotlib: A 2D graphics environment. *Comput. Sci. Eng.* 9(3), 90–95. doi:10.1109/MCSE.2007.55

Javidan, S. M., Banakar, A., Vakilian, K. A., Ampatzidis, Y., and Rahnama, K. (2024). Early detection and spectral signature identification of tomato fungal diseases (*Alternaria alternata*, *Alternaria solani*, *Botrytis cinerea*, and *Fusarium oxysporum*) by RGB and hyperspectral image analysis and machine learning. *Heliyon* 10. doi: 10.1016/j.heliyon.2024.e38017

Johnson, J. M., and Khoshgoftaar, T. M. (2019). Survey on deep learning with class imbalance. *J. Big Data* 6. doi: 10.1186/s40537-019-0192-5

Kado, C. I., and Heskett, M. G. (1970). Selective media for isolation of *Agrobacterium*, *Corynebacterium*, *Erwinia*, *Pseudomonas*, and *Xanthomonas*. *Phytopathology* 60, 969–976. doi: 10.1094/Phyto-60-969

Kim, M. S., Chen, Y. R., and Mehl, P. M. (2001). Hyperspectral reflectance and fluorescence imaging system for food quality and safety. *Trans. ASAE* 44, 721–729.

Lecun, Y., Bengio, Y., and Hinton, G. (2015). Deep learning. *Nature* 521, 436–444. doi: 10.1038/nature14539

Lee, C. C., Koo, V. C., Lim, T. S., Lee, Y. P., and Abidin, H. (2022). A multi-layer perceptron-based approach for early detection of BSR disease in oil palm trees using hyperspectral images. *Heliyon* 8. doi: 10.1016/j.heliyon.2022.e09252

López, O. A. M., López, A. M., and Crossa, J. (2022). “Overfitting, Model Tuning, and Evaluation of Prediction Performance,” in Multivariate Statistical Machine Learning Methods for Genomic Prediction, eds. O. A. M. López, A. M. López, and J. Crossa (Springer International Publishing), 109–139. doi: 10.1007/978-3-030-89010-0

Mammone, A., Turchi, M., and Cristianini, N. (2009). Support vector machines. *Wiley Interdiscip. Rev. Comput. Stat.* 1, 283–289. doi: 10.1002/wics.049

Mansfield, J., Genin, S., Magori, S., Citovsky, V., Sriariyanum, M., Ronald, P., et al. (2012). Top 10 plant pathogenic bacteria in molecular plant pathology. *Mol. Plant. Pathol.* 13, 614–629. doi: 10.1111/j.1364-3703.2012.00804.x

- Mountrakis, G., Im, J., and Ogole, C. (2011). Support vector machines in remote sensing: A review. *ISPRS J. Photogramm. Remote Sens.* 66, 247–259. doi: 10.1016/j.isprsjprs.2010.11.001
- Nagasubramanian, K., Jones, S., Sarkar, S., Singh, A. K., Singh, A., and Ganapathysubramanian, B. (2018). Hyperspectral band selection using genetic algorithm and support vector machines for early identification of charcoal rot disease in soybean stems. *Plant Methods* 14. doi: 10.1186/s13007-018-0349-9
- Nti, I. K., Zaman, A., Nyarko-Boateng, O., Adekoya, A. F., and Keyeremeh, F. (2023). A predictive analytics model for crop suitability and productivity with tree-based ensemble learning. *Decis. Anal. J.* 8. doi: 10.1016/j.dajour.2023.100311
- Omaye, J. D., Ogbuju, E., Ataguba, G., Jaiyeoba, O., Aneke, J., and Oladipo, F. (2024). Cross-comparative review of Machine learning for plant disease detection: apple, cassava, cotton and potato plants. *Artif. Intell. Agric.* 12, 127–151. doi: 10.1016/j.aiia.2024.04.002
- Ortenberg, F. (2018). “Hyperspectral Sensor Characteristics: Airborne, Spaceborne, Hand-Held, and Truck-Mounted; Integration of Hyperspectral Data with LIDAR,” in *Fundamentals, Sensor Systems, Spectral Libraries, and Data Mining for Vegetation*, eds. P. S. Thenkabail, J. G. Lyon, and A. Huete (New York: CRC Press), 41–69. doi: 10.13140/2.1.2089.3447
- Pandian, J. A., Kumar, V. D., Geman, O., Hnatiuc, M., Arif, M., and Kanchanadevi, K. (2022). Plant Disease Detection Using Deep Convolutional Neural Network. *Appl. Sci. (Switzerland)* 12. doi: 10.3390/app12146982
- Pathak, D. K., Kalita, S. K., and Bhattacharya, D. K. (2022). Hyperspectral image classification using support vector machine: a spectral spatial feature based approach. *Evol. Intell.* 15, 1809–1823. doi: 10.1007/s12065-021-00591-0
- Pedregosa, F., Varoquaux, G., Gramfort, A., Michel, V., Thirion, B., Grisel, O., et al. (2011). Scikit-learn: Machine learning in Python. *J. Mach. Learn. Res.* 12, 2825–2830.
- Quinlan, J. R. (1986). Induction of Decision Trees. *Mach. Learn.* 1, 81–106.
- Rasamoelina, A. D., Adjailia, F., and Sinčák, P. (2020). A Review of Activation Function for Artificial Neural Network. *2020 IEEE 18th World Symp. Appl. Mach. Intell. Informatics (SAMI)*. doi: 10.1109/SAMI48414.2020.9108717
- Rasoul Safavian, S., and Landgrebe, D. (1991). A Survey of Decision Wee Classifier Methodology. *IEEE Trans. Syst. Man Cybern.* 21, 660–674.

Rubio, J. S. R., López Carrascal, C. E., and Melgarejo, L. M. (2017). Physiological behavior of cassava plants (*Manihot esculenta* Crantz) in response to infection by *Xanthomonas axonopodis* pv. *manihotis* under greenhouse conditions. *Physiol. Mol. Plant Pathol.* 100, 136–141. doi: 10.1016/j.pmpp.2017.09.004

Sankaran, S., Mishra, A., Ehsani, R., and Davis, C. (2010). A review of advanced techniques for detecting plant diseases. *Comput. Electron. Agric.* 72, 1–13. doi: 10.1016/j.compag.2010.02.007

Schmidhuber, J. (2015). Deep Learning in neural networks: An overview. *Neural Netw.* 61, 85–117. doi: 10.1016/j.neunet.2014.09.003

Skoneczny, H., Kubiak, K., Spiralski, M., and Kotlarz, J. (2020). Fire blight disease detection for apple trees: Hyperspectral analysis of healthy, infected and dry leaves. *Remote Sens.* 12. doi: 10.3390/rs12132101

Uddin, S., Haque, I., Lu, H., Moni, M. A., and Gide, E. (2022). Comparative performance analysis of K-nearest neighbour (KNN) algorithm and its different variants for disease prediction. *Sci Rep* 12. doi: 10.1038/s41598-022-10358-x

Van De Vijver, R., Mertens, K., Heungens, K., Somers, B., Nuyttens, D., Borra-Serrano, I., et al. (2020). In-field detection of *Alternaria solani* in potato crops using hyperspectral imaging. *Comput. Electron. Agric.* 168. doi: 10.1016/j.compag.2019.105106

Wardhani, N. W. S., Rochayani, M. Y., Iriany, A., Sulistyono, A. D., and Lestantyo, P. (2019). Cross-validation Metrics for Evaluating Classification Performance on Imbalanced Data. *2019 International Conference on Computer, Control, Informatics and its Applications*. doi:10.1109/IC3INA48034.2019.8949568

Waskom, M., Botvinnik, O., O'Kane, D., Hobson, P., Lukauskas, S., Gemperline, D. C., et al. (2017). *mwaskom/seaborn: v0.8.1 (September 2017)*. Zenodo. Available at: <https://doi.org/10.5281/zenodo.883859>

Zárate-Chaves, C. A., Osorio-Rodríguez, D., Mora, R. E., Pérez-Quintero, Á. L., Dereeper, A., Restrepo, S., et al. (2021). TAL Effector Repertoires of Strains of *Xanthomonas phaseoli* pv. *manihotis* in Commercial Cassava Crops Reveal High Diversity at the Country Scale. *Microorganisms* 9, 1–26. doi: 10.3390/microorganisms

Zhang, J., Yang, Y., Feng, X., Xu, H., Chen, J., and He, Y. (2020). Identification of Bacterial Blight Resistant Rice Seeds Using Terahertz Imaging and Hyperspectral Imaging Combined With Convolutional Neural Network. *Front. Plant. Sci.* 11. doi: 10.3389/fpls.2020.00821

Zhang, X., Vinatzer, B. A., and Li, S. (2024). Hyperspectral imaging analysis for early detection of tomato bacterial leaf spot disease. *Sci. Rep.* 14, 27666. doi: 10.1038/s41598-024-78650-6

## **CONCLUSÕES GERAIS**

---

---

1. O teste LAMP desenvolvido neste estudo demonstrou alta sensibilidade, sendo capaz de detectar até 100 fg de DNA do isolado tipo (IBSBF 278), e alta especificidade, sem gerar reações cruzadas com outras espécies bacterianas ou patovares, amplificando exclusivamente isolados de Xpm. O método mostrou-se eficaz para detectar Xpm em folhas de mandioca infectadas quando maceradas, sem a necessidade de tratamento adicional das amostras, tornando-o adequado para o monitoramento da doença, tanto em laboratório quanto em campo.
2. A avaliação da resistência de genótipos de mandioca resultou na formação de três grupos: moderadamente resistentes, moderadamente suscetíveis e suscetíveis, com base na escala de severidade e na Área Abaixo da Curva de Progresso da Doença (AUDPC). Nenhum genótipo foi classificado como resistente, o que destaca a importância da realização de múltiplos ensaios sob diferentes condições ambientais para uma compreensão mais aprofundada do comportamento dos genótipos.
3. Na análise por imagens hiperespectrais (HSI), o modelo baseado em Support Vector Machine (SVM) obteve o melhor desempenho, com 91,41% de acurácia e AUC-ROC de 0,9684, seguido por Multiple-Layer Perceptron (MLP) (87,5%), Random Forest - RF (76,56%) e XGBoost (80,08%). K-Nearest Neighbors (KNN) e Decision Tree (DT) apresentaram os piores resultados, com acuráncias de 70,31% e 71,88%, respectivamente. Esses resultados indicam que a combinação de HSI com SVM é a melhor para discriminar folhas doentes e sadias no patossistema Xpm-mandioca, com potencial para aplicações em campo.